AMXTH-CD-TR-86055

④

NONLINEAR DYNAMIC RESPONSE ANALYSIS OF 115 MM CHEMICAL ROCKET PACKING IMPACTS

AD-A190 702

by
Stephen E. Stewart
P. A. Cox

FINAL REPORT
SwRI Project No. 06-8461-001

June 1985

DTIC
ELECTE
JAN 1 9 1988
S
H
D

DISTRIBUTION UNLIMITED / APPROVED FOR PUBLIC RELEASE

Prepared for

**U.S. ARMY TOXIC AND HAZARDOUS MATERIALS AGENCY
ABERDEEN PROVING GROUND, MARYLAND 21010-5401**

DISCLAIMER

The findings in this report are not to be construed as an official Department of the Army position unless so designated by other authorizing documents.

REPORT DOCUMENTATION PAGE

1a. REPORT SECURITY CLASSIFICATION	1b RESTRICTIVE MARKINGS
Unclassified	None

2a. SECURITY CLASSIFICATION AUTHORITY	3 DISTRIBUTION/AVAILABILITY OF REPORT
NA	Distribution Unlimited/Approved for Public Release
2b. DECLASSIFICATION/DOWNGRADING SCHEDULE	
NA	

4 PERFORMING ORGANIZATION REPORT NUMBER(S)	5 MONITORING ORGANIZATION REPORT NUMBER(S)
06-8461-001	AMXTH-CD-TR-86055

6a NAME OF PERFORMING ORGANIZATION	6b OFFICE SYMBOL (If applicable)	7a. NAME OF MONITORING ORGANIZATION
Southwest Research Institute		U.S. Army Toxic and Hazardous Materials Agency

6c ADDRESS (City, State, and ZIP Code)	7b. ADDRESS (City, State, and ZIP Code)
P. O. Drawer 28510 6220 Culebra Road San Antonio, Texas 78284	Aberdeen Proving Ground, MD 21010-5401

8a NAME OF FUNDING/SPONSORING ORGANIZATION	8b. OFFICE SYMBOL (If applicable)	9. PROCUREMENT INSTRUMENT IDENTIFICATION NUMBER
H&R Technical Associates, Inc.		

8c. ADDRESS (City, State, and ZIP Code)	10 SOURCE OF FUNDING NUMBERS			
P. O. Box 215 Oak Ridge, Tennessee 37831	PROGRAM ELEMENT NO	PROJECT NO	TASK NO	WORK UNIT ACCESSION NO

11. TITLE (Include Security Classification)

Nonlinear Dynamic Response Analysis of 115mm Chemical Rocket Packing Impacts

12. PERSONAL AUTHOR(S)
Stewart, Stephen E.; Cox, P. A.

13a TYPE OF REPORT	13b TIME COVERED	14 DATE OF REPORT (Year, Month, Day)	15 PAGE COUNT
Final	FROM _____ TO _____	85,06	128

16 SUPPLEMENTARY NOTATION

17 COSATI CODES			18 SUBJECT TERMS (Continue on reverse if necessary and identify by block number)
FIELD	GROUP	SUB-GROUP	M55 Chemical Rocket, Rocket Packing, Impact Response, CAMPACT
15	02		

19. ABSTRACT (Continue on reverse if necessary and identify by block number)

Nonlinear dynamic impact response analyses were performed on 115mm chemical rocket packing assemblies. Three different orientations of the packing assembly during impact with an unyielding surface were examined: impacts of the packing assembly bottom, side and end. For impacts on unyielding surfaces due to drops from 40 feet, failures of one or more rocket agent cannisters were probable if the packing was oriented so that the end or side struck the unyielding surface. It was concluded that bottom impacts from 40 feet would not cause leakage of rocket agent cannisters. Calculations of the interaction effects between rocket packing assemblies inside a CAMPACT and the CAMPACT structure indicated the CAMPACT would have a significant ameliorating effect on packing response during end impacts from 40 feet.

20 DISTRIBUTION/AVAILABILITY OF ABSTRACT	21 ABSTRACT SECURITY CLASSIFICATION
[ ] UNCLASSIFIED/UNLIMITED [X] SAME AS RPT [ ] DTIC USERS	Unclassified

22a NAME OF RESPONSIBLE INDIVIDUAL	22b TELEPHONE (Include Area Code)	22c OFFICE SYMBOL
CPT Kevin J. Flamm	(301) 671-2424	AMXTH-CD-L

DD FORM 1473, 84 MAR   83 APR edition may be used until exhausted
All other editions are obsolete

SECURITY CLASSIFICATION OF THIS PAGE

SOUTHWEST RESEARCH INSTITUTE
Post Office Drawer 28510, 6220 Culebra Road
San Antonio, Texas 78284

NONLINEAR DYNAMIC RESPONSE ANALYSIS OF 115 MM CHEMICAL ROCKET PACKING IMPACTS

by

Stephen E. Stewart
P.A. Cox

FINAL REPORT
SwRI Project No. 06-8461-001

for

H&R Technical Associates
977 Oak Ridge Turnpike
Oak Ridge, Tennessee

June 1985

Approved:

Alex B. Wenzel, Director
Department of Energetic Systems

Table of Contents

List of Figures

List of Tables

iii

ABBREVIATIONS

The following abbreviations are used in this document:

ADINA   - Automatic Dynamic Incremental Nonlinear Analysis Code

CAMPACT - Container for Armaments Protection and Transport

DOF   - degree(s) of freedom

FE   - finite element

FEM   - finite element method

H&R   - H&R Technical Associates

M55   - 115 mm chemical agent rocket weapon

SwRI   - Southwest Research Institute

2-D   - two dimensional

3-D   - three dimensional

1.0 BACKGROUND AND SUMMARY

H&R Technical Associates has been contracted to assess the risks associated with the transport of M55 chemical agent munitions. In support of these studies, SwRI has analyzed for H&R various sub-problems in the areas of thermal cook-off, structural damage, and penetration of these munitions and their shipping containers. Separate reports have been issued by SwRI stating the results of these analyses.

This particular document addresses the impact analyses performed on the rocket packing assembly, hereinafter referred to as the "pallet assembly." The concern motivating these analyses can be stated as follows. What is the highest distance from which the pallet can be dropped onto an unyielding surface without inducing leakage in in the agent cannister? In response to this concern, a pallet of M55 rockets, illustrated in Figure 1, was analyzed to determine if it could be dropped onto a unyielding surface from 40 feet on each of its faces (end, side, and bottom faces) and not induce failure of the agent cannister.

It is anticipated that pallet assemblies of M55 munitions will be shipped in a protective containers named "CAMPACT." On the exterior, CAMPACTs resemble ordinary 20-foot shipping containers. They are especially constructed for transporting hazardous materials, however. CAMPACT construction features include a thick foam inner lining, aluminum honeycomb and Kevlar sidewalls, and an interior truss for added strength. The sidewall, truss, and inner lining provide a substantial increase in rigidity and thermal/fire protection over conventional container construction. Figure 2 illustrates this container.

If a loaded CAMPACT container is dropped, the foam lining of the CAMPACT might have an ameliorating effect on the agent cannister response. On the other hand, the additional mass of pallet assemblies above the agent cannister of interest might significantly increase the cannister response. To establish in a qualitative manner the effects of the foam lining and pallet interaction, additional calculations were also performed on a simple pallet model modified to reflect the cushioning of the foam inner lining and the added inertia of other pallets. (For detailed calculations of the structural response of the CAMPACT to impact see [1]).

It is important to briefly mention at this point some conditions that were assumed to make the impact analyses tractable and the scope of the work performed. Firstly, it was assumed that the agent cannister was in a new condition, that is, aging effects such as load history, corrosion, creep and pallet degradation were not in any way assessed or accounted for. Secondly, it was assumed that agent cannisters were not leaking at the time of transportation. Thirdly, in regards to the scope of this work, these analyses quantitatively address only the impact of the pallet on a unyielding surface, separate from any shipping container which might be used to transport pallets. Interaction effects have been addressed, in a qualitative way, for the longitudinal impact case, however.

Results of the pallet impact analyses can be briefly summarized. In the case of bottom or vertical impacts onto unyielding surfaces from 40 foot

1

Plywood End Cap

Longitudinal Stringer
(Typical)

Base Stringer and
Rubbing Strip
(Typical)

Wood Crate

Length   83 inches

Width   30 inches

Height   28 inches
(Including skids)

Weight   1,350
(filled)

Cubage   41.7 cu feet

Wooden Spacer
(Typical)
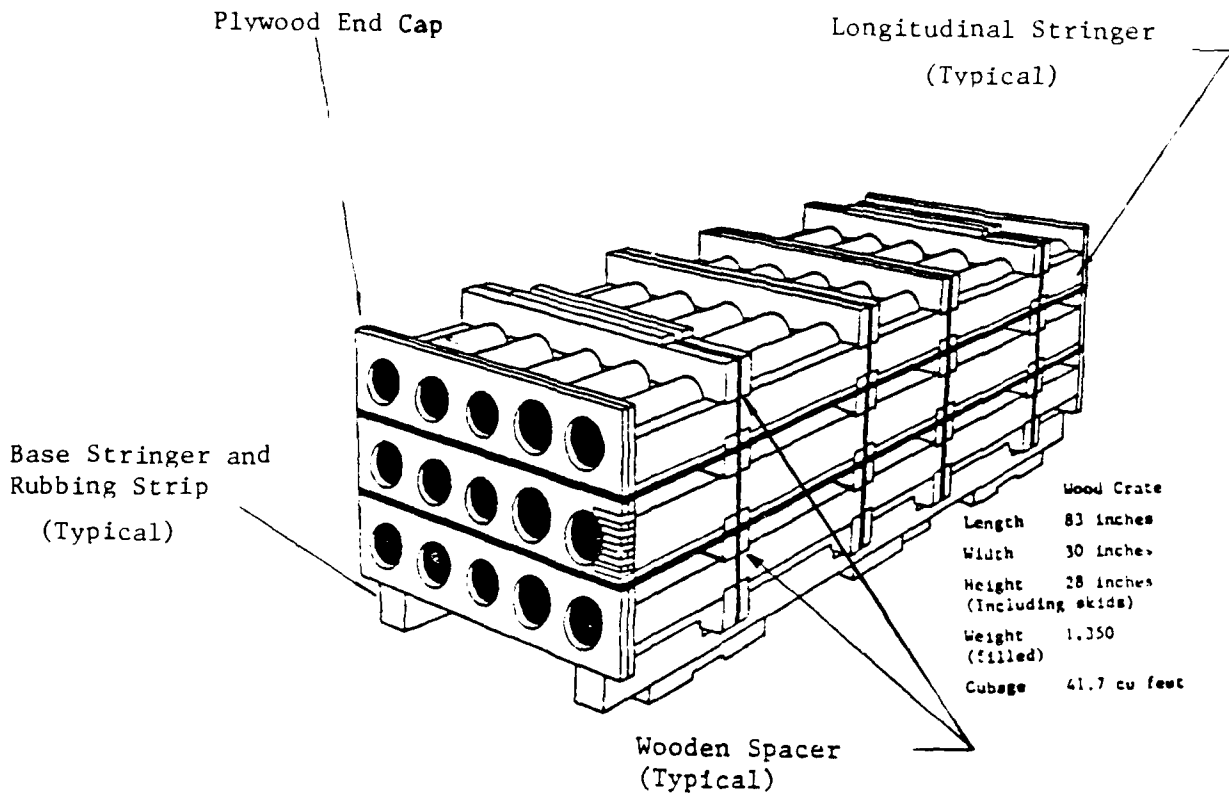
Figure 1.   Pallet of M55 Missiles (in Launch Tubes)

Figure 2. Principal Features of CAMPACT Container

3

heights, it was concluded that failure of the agent cannister would not occur. For end or longitudinal unyielding surface impacts from 40 feet, the analyses indicated that strains in the agent cannister exceeded the failure criteria and leakage of the agent cannister probably would occur. Longitudinal impacts onto unyielding surfaces from 30 feet did not cause failure of the agent cannister, however. Analyses of side or lateral impacts of the pallet onto unyielding surfaces from 40 feet showed that cannister failures would probably occur. Calculations of the interactions between pallets and the CAMPACT indicated that the CAMPACT could have a significant ameliorating effect on the pallet response during longitudinal impacts from 40 foot heights.
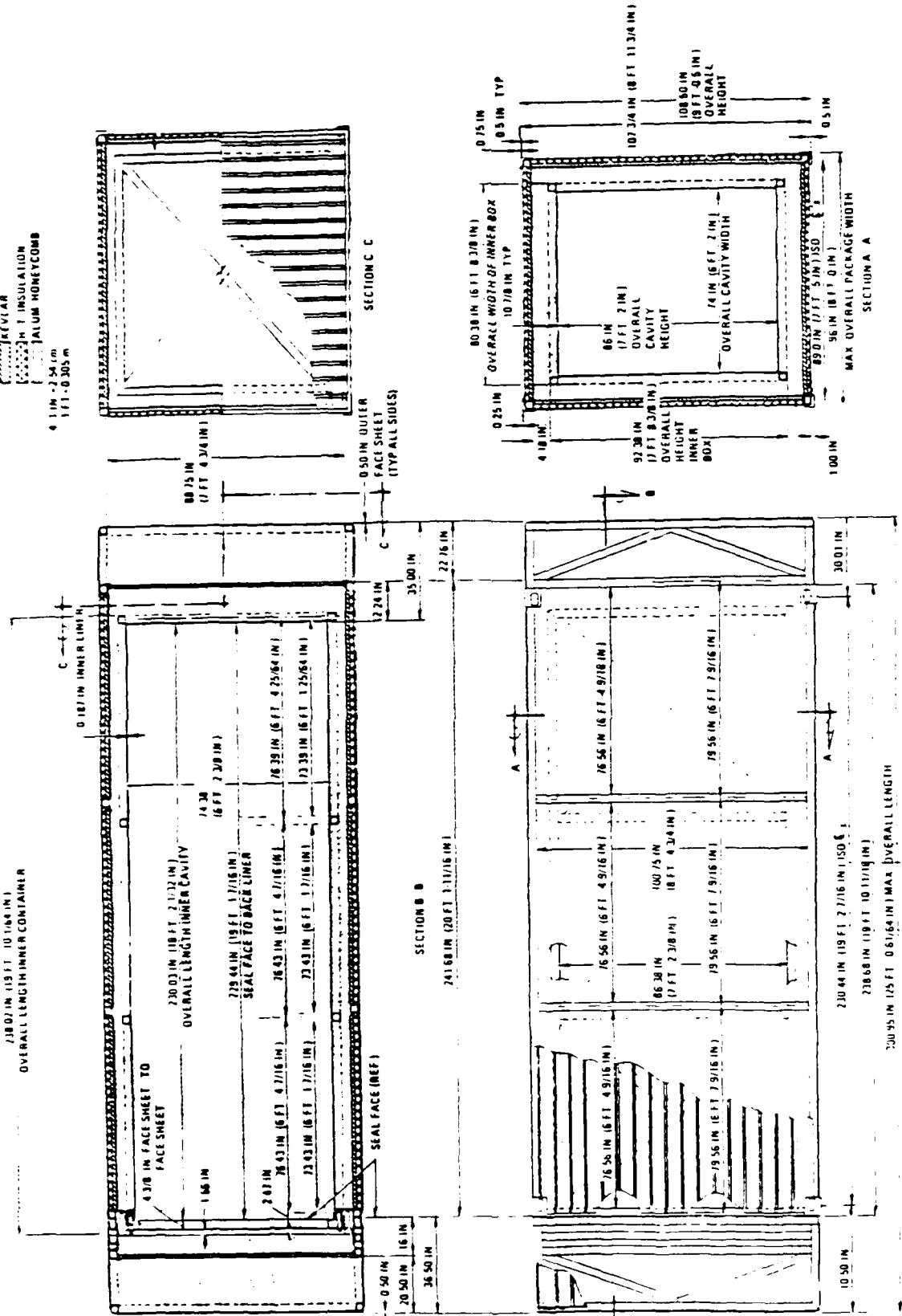
This report has been organized to assist the technical reader in understanding the results achieved, and also how they were derived. It consists of two major parts. The first, or methodology section, describes the problems solved, the details of the finite element models used to generate strain-time histories in the agent cannister, and general features of the nonlinear computational scheme. The second part presents the results, primarily in the form of strain-time histories for nodes at several positions along the agent cannister. These plots are discussed in light of the failure criteria adopted and conclusions are then drawn regarding leakage of agent.

2.0 ANALYSIS METHODOLOGY

2.1 Overview

It does not require much stretching of the imagination to suspect that dropping pallets from 40-foot heights onto unyielding surfaces could cause yielding or failure of pallet components. Responses of this type have the general classification of nonlinear response. What is meant by nonlinear response is that computed displacements are not linear functions of the applied loads. This is a mathematically correct, but physically an unappealing explanation.

Several physical phenomena can be identified as causing nonlinear response: material yielding, changes in boundary conditions, and large displacements. Material yielding results in a nonlinear relation between material stress and strains; large displacements can cause yielding also, but they change the directions of the applied loads on the structure as well. Changes in boundary conditions generally occur when the structure makes contact with other structures, usually after some initial displacement. This action results in a nonlinear response because there is a "step change" in structural stiffness [2].

Analyses of the pallet assembly involved all these types of nonlinearities. It was nearly certain from the outset of this project that the applied loads and low yield points of some pallet components would result in inelastic material behavior. Although not so obvious, it also became clear that large displacements would be induced as well; some component displacements exceeded one inch. Finally, the structure of the pallet is such that with large displacements, some components could make contact with the impact surface and therefore, changes in boundary conditions could also occur.

The computer program proposed and used for the pallet impact problems was ADINA. In ADINA, four levels of computational complexity exist: linear elastic, materially nonlinear, total Lagrangian, and updated Lagrangian analysis. Each computational level is more complex because fewer assumptions about the structural response are made, e.g., small strains, linear materials, small displacements, and constant boundary conditions. It appeared at the beginning that few assumptions like these could be made in the case of pallet impacts, and the results have indeed validated this approach. Thus, for the pallet impact problems, an updated Lagrangian; the most computationally expensive technique, was employed to construct solutions. That is, materials were assumed to behave nonlinearly, displacements were allowed to become large and changes in loading directions and boundary conditions were accounted for.

It has been pointed out that one of the features of these impact problems is that certain assumptions made in more common engineering problems could not be made. Although it was not possible to reduce the computational effort required to construct solutions, it was possible to reduce the problem size. Finite element models were kept to a reasonable size (less than 250 simultaneous equations) by making plausible assumptions about pallet behavior during a particular impact orientation. These presumptions about pallet dynamic response set the general features of the FE models that were ultimately developed.

First, it was presumed that in each of the various impact scenarios, only certain elements of the pallet assembly would be significantly loaded. Thus, the rest of the pallet need not be explicitly modeled so long as its inertia was accounted for. A second presumption made was that the impact response consisted of rocket bending and cross section crushing loads (at the rocket supports) and that these phenomena could be treated separately. Thus, bending and crushing strains were computed using different FE models and results were superposed.

In consequence of these initial assumptions about the pallet response behavior, five finite element models were created to analyze bottom (vertical), side (lateral), and end (longitudinal) face impacts. Vertical and lateral impact analyses utilized two models each: a beam and truss element model of one-quarter of the pallet assembly to obtain bending strains, and a two-dimensional model of the rocket support region to obtain strains in the agent cannister due to crushing or squeezing. The end face or longitudinal impact scenario does not involve any crushing or squeezing of the agent cannister between lateral supports so only one model was constructed.

Assumptions about pallet response behavior also guided the selection of the nonlinear material models used for pallet components. Where strains were expected to remain in the elastic range linear, elastic models were used. Where strains might exceed yield values, elastic-plastic models were selected appropriate for the material. Nonlinear material models used in these analyses were isotropic elastic-plastic, elastic-perfectly plastic, nonlinear elastic, or orthotropic elastic [3]. For nonlinear elastic-plastic models, a material elastic modulus, yield strength, and tangent modulus are specified; isotropic strain hardening is assumed in this material model. Elastic-perfectly plastic models appear to be nearly mathematically identical to elastic-plastic models but the tangent modulus is input as zero. These models constituted the principal material representations in the 3-D analysis. Nonlinear elastic material models were invoked to represent rocket tube crushing phenomena and the CAMPACT foam; orthotropic elastic material models were used to represent the wood in the rocket tube 2-D crushing analyses.

In the version of ADINA available at SwRI, there is currently only one orthotropic material model active: a linear elastic material model. For the 2-D models described below, such a material model was considered acceptable. The 2-D models were used to obtain crushing or squeezing stress-strain characteristics of M55 assemblies resting on lateral supports. Only localized plasticity of the wood supports was expected in these analyses, hence, a purely elastic representation of the support was considered to give reasonable results. In the 3-D models, on the other hand, large amounts of plasticity were expected in the bending of the wood supports. Thus, a linear-elastic model was not sufficiently accurate. In this case, isotropic material models were used. Material properties selected for these "isotropic" wood materials were the orthotropic parameters corresponding to the most heavily loaded orthotropic axis. For example, in the vertical impact model, where the wooden lateral supports undergo bending about axes normal to the grain direction, grain direction mechanical properties were input as the "isotropic" material model, as the principal bending stresses would occur in the grain direction.

Because the version of ADINA available at SwRI does not contain gap elements - elements specifically designed to address contact phenomena - it

was difficult to adequately address these conditions in the lateral pallet impact problem. A nonlinear elastic element with increasing stiffness was created for the vertical pallet problem; and used with some success to represent contact between lateral supports and the ground. Details are given in Section 2.4.

Some assumptions were also made concerning failure. Failure by excessive straining was assumed to occur when the total strain at any point the agent cannister exceeded a predetermined value. The Structural Alloys Handbook gives the ultimate strain of 606'-T6, the cannister material, as 8% [4]. While a strain of 8% at failure might be reached in a test coupon, it was believed that 4% was a more realistic failure strain for the agent cannister. This reduced allowable strain reflects uncertainties about the actual agent cannister strength capacity and the probability that some stress concentrations exist for the cannister which are not accounted for in the FE model.

Buckling failure modes were considered for end face, or longitudinal impacts. Failure by buckling was determined by comparing the critical stress for an empty cylindrical shell (having cross-sectional dimensions equal to the agent cannister) with the maximum buckling stress caused by a longitudinal impact. Failure by buckling was presumed if, during the impact, loads exceeded the buckling critical value. Note that this approach may be conservative. In general, the agent cannister is considerably more than half full of agent; the fluid could significantly stiffen the agent cannister and thereby increase the critical buckling stress.

In the sections below, each of these finite element models are discussed in detail. These discussions include descriptions of the nonlinear material model, active degrees of freedom, special purpose elements, boundary conditions assumed and the applied initial conditions. Models are discussed in order of increasing complexity: longitudinal, lateral and vertical impact analyses.

2.2 Longitudinal Impact

2.2.1 Analyses Performed

End face or longitudinal impacts of pallet assemblies actually involved analysis of only the M55 rocket sub-assembly. It was assumed for this loading scenario that no interaction took place between wooden pallet members or fiberglass launching tubes and the rockets. (Calculations in Appendix D show that this assumption appears to be a valid one). Therefore, the finite element models of the "pallet assembly" consisted of a single M55 rocket, oriented nose downward, with boundary conditions simulating a rigid impact surface. Neither the compliance of the plywood end caps (see Figure 1) or the launching tube end plugs were included in the longitudinal impact analyses. This approach is conservative although it was judged that their effect on the agent cannister response would be small.

SwRI numerically calculated the nonlinear dynamic response of a single M55 rocket impacting unyielding surfaces from heights of 30 and 40 feet and estimated the effects of the CAMPACT structure and its internal pallet arrangement on the safe/not safe drop height.

7

Before computing the dynamic impact response of the M55, the finite element model was checked. Hand calculations were made of the rocket weight and the first longitudinal natural frequency. The estimated rocket weight of 57 lbs. agreed very well with the numerically computed weight of 57.01 lbs. The computed first longitudinal frequency was 210 Hz. Closed form solutions, assuming a uniform distribution of mass and stiffness, gave the first longitudinal natural frequency as 216.4 Hz. These closed form solutions are contained in Appendix A.

2.2.2 Model Development

To analyze impact on unyielding surfaces, the investigators used a beam element model of the M55. This model consisted of 28 beam elements having only one translational degree of freedom (in the rocket's axial direction) at each node. Features of this model are shown in Figure 3. In general, only the rocket casing, and not rocket internals, was considered in establishing the model's axial stiffness. An exception occurred in the warhead region, where effective cross sectional properties were computed that accounted for the additional stiffness of the burster casing. Details are in Appendix A. Note that the burster's internal steel sleeve and plastic tube were not considered to add to the warhead's axial stiffness, primarily because of their lack of longitudinal end-fixity [5].

Since tapered beam elements are not available in ADINA, tapered sections of the rocket were represented by short beam elements, each of uniform cross section, but increasing in area in the direction of increasing section diameter. Each element in a tapered region had outside diameters equal to the average outer diameter of the tapered section represented.

To achieve a correct distribution of mass along the rocket's length, effective densities were computed for each element. These effective densities accounted for rocket casing and internal weights such as the fuze mechanism, the chemical agent, and the solid fuel. The exact density of the chemical agent could not be determined, so the density of water was used. Because the agent density was unknown, there may be some error in the FE model's mass distribution. Total rocket mass used in the analyses was correct, however, and equaled 57 lbs.

Each M55 in the pallet assembly is inside a fiberglass launching tube having closed ends. These tube end plugs are fabricated from aluminum and are counterbored or milled to accept the rocket tip or fins. For the longitudinal impact analysis, the plug at the nose of the rocket is of interest. This fitting, three inches thick, is counterbored for three-quarters of its thickness so as to accept the M55 fuze assembly. As this puts very little material between the rocket nose and the impact surface, the end plug stiffness was ignored in the calculation of rocket impact response. Shear loads between the counterbore in the plug and the fuze were not computed.

In addition, a plywood end cap at each end of the pallet prevents longitudinal motion of the rocket/tube assemblies during transport. End caps are 3/4-inch thick plywood sheets with holes located at each launching tube end plug. End cap hole diameters are smaller than end plugs. Again, compliance of the plywood end cap was ignored, resulting in a conservative calculation of the rocket response during longitudinal impact.
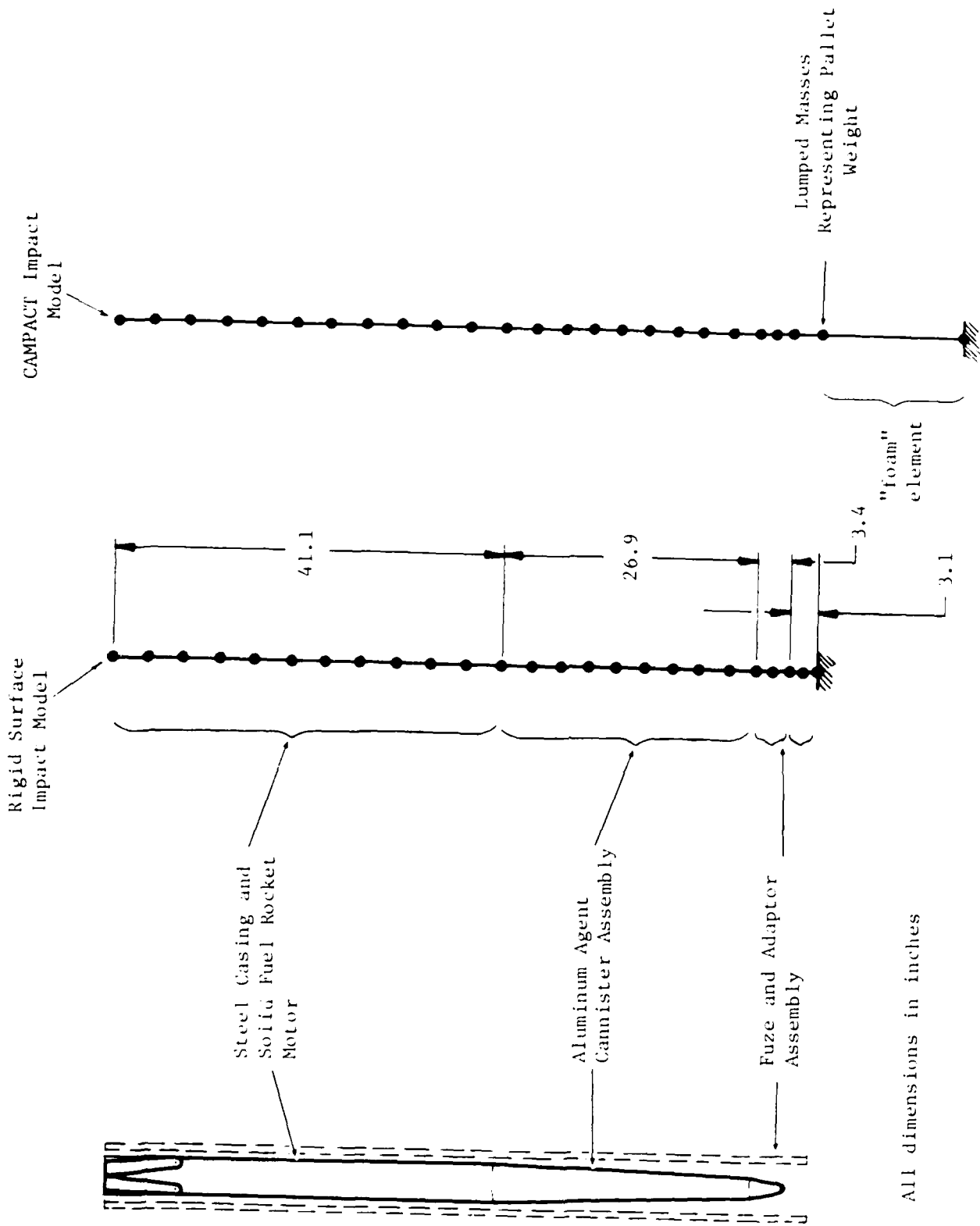
8

CAMPACT Impact Model

Lumped Masses Representing Pallet Weight

Rigid Surface Impact Model

41.1

26.9

3.4

"foam" element

3.1

Steel Casing and Solid Fuel Rocket Motor

Aluminum Agent Cannister Assembly

Fuze and Adapter Assembly

All dimensions in inches

Figure 3. Rocket Model for Longitudinal Impact Loading

9

Figure 3 also shows the model that was developed to estimate the effect on the rockets in a CAMPACT container undergoing a longitudinal impact. Results obtained from this model should not be considered definitive, but rather should indicate whether longitudinal impacts for rockets inside CAMPACTs should be more or less severe than impacts on unyielding surfaces.

This model is a simple extension of the M55 FE model just described. At the nose, a nonlinear elastic element has been added to represent the thick foam insulation on the CAMPACT door. Also at the nose, a lumped mass has been added to represent the pallet components behind the modeled M55 rocket, the weight of the pallet containing the modeled M55 rocket, and the internal truss and roller assembly of the compact. These weights are added at the front of the M55 rocket (rather than the rear) so that their loading effect is felt by the foam only, and not the rocket. It is assumed in a CAMPACT longitudinal impact, that no pallet inertia loads pass through the rockets, but only through other pallet members and then into the foam. This assumption is supported by the calculations of Appendix D.

2.2.3 Finite Element Characteristics and Material Models

The M55 casing is fabricated from steel and aluminum. From drawings provided to SwRI, required minimum mechanical properties and or the chemical composition of the casing materials were found. From these data, the agent cannister (aluminum) was taken to be 6061 in the T6 temper condition, and the rocket casing (steel) to be AISI 1030, water-quenched and tempered at 600°F. For aluminum or steel finite elements, a bilinear elastic-plastic material model was used. The tangent moduli for the steel and the aluminum were calculated based upon 19% and 4% strain at failure, respectively. As previously discussed, this value represents one-half of the uniaxial tension test value for the aluminum. Pertinent material model input data are summarized below.

Table 1.

Mechanical Properties of AISI 1030 Steel
Longitudinal Impact FE Model

Property	Value
Elastic Modulus, E	30.0 E 6 psi
Poisson's Ratio	0.270
Yield Strength	90.0 E 3 psi
Tangent Modulus, E'	1.39 E 5 psi

Table 2.

Mechanical Properties of 6061-T6 Aluminum
Longitudinal Impact FE Model

Property	Value	
Elastic Modulus, E	10.0 E 6	psi
Poisson's Ratio	0.300	
Yield Strength	38.8 E 3	psi
Tangent Modulus, E1	88.5 E 3	psi

The truss element representing a portion of the thick foam layer on the
CAMPACT door was developed from test data [6]. The length of this element
approximately equalled the foam layer thickness and its cross sectional area
equalled 1/60th of the door area. (In the CAMPACT, 60 rockets impact the door
during a longitudinal impact). The stress-strain characteristic of the foam
is essentially piece-wise linear and consists of three pieces. The modulus of
the elastic region is defined as "E" and tangent moduli of plastic regions are
defined as "E1" and "E2", respectively.

Table 3.

Mechanical Properties of CAMPACT Foam
Longitudinal Impact FE Model

Property	Value	
Elastic Modulus, E	35.0 E 2	psi
Yield Strength	14.0 E 1	psi
Tangent Modulus, E1 (at 4% strain)	0.0	psi
Tangent Modulus, E2 (at 52% strain)	99.2 E 1	psi

2.3 Lateral Impact

2.3.1 Analyses Performed

SwRI calculated the dynamic response of a pallet when falling from 40
feet in a lateral orientation and impacting an unyielding surface. Dynamic
response of the agent cannister due to impact was assumed to consist of two
separate phenomenon: bending of the rockets and squeezing of the rockets and
tube assemblies between the lateral wooden supports. Strains and stresses
induced by these phenomena were calculated separately and superposed to obtain
the total strain or stress in the agent cannister.

A two-dimensional plane stress FE model of the rocket, launching tube,
and lateral support and a three-dimensional model of the middle row of M55

11

rockets in the pallet assembly were created to compute the squeezing and bending results. Figures 4 and 5 illustrate the principal features contained in these finite element models.

The 2-D squeezing analysis (Figure 4) was a calculation of the quasi-static response of the tube, agent cannister and support under a steadily increasing lateral shear load. From this analysis, shear failure load of the rocket/tube assembly at the support could be assessed. Figure 5 shows the fiberglass maximum principal stress versus the total shear load, as well as the aluminum cannister strain versus total shear load. By comparing the plots, one can see that when the fiberglass reaches a stress of 2' ksi (its failure stress), strain in the aluminum agent cannister is nearly 2%. This failure stress and cannister strain correspond to a total shear load of approximately 25 kips. Although the 2-D analysis was continued for shear loads greater than 25 kips, these results include the stiffness of the fiberglass and are not very meaningful.

It is postulated that at the 25 kips shear load level the fiberglass failed completely. The strain in the aluminum at this load level, nearly 2%, is presumed to step change to a value greater than 4%, upon failure of the fiberglass. Hence, a simultaneous failure of the agent cannister and fiberglass launching tube is presumed to occur. For this reason, 25 kips is adopted as the cannister failure shear load at the support.

The three-dimensional bending model (Figure 5) was formulated to give the maximum bending strain and the maximum shear load in the rocket cannister. It was anticipated that squeezing and bending components would be superposed to estimate the total strain state in the agent cannister. Superposition would be performed at times when either the agent cannister bending strain maxima or the cannister squeezing strain maxima occurred. As indicated in the results section, this superposition was not ultimately required because the squeezing strain component at the lateral support, by itself, exceeded the failure criteria.

Both a weight check and an eigenvalue check were made on the 3-D pallet model. The purpose of these check runs was to assure the investigators that the model had the correct mass and stiffness properties. The weight of the middle row of rockets and lateral supports was calculated by hand to be 147 lbs. Weight of the finite element model was 146 lbs. Similar agreement was obtained between closed form and numerical calculations of eigenvalues. A first bending mode of the rocket/tube assembly was calculated to be 279 Hz. A similar mode was calculated numerically as 241 Hz. Closed form eigenvalue calculations are contained in Appendix B.

2.3.2 Model Development

As previously mentioned, Figure 4 illustrates the features of the squeezing model used in the lateral impact analysis. The developed finite element model consisted of approximately 100 2-D plane stress elements having a thickness approximately equal to the lateral support thickness.

For lateral squeezing of the agent cannister and launching tube, only one plane of symmetry exists, the plane containing the lateral centerline of the rocket/tube assembly. Thus, the entire bottom half of the rocket and tube

12

Figure 4. Principal Features of Lateral Impact Crushing Model

All dimensions in inches.

Represents Fiberglass Launching
Tube and Aluminum Warhead Casing,
Nonlinear Elastic-plastic Material
Model (2 beams, coupled in
translation DOF, typical)

Represents Mass of Overhanging
Lateral Support Beams (concentrated
mass)

Represents Wooden Saddle
Lateral Stiffness, Elastic-
plastic Isotropic Material
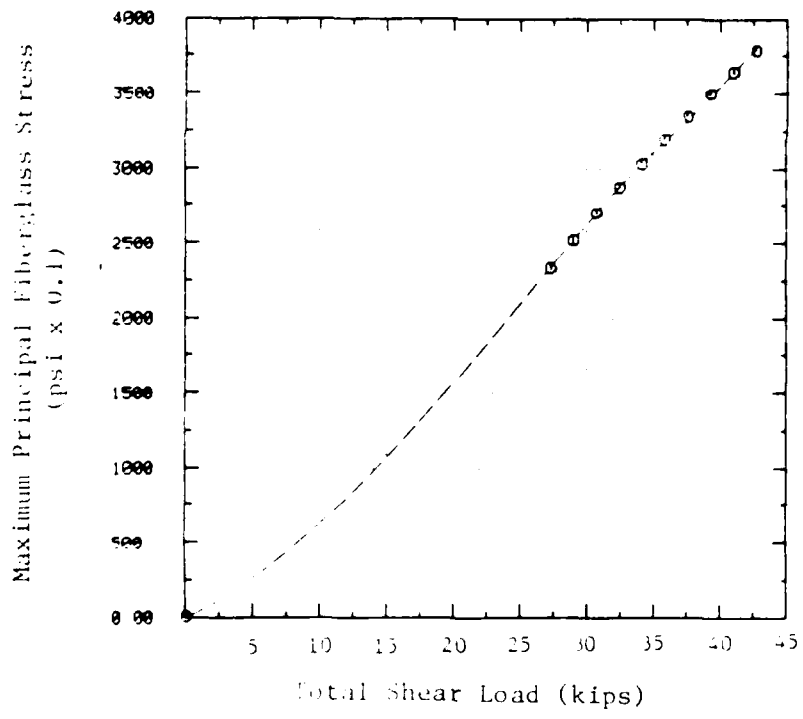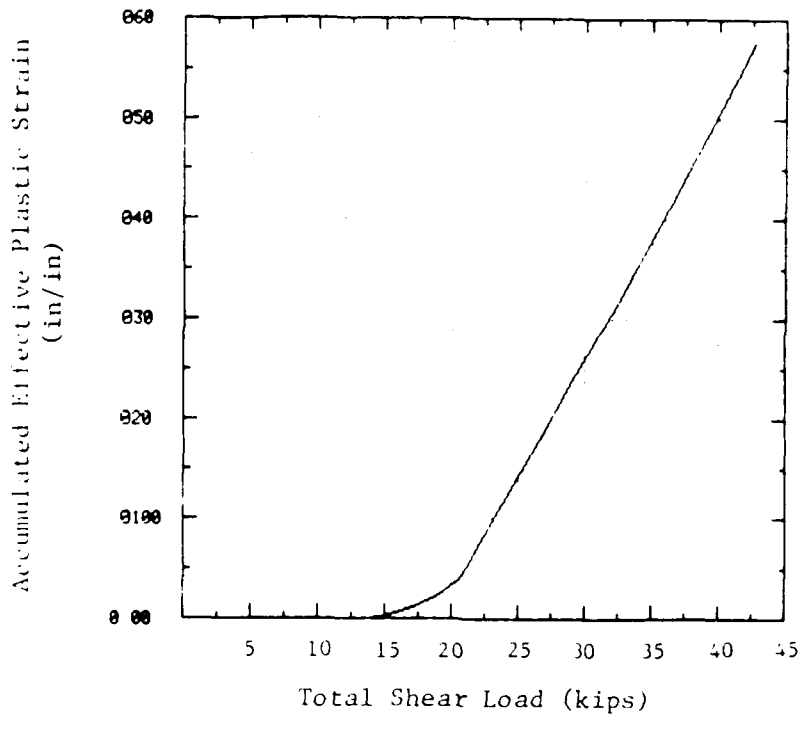Model, Grain Direction Material
Properties (typical)

Figure 5. Pallet Model for Lateral Impact Loading

14

Figure 6. Fiberglass Principal Stress and Aluminum
Cannister Strain Versus Total Shear Load

15

assembly are represented in this model. They are modeled with beam and plate elements so that, with minimal modification, the lateral squeezing model could also be used in the vertical crushing analysis. It is not necessary to represent in the model the entire bottom half of the wooden support. Under the lateral shear loads indicated in Figure 4, only the right portion of the support is loaded and thus only this region is represented.

Boundary conditions at the edges of the lateral support, and the rocket casing and launching tube centerplanes are as indicated in Figure 4. In addition, nodes along the agent cannister-launching tube, and tube-support interfaces are coupled in the radial direction. The purpose of these constraint equations is to allow circumferential slippage between the M55 rocket and its launching tube, as occurs in reality. Beam and plate elements representing the launching tube and agent cannister are also coupled via constraint equations. These equations rectified the beam rotational with the plate translational degrees of freedom.

Figure 5 illustrates the features of the 3-D bending model. Only the middle row of M55's in the pallet assembly are represented. Because there are no significant load paths between rows of rockets in the pallet, interaction between rows under lateral impact is neglected. The FE model accounts for interaction between rockets comprising the middle row by connecting rocket tube assemblies with truss elements representing the grain-direction stiffness of the lateral wooden supports.

To obtain correct stresses and strains at launching tube and agent cannister cross sections, rocket/tube assemblies were modeled by coupled sets of beam elements, one set of elements representing the tubes, one set representing the rockets. Constraint equations were applied that required translations (in the impact direction only) of rocket and tube be identical. These coupled beam sets are represented by a single line in Figure 5. Derivations of the constraints are given in Appendix B.

Only half the longitudinal length of the pallet is represented by the FE model. Symmetry has been assumed about the pallet lateral centerplane; the effects of asymmetrical response modes under lateral impact are assumed to be negligible at the agent cannister. Boundary conditions at the rockets' midpoints are as shown in Figure 5. Launching tubes had identical boundary conditions at corresponding nodes. Elements representing the rockets had annular cross sections and densities which accounted for casing and internal weights such as the chemical agent and solid rocket fuel.

2.3.3 Finite Element Characteristics and Material Models

The squeezing and bending materials developed for the lateral impact problem were identical except that one additional material model existed in the 3-D model that did not exist in the 2-D analysis (AISI 1030 steel). As in the case of the longitudinal impact problem, aluminum and steel rocket casings were represented as elastic-plastic materials with tangent moduli calculated based upon failure strains. Again, for the aluminum, the value used represented one-half of the uniaxial tension test data. Pertinent material model input data are summarized below.

16

Table 4.

Mechanical Properties of AISI 1030 Steel
Lateral Impact FE Model

Property	Value
Elastic Modulus, E	30.0 E 6 psi
Poisson's Ratio	0.270
Yield Strength	90.0 E 3 psi
Tangent Modulus, E'	1.39 E 5 psi

Table 5.

Mechanical Properties of 6061-T6 Aluminum
Lateral Impact FE Model

Property	Value
Elastic Modulus, E	10.0 E 6 psi
Poisson's Ratio	0.300
Yield Strength	38.8 E 3 psi
Tangent Modulus, E'	38.5 E 3 psi

Fiberglass material data were developed from the tube specification given in the pallet assembly drawings and from Owens-Corning Fiberglass Company data found in reference 7. An average glass to resin ratio of 35% was assumed. A sufficient amount of this glass was assumed to be in mat form to result in isotropy.

Fiberglass is a brittle elastic material, i.e., there is a linear relation between stress and strain up until failure; however, material models with ultimate strength cut-offs do not exist in the SwRI version of ADINA. Hence, for the purposes of computation, an elastic-perfectly plastic material model was used for the fiberglass launching tubes. Following calculation of a solution, launching tube elements were manually checked for "plasticity" (failure). For the 40 foot drop height, "plasticity" in the fiberglass was insignificant, occuring only over a small portion of the tube length and never occurring through the complete wall thickness.

Mechanical properties used for the launching tubes are summarized below.

Table 6.

Mechanical Properties of Fiberglass Launching Tubes
Lateral Impact FE Model

Property	Value	
Elastic Modulus, E	1.10 E 6	psi
Poisson's Ratio	0.11	
Yield Strength	2.10 E 7	psi
Tangent Modulus, E'	0.0	psi

Axial or grain-direction stiffness of the wooden rocket supports was estimated from an effective cross sectional area for the support. Because supports have a "scalloped" shape, their actual area varies along the support length. To simplify the modeling of these members, an effective beam width was computed based on the beam longitudinal area and length. (See Appendix B.) Because most of the stresses during lateral impact were expected to be axial, the beam element in this model was given isotropic material properties identical to the orthotropic grain properties. Yield strength was taken at 12% moisture content, conforming to seasoned wood [8], [9].

Pertinent characteristics of these elements are shown in the table below.

Table 7.

Mechanical Properties Wooden Lateral Supports
Lateral Impact Model

Property	Value	
Elastic Modulus, E_r	1.353 E 6	psi
Poisson's Ratio	0.239	
Yield Strength	5700.0	psi
Tangent Modulus, E_T	0.0	psi

2.4 Vertical Impact

2.4.1 Analyses Performed

SwRI computed the response of the pallet assembly when falling 40 feet onto a unyielding surface, in its normal, upright orientation. Dynamic response of the agent cannister to impact was assumed to consist of two independent phenomena: bending of the rockets between lateral supports, and diametral crushing of the launching tube and rocket cross sections by the supports. Strains and stresses induced by these phenomena were computed independently and superposed to obtain the total strain or stress in the agent cannister.

The investigators created finite element idealizations to compute bending and crushing results. A two-dimensional, plane stress model of the rocket, launching tube, and support interface, and a three-dimensional model of one quarter of the pallet assembly were used to obtain crushing and bending responses. Figures 7 and 8 illustrate the main features of these models, and Appendix B details the effective density, concentrated mass, and beam property calculations made in creating the FE models.

The crushing analysis was a calculation of the quasi-static response of the tube, agent cannister, and wooden support under a monotonically increasing crushing load. From these computations, a crushing force-cannister strain characteristic was developed. Initial conditions for the dynamic response analysis of the three-dimensional model corresponded to the 40 foot drop height. Results from this model were strain-time histories in the rocket casing due to bending, and the crushing force-time history at the rocket-lateral support connections.

The crushing force-cannister strain characteristic was obtained first. From these data, a nonlinear elastic truss element ("the crushing spring") was developed which reflected the computed rocket/tube and lateral support crushing stiffness. These truss elements became part of the 3-D bending model. Hence, the dynamic response computed using the 3-D model reflected both bending and crushing energy absorption.

Both a weight check and an eigenvalue check were made on the 3-D pallet model before computing dynamic response. The purpose of these calculations was to assure the investigators that the model had the correct mass and stiffness properties. The weight of the quarter pallet modeled was estimated to be 226 lbs. A weight of 226.4 lbs. was calculated from the FE model. Very good agreement was also obtained between closed form and numerical solutions for eigenvalues. A first bending mode of the rocket tube assembly was calculated to be 304 Hz. A similar rocket/tube bending mode was calculated numerically as 293 Hz. Eigenvalue calculations are shown in Appendix C.

2.4.2 Model Development

To obtain the crushing force-cannister strain characteristic, a finite element model of the rocket, tube and support interface was created. Because loading and geometrical symmetry exists about the vertical and horizontal centerplanes of this connection, only one-quarter of the tube and support region need be modeled. Figure 7 shows the principle features of the finite element model developed. This idealization consisted of about 100 2-D plate elements having 2 DOF at each node. The thickness of these elements equalled the thickness of the wooden lateral support.

Boundary conditions at the edges of the lateral support member, and the rocket casing, and launching tube centerplanes are indicated in Figure 7. In addition, nodes along the agent cannister-launching tube and tube-support interfaces are coupled in the radial direction. These constraints allow circumferential slippage between the M55 and its launching tube as actually occurs.

Figure 8 shows the features of the bending model. One-quarter of the pallet containing three columns of rockets and tubes are represented. The two

19

Denotes Coupling in Radial Direction

Aluminum Warhead Casing, Isotropic, Nonlinear, Elastic-plastic Material Model

"Cross-grain" or Tangential Orthotropic Axis

"Grain" or Longitudinal Orthotropic Axis

1-13/16

2.844

Fiberglass Launching Tube, Isotropic Linear Elastic Material Model, Elements Become Inactive After Principal Strains Exceed Ultimate

Wooden Support, Elastic Orthotropic Material Model

x

Vertically Applied Distributed Load

20

All dimensions in inches

Figure 7. Principal Features of Vertical Impact Crushing Model

Represents Fiberglass Launching Tube and
Aluminum Warhead Casing, Isotropic
Nonlinear Elastic-plastic Material Model
(2 beams, coupled in translation DOF, typical)

Nonlinear Spring Representing
Crushing Stiffness (k_s calculated
from crushing model)

Element Representing Contact
With Impact Surface

Concentrated Masses Representing Center
Columns of Rockets (typical)

Represents Wooden Saddle
Support, Isotropic, Elastic-
plastic Nonlinear Material
Model, Grain Direction
Properties (typical)

Represents Wooden Stringer, Isotropic,
Nonlinear Elastic-perfectly Plastic
Material Model, Cross-grain Material
Properties, (typical)

Represents Wooden Rubbing Strip
and Base Stringer, Isotropic,
Nonlinear, Elastic-perfectly
Plastic Material Model, Cross-
grain Material Properties
(typical)

X
Y
Z

21

Figure 8. Pallet Model for Vertical Impact Loading

off-center columns of rockets are idealized as lumped masses on the lateral support beams, while the center column of rockets are more explicitly modeled using beam elements. "Crushing spring" elements are indicated in the figure.

In order to account for possible contact between the impact surface and the lateral support, a truss element has been installed at the support center point (see Figure 3). This element had little axial stiffness for displacements less than the support-surface gap; for greater displacements, the element stiffness increased sharply.

Again, only half the longitudinal length of the pallet is represented by the model. Symmetry has been assumed about the pallet lateral centerplane, and the effect of asymmetrical modes under vertical impact are assumed to be small at the agent cannister.

2.4.3 Finite Element Characteristics and Material Models

The 3-D model developed for the pallet vertical impact problem was the most complex of the pallet models constructed. This idealization of one-quarter of the pallet consisted of over 100 beam and truss elements classified into six different groups, each group having particular dimensional or constitutive features. In the following paragraphs, each group is discussed in turn.

Lateral wooden supports in the pallet were idealized as beams of uniform cross section and homogenous, isotropic material. Because lateral supports have a "scalloped" shape so as to conform to the launching tubes, their actual cross sectional area varies along the support length. To simplify the modeling of these members while accounting for the regions of increased cross sectional area between "scallops", an effective beam width was computed based upon the actual beam longitudinal area and length (see Appendix C). Because most of the stress was expected to be caused by support bending along the grain direction, this beam was given isotropic material properties corresponding to the grain direction orthotropic properties. Because post yield characteristics of woods are not well understood, it was assumed that the supports had elastic-perfectly plastic behavior. Yield strength for the support was taken for wood at 12% moisture content (seasoned wood). Poisson's ratio was taken as the average of the radial-grain and tangential-grain ratios.

Pertinent characteristics of these elements are summarized in the next table.

Table 8.

Mechanical Properties Wooden Lateral Supports
Vertical Impact Model

Property	Value	
Elastic Modulus, E_L	1.353 E 6	psi
Poisson's Ratio	0.239	
Yield Strength	5700.0	psi
Tangent Modulus, E_T	0.0	psi

22

The wooden base stringer and rubbing strips along the bottom of the pallet were assumed to sustain only cross-grain compressive loads during these impacts. Thus, like the lateral supports, these pallet components were idealized as isotropic, elastic-perfectly plastic materials with moduli and mechanical properties corresponding to the cross-grain wood orthotropic axis.

Parameters input for these finite elements are shown below.

Table 9.

Mechanical Properties for Base Stringer and Rubbing Strip
Vertical Impact FE Model

Property	Value	
Elastic Modulus, E_R	0.064 E 6	psi
Yield Strength	510.0	psi
Tangent Modulus, E_T	0.0	psi

As in the case of the longitudinal and lateral impact problems, rocket casing materials were considered to be isotropic, elastic-plastic materials with the following properties.

Table 10.

Mechanical Properties of AISI 1031 Steel
Vertical Impact FE Model

Property	Value	
Elastic Modulus, E	30.0 E 6	psi
Poisson's Ratio	0.270	
Yield Strength	90.0 E 3	psi
Tangent Modulus, E'	1.39 E 5	psi

Table 11.

Mechanical Properties of 6061-T6 Aluminum
Vertical Impact FE Model

Property	Value	
Elastic Modulus, E	10.0 E 6	psi
Poisson's Ratio	0.300	
Yield Strength	38.8 E 3	psi
Tangent Modulus, E'	88.5 E 3	psi

23

Fiberglass material data were developed from the tube specification given in the pallet assembly drawings and from Owens-Corning Fiberglass Company data found in reference 6. An average glass to resin ratio of 35% was assumed. A sufficient amount of this glass was assumed to be in mat form to result in isotropy. Fiberglass is a brittle elastic material, i.e., there is a linear relation between stress and strain up until failure. Material models with ultimate strength cut-offs do not exist in the SWRI version of ADINA. Hence, for computations, an elastic-perfectly plastic material model was used for the fiberglass launching tubes. Following calculation of a solution, launching tube elements were manually checked for "plasticity" failure. For the 40 foot drop height, no "plasticity" occurred.

Mechanical properties used for the launching tubes are summarized below.

Table 12.

Mechanical Properties of Fiberglass Launching Tubes
Vertical Impact FE Model

Property	Value	
Elastic Modulus, E	1.10 E 6	psi
Poisson's Ratio	0.11	
Yield Strength	2.10 E 7	
Tangent Modulus, Et	0.0	psi

The nonlinear elastic truss element representing the diametral crushing stiffness of the cannister cross section was developed from the crushing force data computed using the 2-D model. Displacement at δ, indicated in Figure 7, and the total applied force were tabulated from the 2-D analyses. These data were converted into an equivalent stress-strain characteristic by assuming an element length and cross sectional area of
3.03 inches and 1 square inch, respectively. Figure 9 shows the force-displacement data obtained from the 2-D results. The data point at δ = 0.19 inch, F = 7200 lbs. corresponds to failure at the agent cannister, i.e., a 4% strain through the wall of the cannister. Appendix C contains a tabulation of the displacement-maximum cannister strain results.

Lateral supports in the pallet assembly are separated by longitudinal stringers, also fabricated from wood. Under vertically-oriented pallet impacts, these longitudinal stringers undergo compression perpendicular to the wood grain. Because cross-grain crushing of the longitudinal stringers is a local phenomenon, not occuring over a significant percentage of the stringer length, stringer stiffness was modeled using single truss elements between the lateral support beams in the finite element model. As indicated in Figure 8, these element's material models were nonlinear, elastic-perfectly plastic models with isotropic moduli equal to the cross-grain orthotropic parameters. Data for these elements are summarized in the next table.

24
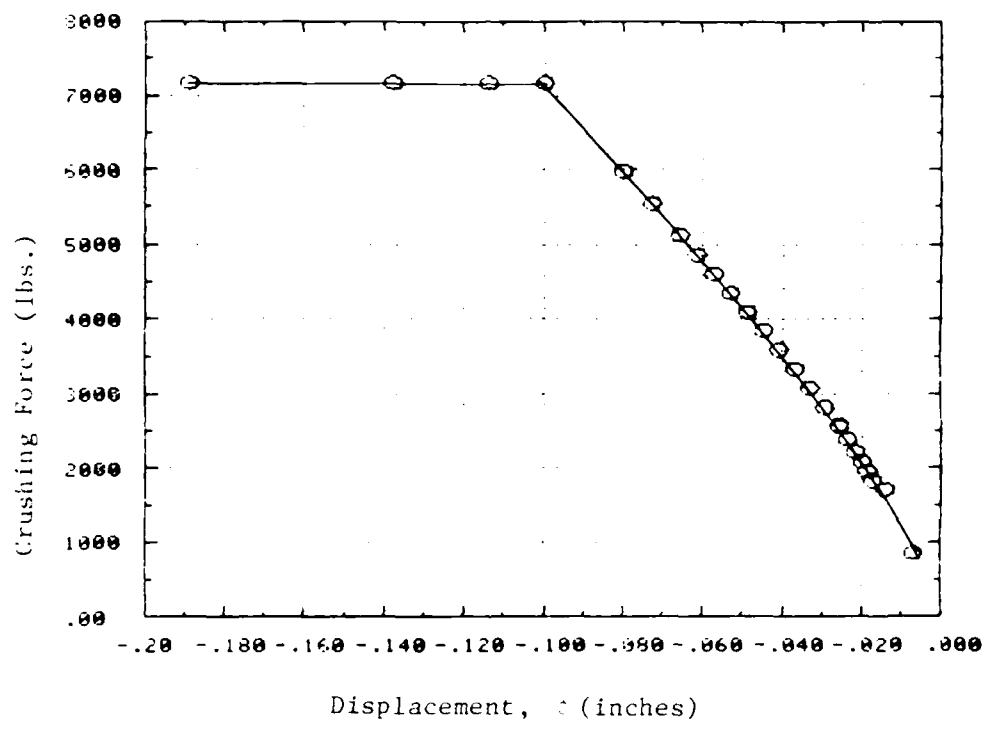
Figure 9.   Crushing Force - Displacement Characteristic

Table 13.

Mechanical Properties of Longitudinal Stringers
Vertical Impact FE Model

Property	Value	
Elastic Modulus, E_R	0.064 E 6	psi
Yield Strength	510.0	psi
Tangent Modulus, E_T	0.0	psi

Under static loads, such as gravity, the pallet assembly is supported entirely by the large base stringer and rubbing strip. Under impact loads, however, inertia loadings may be sufficiently high so that lateral support beams undergoing bending also contact the impact surface. To represent this change in boundary conditions ordinarily calls for a nonlinear element specifically adapted to contact problems. In SwRI's version of ADINA, such an element does not exist. To address this difficulty, the investigators created a nonlinear elastic truss element with increasing stiffness. This element, shown in Figure 8, was installed at the midpoint of the lateral support. For support displacements less than or equal to the distance from the support to the impact surface, this element's stiffness was very low. For large displacements, the element's stiffness increased rapidly, representing support contact with the impact surface.

3.1 Longitudinal Impacts

As mentioned previously, SwRI considered three impact scenarios: impacts caused by drops from 40 and 30 feet onto rigid, unyielding surfaces, and an impact scenario that considered the additional mass and energy absorbing materials (foam) of the CAMPACT. In addition, the possibility of failure of the agent cannister by buckling was also examined.

Figures 10-12 summarize the results of the longitudinal unyielding surface impact analyses. Figure 10 shows the locations along the agent cannister where axial strain data were tabulated. Figure 11 contains three plots of the strain-time history for the 40 foot impact. The plots show strains at the forward, middle, and aft end of the agent cannister. Similarly, Figure 12 shows plots of the strain-time history for the 30 foot impact case. It consists of plots of the strain response at 6 locations along the agent cannister.

For the 40 foot drop, the strains in Element 5 (topmost plot of Figure 11) exceeded the agent cannister failure criterion by a good margin, reaching 8% at .0035 seconds after impact. These high strains occurred in the forward, tapered region of the cannister. At points aft of the tapered region where cross-sectional areas are larger, lower strains were recorded. At Elements 11 and 15, maximum strains computed were 0.35% and 0.1%, respectively.

Close examination of these plots, particularly the topmost plot of Figure 11, reveals flat regions in the strain-time history. These flat response regions are generally preceded by a rapid increase in strain and only occur after material strains have exceeded 0.4% (yield strain).

The rapid rise in strain before the flat regions signifies that the applied load is rising and that material yielding is occurring; the strain increases rapidly because the plastic stress-strain modulus is very low compared to the elastic modulus. After the load begins to decrease, however; the material response can again be elastic. If the applied load increases for a second time, the change in strain will be relatively small until the new yield point is exceeded. These flat spots in the strain response represent points in the strain time history where this elastic behavior, below a newly defined yield point, is occurring.

An equivalent crush force for impact conditions was computed for this scenario by equating the pallet's kinetic energy at impact to the work necessary to deform the structure. For longitudinal impact, this equivalent crush force was 546,800 lbs. (see Appendix E). Note that failure of the rocket occurred in this impact scenario.

For the 30 foot impact analysis, strains at 6 points along the agent cannister were plotted (Figure 12). Again, as in the 40 foot impact case, strains were greatest in the forward, tapered regions of the cannister and decreased at aft sections. Strains at all sections were consistently lower than the 40 foot case, as expected. Maximum strain at the foremost cannister section was less than 1.5%, indicating that yielding of the casing had occurred, but it was not sufficient to cause failure (yield in aluminum begins at approximately 0.4% strain). Maximum strains at aft sections were approximately 0.31%, 0.30%, 0.29%, and .285%, respectively. Strains at the
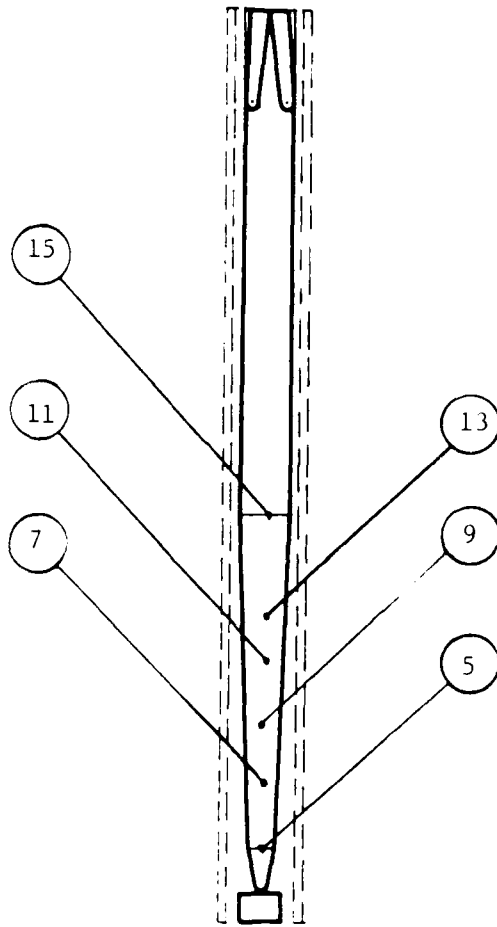
Figure 10. Approximate Locations of Elements for Which
Axial Strain Data Was Tabulated

Element 5 Strain (in/in)

Time (sec)

Element 11 Strain (in/in)

Time (sec)

Element 15 Strain (in/in)

Time (sec)
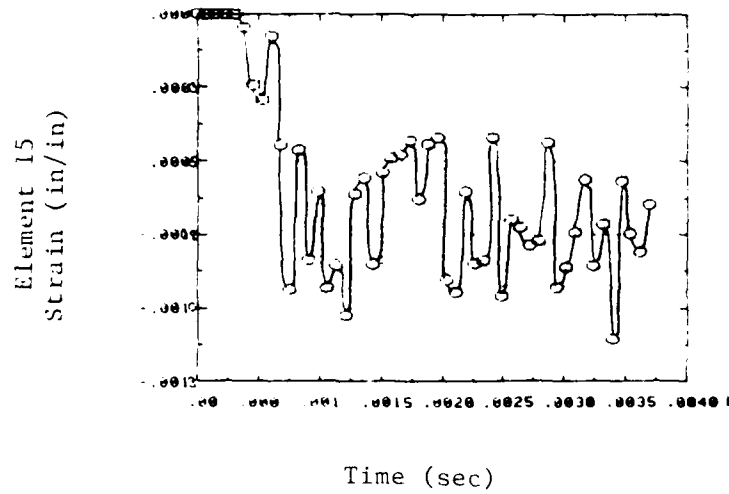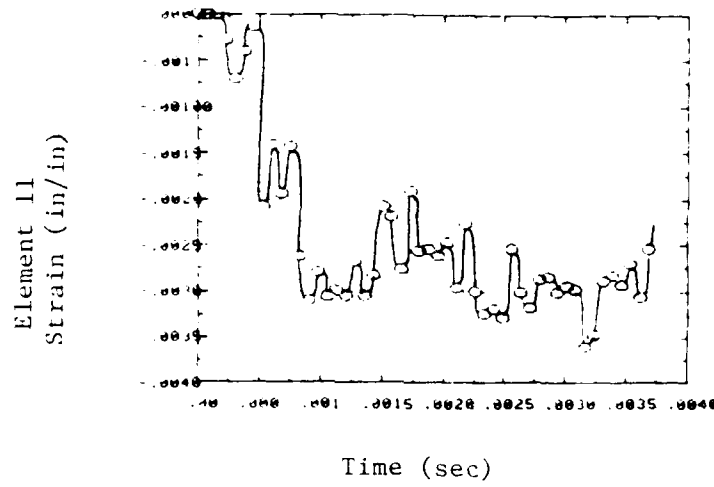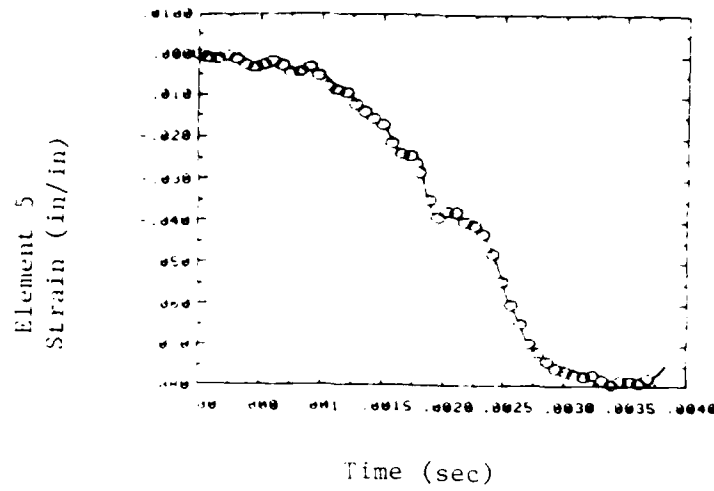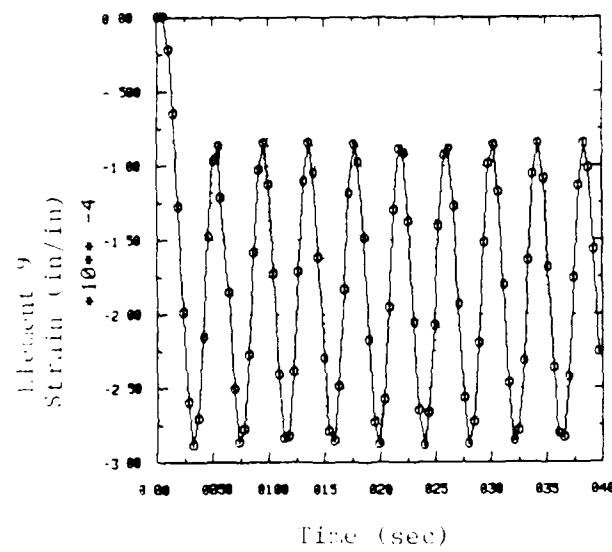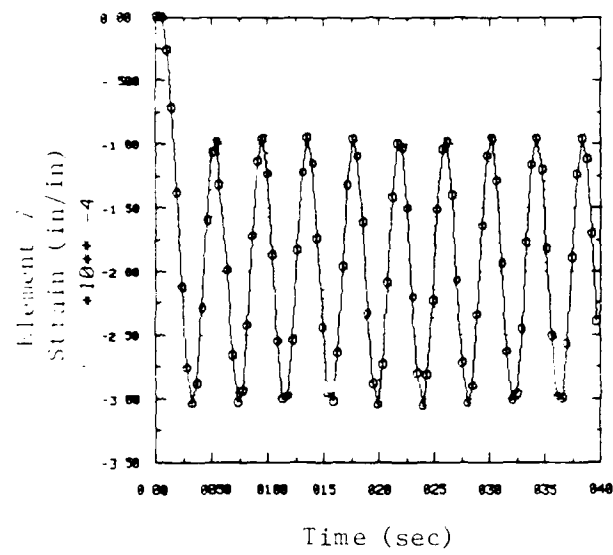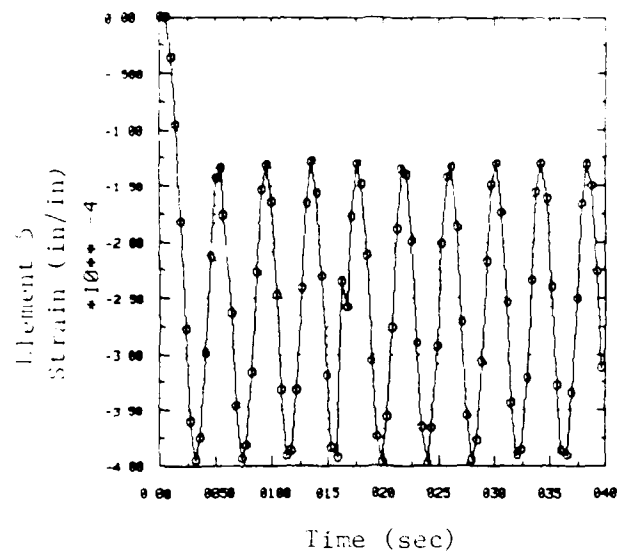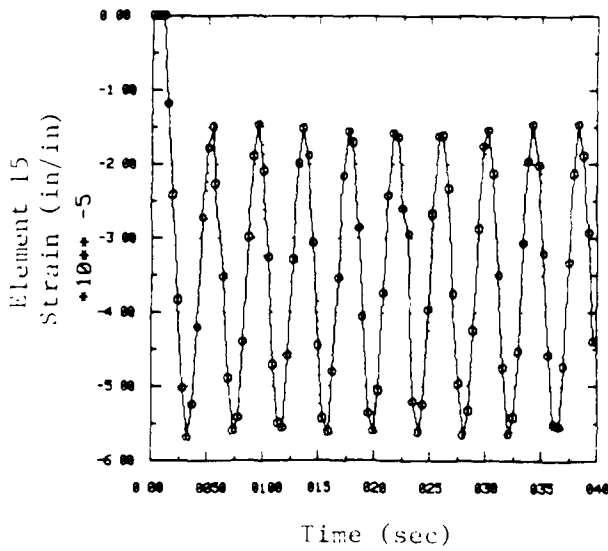
Figure 11. Axial Strains in M55 Rocket Undergoing
Longitudinal Impact (from 40 feet)

29
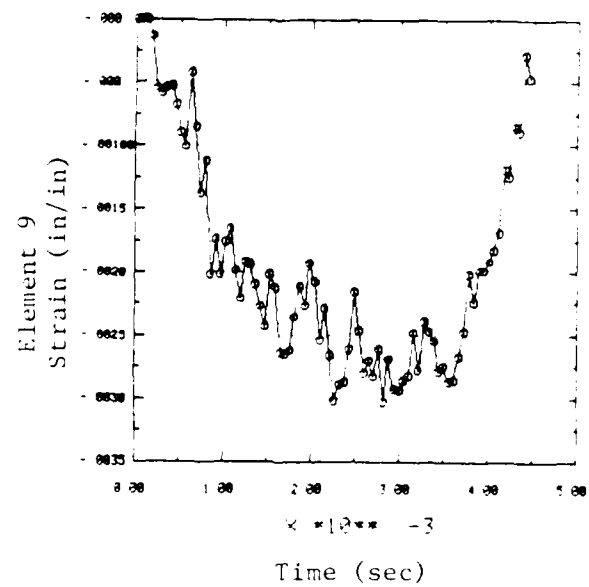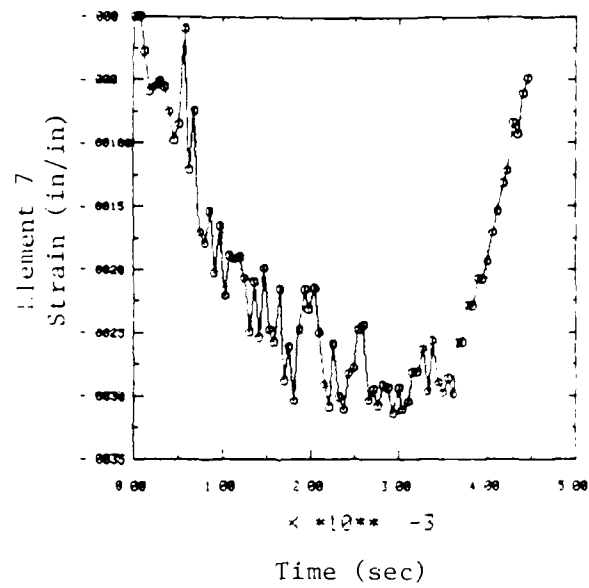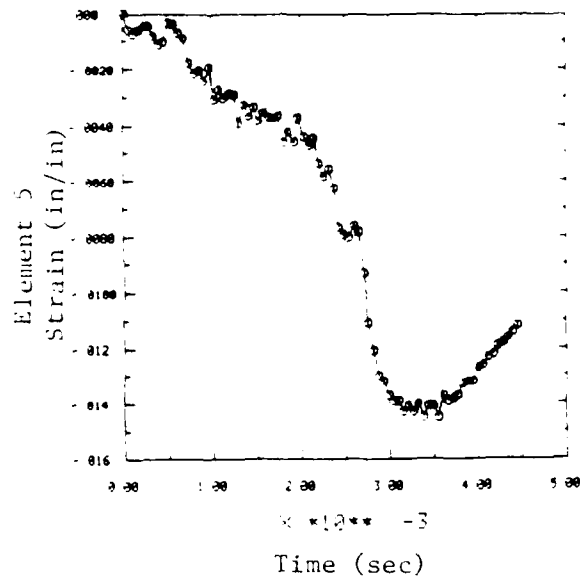
Figure 12.   Axial Strains in M55 Rocket Undergoing
Longitudinal Impact (from 30 feet)

30
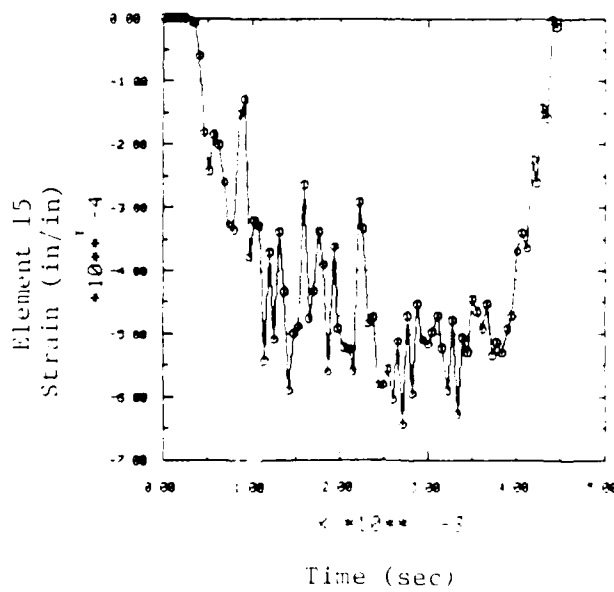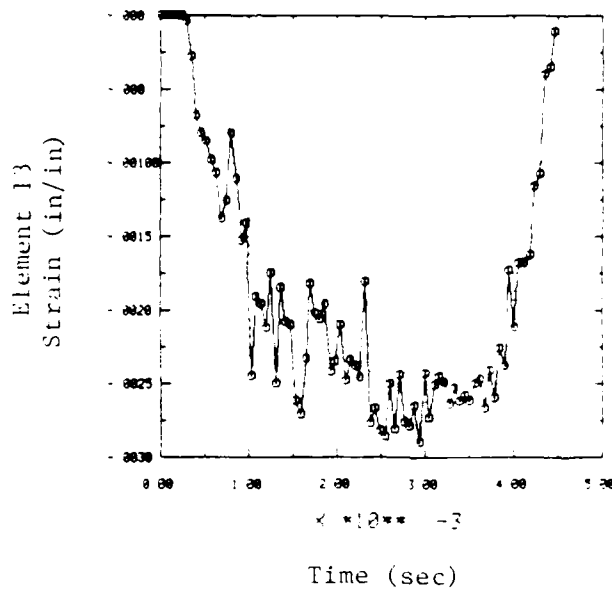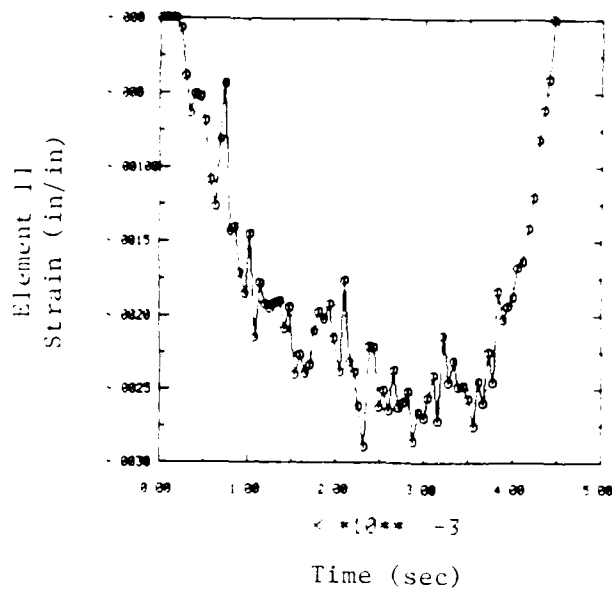
Figure 12. (cont'd) Axial Strains in M55 Rocket Undergoing
Longitudinal Impact (from 30 feet)

31

cannister-rocket motor joint were very low, less than 0.07%.

Note that strains caused by 30 and 40 foot impacts are not proportional. Drops from 30 feet cause approximately only one-half the strain in the forward cannister caused by the 40 foot impact. Impact responses of the cannister are not proportional because the cannister response is non-linear. Agent cannister elements 5 through 8, for example, deformed plastically during the 40 foot impact, while during the 30 foot impact only cannister element 5 deformed plastically - the greater part of the agent cannister did not yield.

Figures 13 and 14 summarize the results for the foam impact model. As previously discussed, the model attempts to assess, albeit in a qualitative way, interactions between the pallets and the CAMPACT structure during a longitudinal impact.

It appears that the inner-liner of the CAMPACT has the potential to significantly ameliorate the response of the pallets. Figure 13 shows that, for longitudinal impacts onto thick foam, the M55 rocket response is primarily in one mode (compared to the multiple mode response indicated in Figures 11 and 12 for unyielding surface impacts) and that the maximum strain response is substantially reduced. Maximum computed dynamic strain for the agent cannister in this analysis occurs in the forward tapered section of the cannister and was about .041% as compared to 8% strain for the unyielding surface impact case. (Because structural damping was not included in these analyses, strain response amplitudes do not decrease over time).

Besides failure by overload, another possible failure mode for the agent cannister is buckling between the lateral supports. Four buckling modes were examined in order to assess whether buckling was a critical failure mode for this type of impact. In the first case, the cannister was considered as a Euler column and the critical axial load was computed. Because the agent cannister is a thin walled cylinder, in the second case lobar or circumferential buckling was assessed. In this analysis, the agent cannister was considered to have uniform cross-sectional area, i.e., the forward tapered section was ignored. In the third case, lobar buckling of the taper section was assessed. Fore and aft cross sections of the taper section were presumed to remain circular in this closed form solution. In the last case, the internal burster casing critical buckling load was computed, again assuming that the burster acted as a Euler column. Results of the buckling analyses are summarized in Table 14. In all cases, the probable buckling stress exceeds the agent cannister ultimate stress (42.0 ksi). Hence, for these rocket support conditions, failure by overload should occur before failure by buckling.

These results indicate that a high probability of agent leakage exists for longitudinal, unyielding surface impacts from heights equal to or greater than 40 feet. Pallet assemblies impacting unyielding surfaces from lower heights, have a much lower probability of catastrophic failure of the agent cannister. The results also appear to indicate that the CAMPACT assembly probably ameliorates the effects of longitudinal impact significantly, although without a more complete pallet CAMPACT interaction analysis, it is not possible to say what the safe not safe drop height might be for M55 rockets shipped in the CAMPACT.

32

Figure 13.   Axial Strains in M55 Rocket Undergoing
            Longitudinal Impact Onto Foam
            (from 40 feet)

33
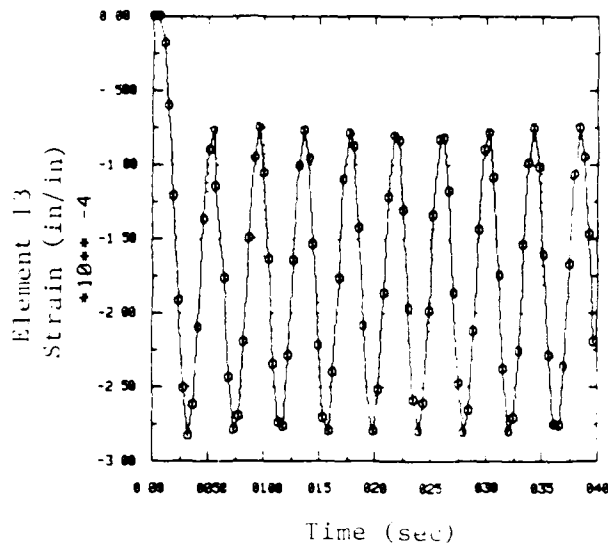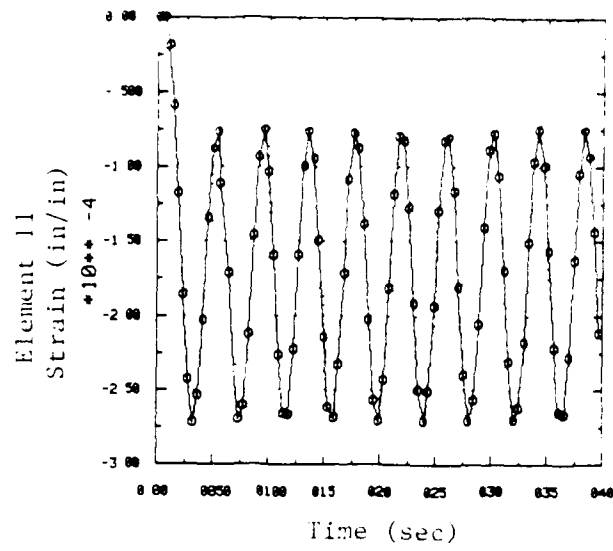
Figure 13. (cont'd) Axial Strains in M55 Rocket Undergoing
Longitudinal Impact Onto Foam
(from 40 feet)

34
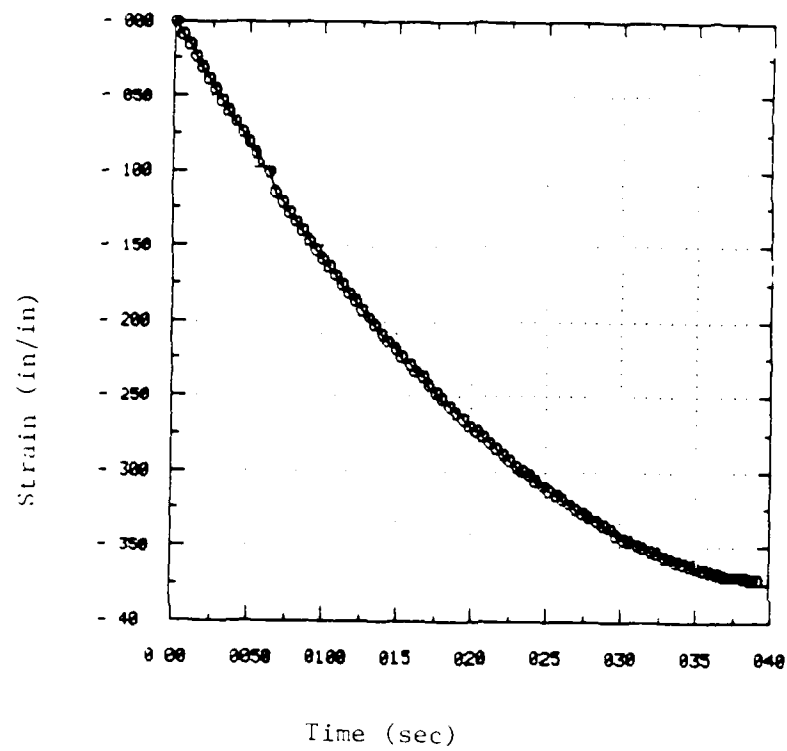
Figure 14.   Strain in Foam Undergoing Impact by M55
(from 40 feet)

Table 14.

Summary of Closed Form Buckling Solutions for Longitudinal Impact

Case	Mode Description	Theoretical Buckling Value (psi)	Probable Buckling Value (psi)	Remarks
1	Columnar buckling of agent cannister between lateral supports (Euler or free-free beam)	592743	same	Actual B.C.'s unknown – theoretical value $>>> s_{yield}$ for aluminum
2	Circumferential buckling of agent cannister approximated as uniform beam	157506	63002	Buckling value may be lower if uniform beam assumption is unconservative
3	Circumferential buckling of tapered section of agent cannister, requiring ends remain circular	154771	57265	Actual B.C.'s unknown
4	Columnar buckling of agent burster casing (Euler or free-free beam)	48420	same	Actual B.C.'s are more like "clamped", and effects of inner steel linear stiffness ignored; hence this value is probably a lower bound on actual

B.C. = Boundary Condition

36

3.2 Lateral Impacts

Figures 15-17 show the results computed for the lateral impact
scenario. Figure 15 illustrates the locations along the M55 rocket where
strain data from the 3-D analysis were obtained. These data appear as the
plots of Figure 16. Elements 38 through 43 represent the agent cannister
region of the rocket, with element 43 representing its forward tapered
section. Figure 17 shows the rocket tube assembly shear force-time history
for the forward and aft support junctions.

The strain response-time histories plotted in Figure 16 are primarily the
result of rocket bending between the supports. The plots indicate that the
impact was not sufficient to cause failure of the cannister at locations away
from the support junctions. The maximum bending strain observed occurred in
Element 39, about 2 milliseconds after impact. This strain exceeded 2%, or
about one-half the failure value. At all other elements along the cannister
region, bending strains were at all times less than 1%.

Squeezing of the rocket/tube assembly between the lateral supports is
quite severe in this loading scenario, however. Figure 17 depicts the
rocket/tube shear force at the support junctions indicated in Figure 15. The
maximum shear force occurs around 2 milliseconds after initial impact at the
aft lateral support junction. This shear force momentarily exceeds 50 kips.
From the quasi-static squeezing analysis, it was determined that a 25 kip
shear force was sufficient to cause cannister failure, i.e., strains exceeding
of 4% (see Section 2.3.1). Hence, it appears that failure of the agent
cannister is likely to occur during lateral impacts.

Again, by equating the work necessary to deform the structure to the
kinetic energy of the pallet, an equivalent crush force was computed for this
impact scenario. This equivalent force equalled 627,950 lbs. (see Appendix
E). Note that in this scenario, the missile failed by localized crushing of
the agent cannister at the lateral support.

3.3 Vertical Impacts

Figures 18-20 show the computed results for the pallet assembly
undergoing a 40 foot drop onto a unyielding surface. Figure 18 indicates the
approximate locations of the elements for which results were plotted.
Elements 21 through 26 model the agent cannister, with Element 21 representing
the forward, tapered region. Element 27 has the properties of the rocket
motor casing. Figure 19 contains the plots of the strain-time histories
obtained from the 3-D finite element model, and Figure 20 summarizes the
diametral crushing displacements.

One mode of response of the M55 rockets during a vertical impact is in
bending, and it is apparent from Figure 19 that the magnitude of the bending
strains are quite low. These low strains indicate that the impact energy was
not being absorbed significantly by rocket bending. (It was for this reason
that the time integration analysis were stopped at 4.5 milliseconds). Results
from the 3-D analysis show that significant strains and yielding occurred
during compression of the base stringer rubbing strip and bending of the
lateral wooden supports. Plasticity was observed in both the rubbing strip
and lateral supports. The maximum displacement of the wooden lateral supports
was less than two inches. Thus, it does not appear that catastrophic failure
of the supports would occur after deflections of this magnitude. Further,
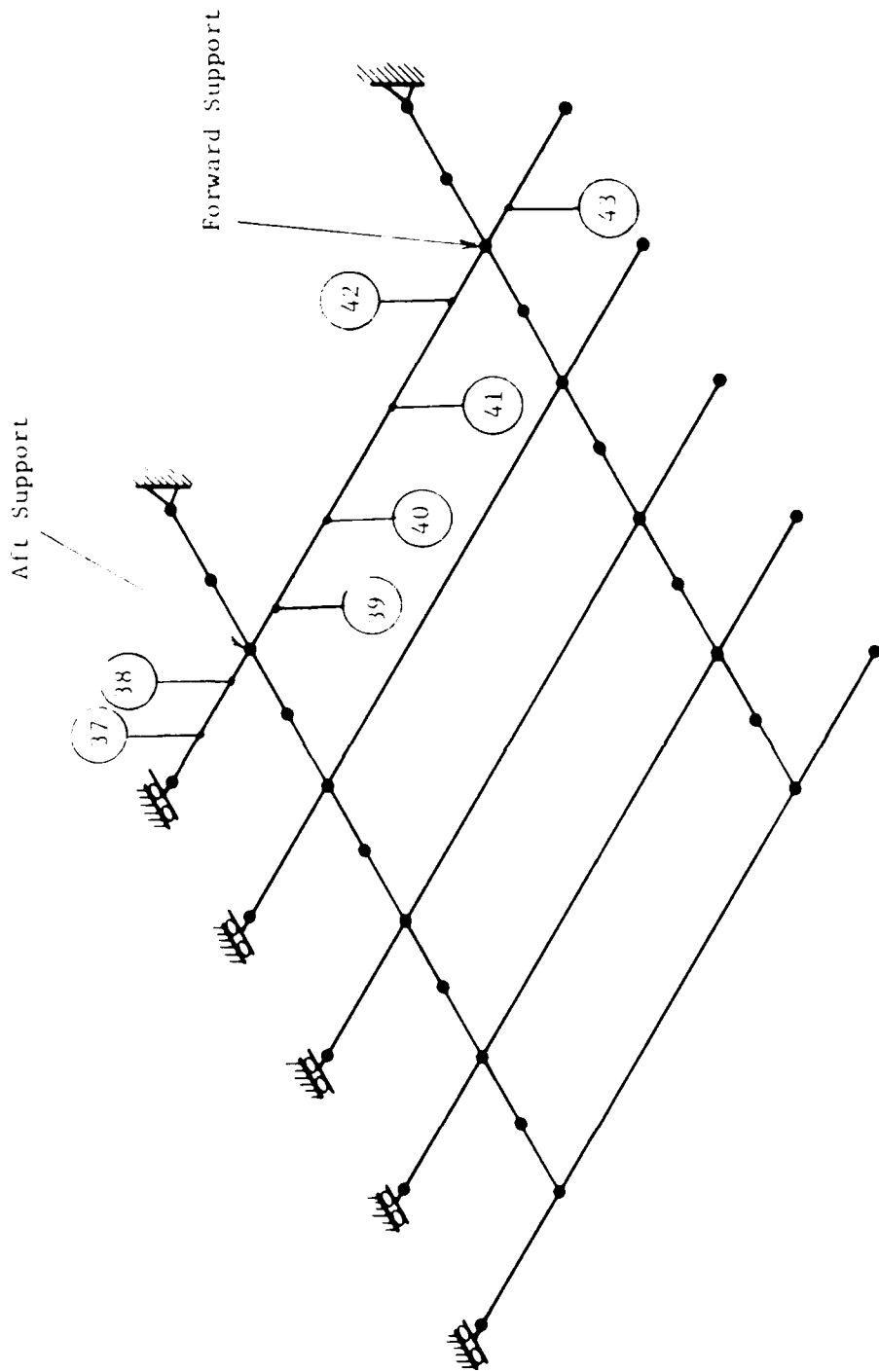
Figure 15. Approximate Locations of Elements for Which Lateral Impact Strain Data Was Plotted

38
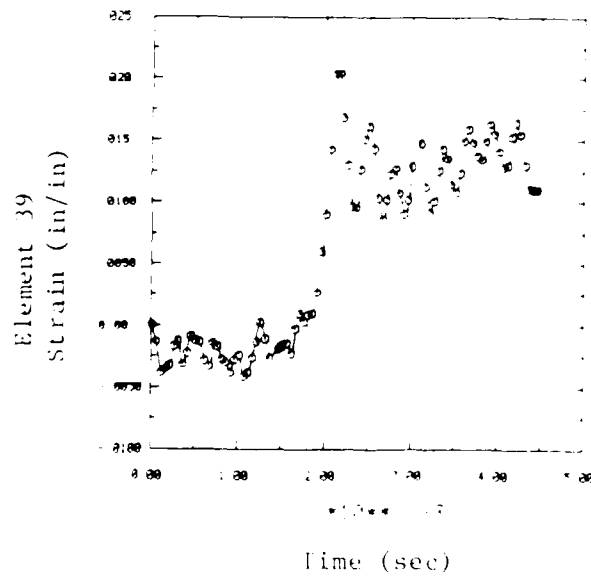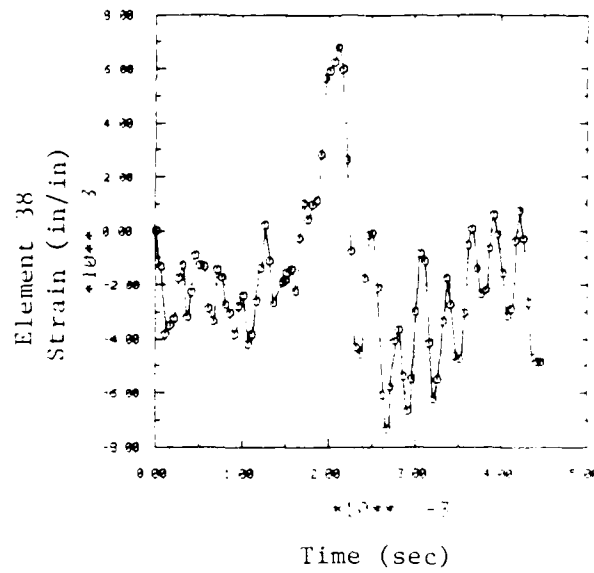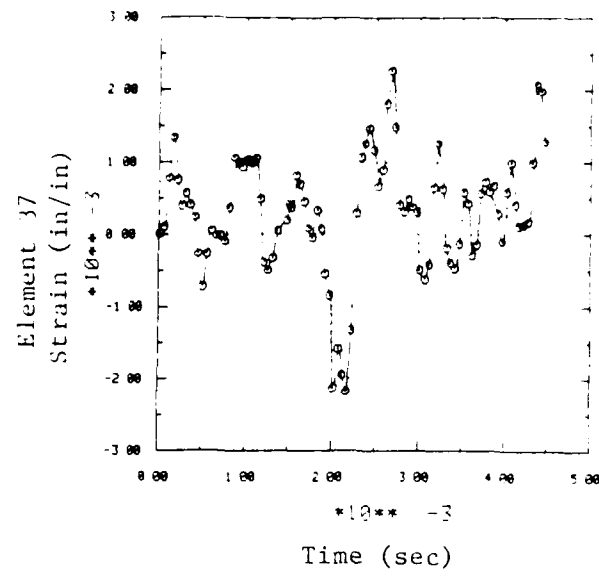
Figure 16.   Strains in M55 Rocket Undergoing
Lateral Impact (from 40 feet)

39
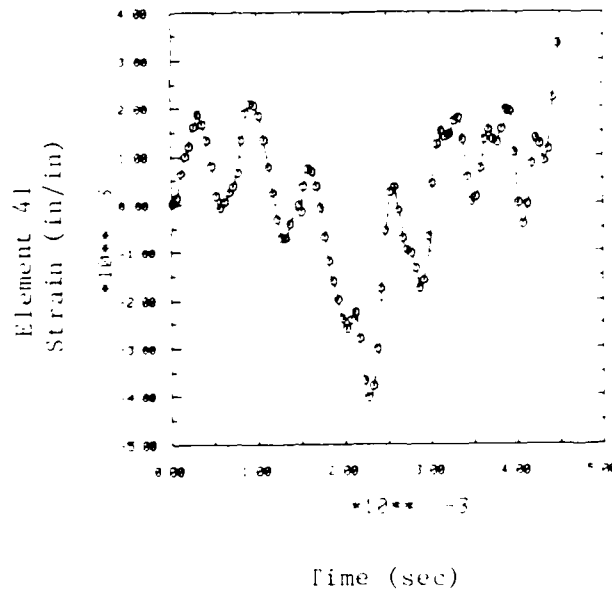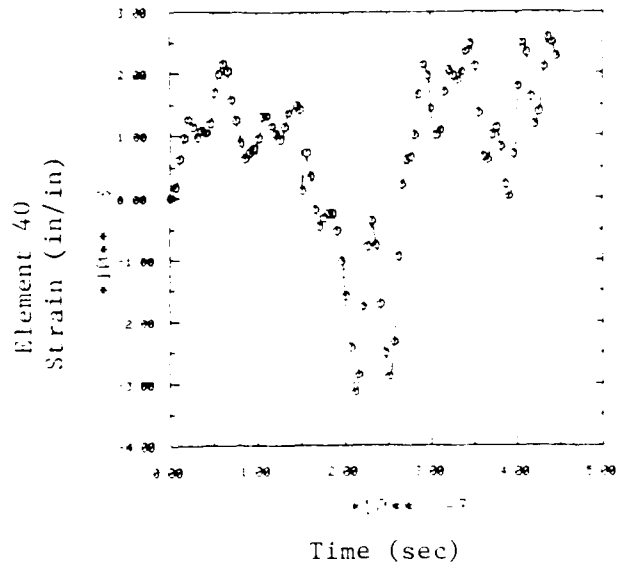
Figure 16. (cont'd) Strain in M55 Rocket Undergoing Lateral
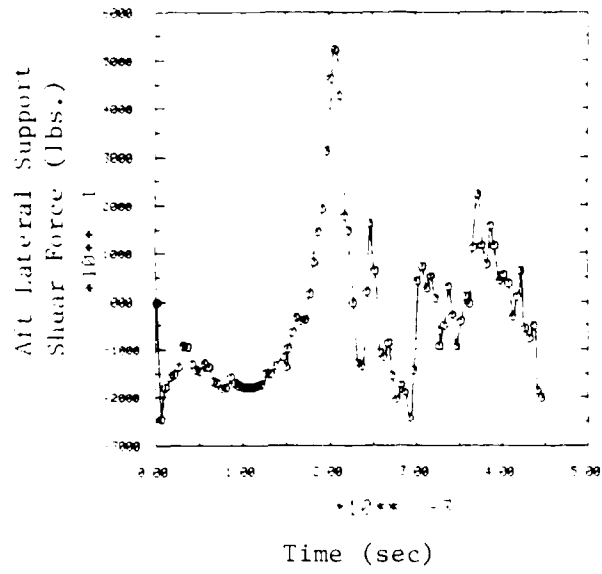Impact (from 40 feet)

Figure 16. (cont'd) Strain in M55 Rocket Undergoing Lateral
Impact (from 40 feet)
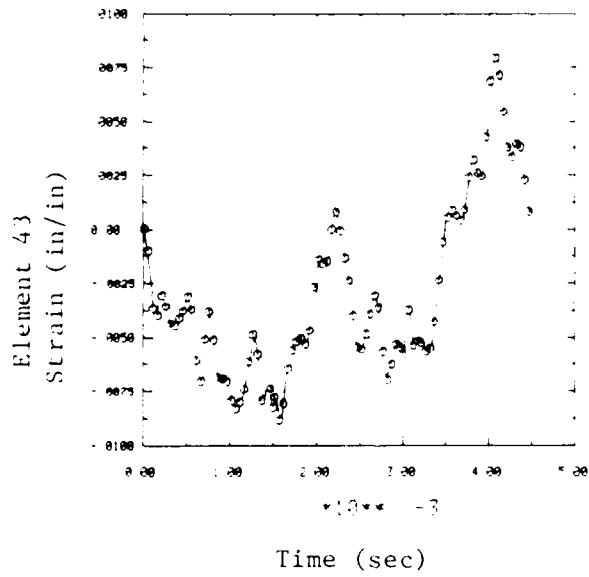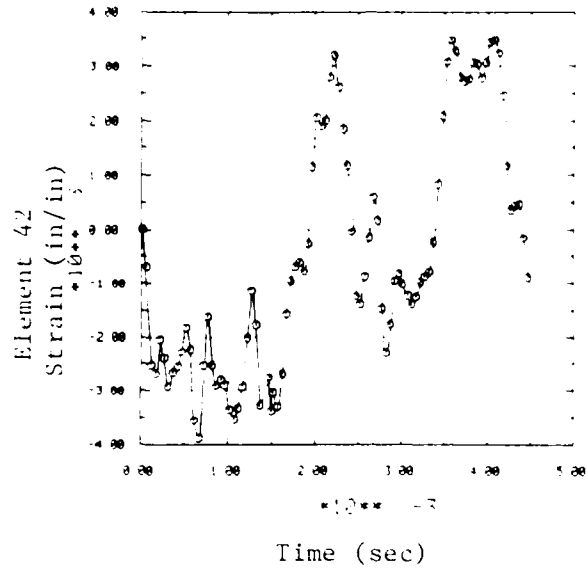
41
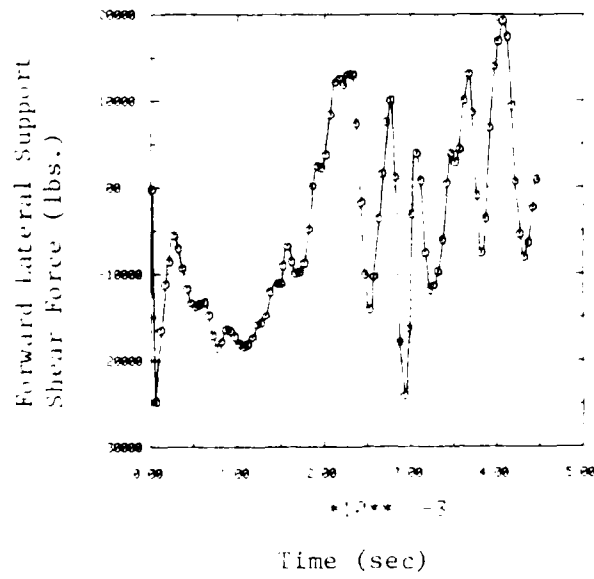
Figure 17. Shear Forces at Rocket/Tube Assembly-
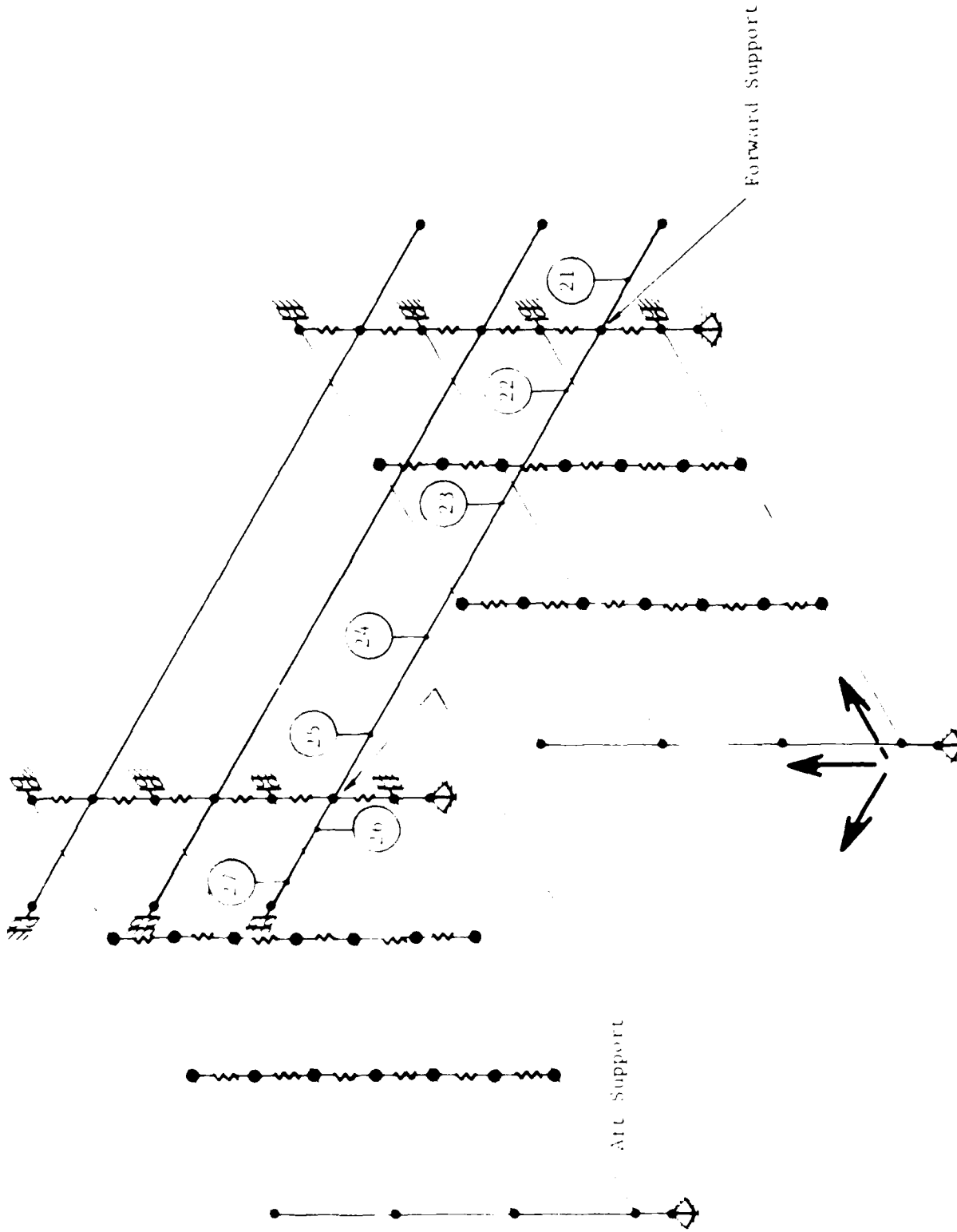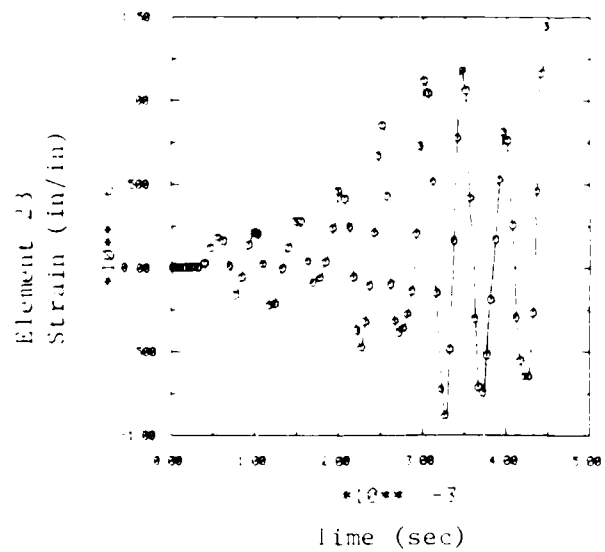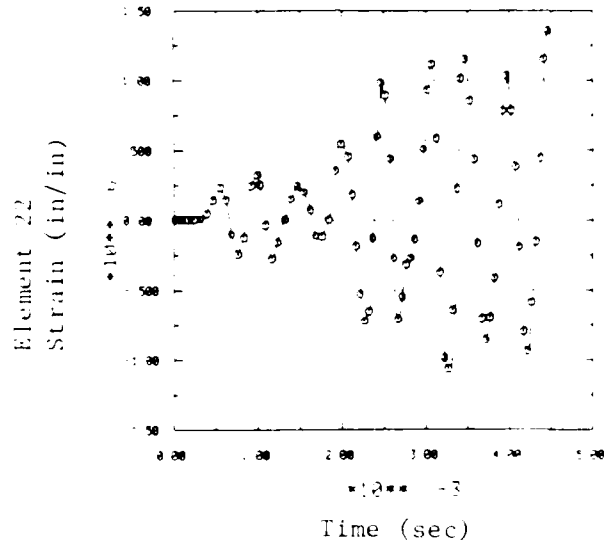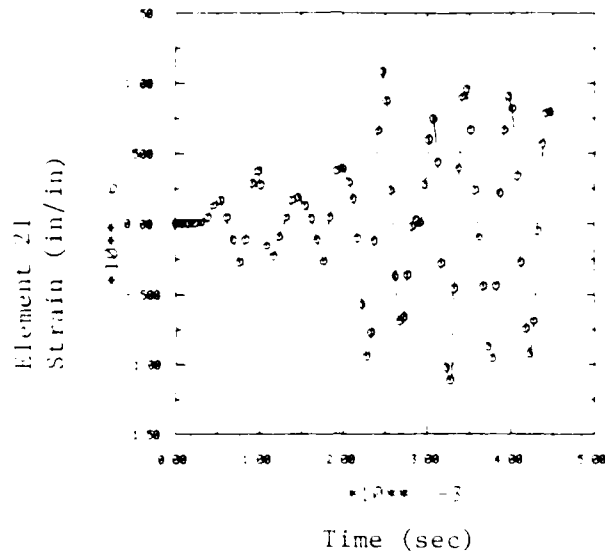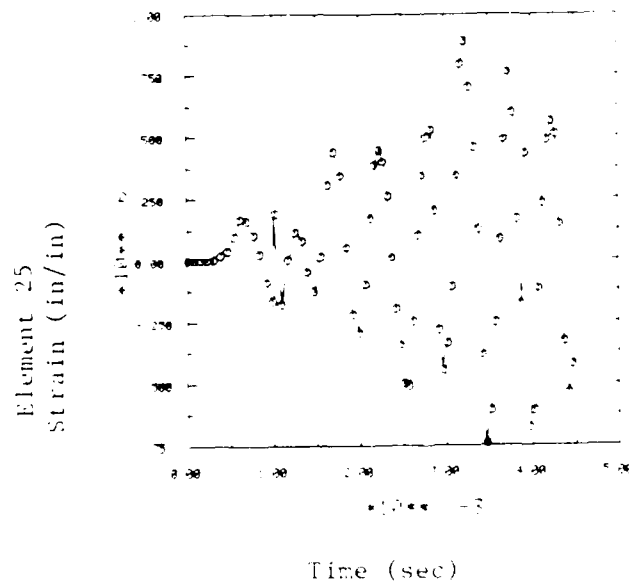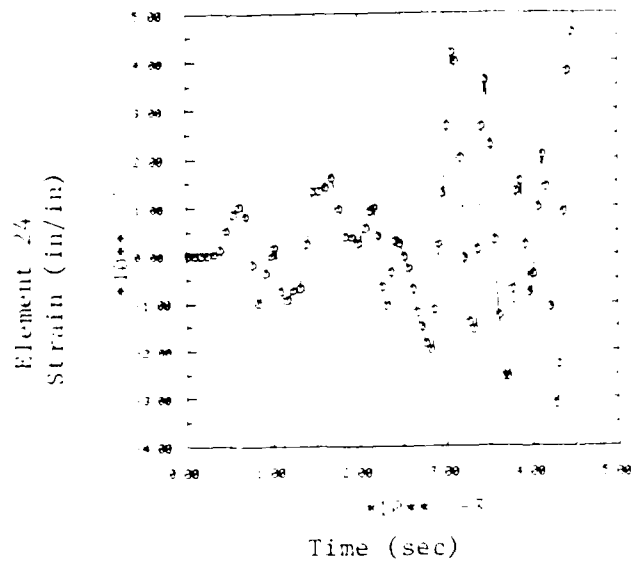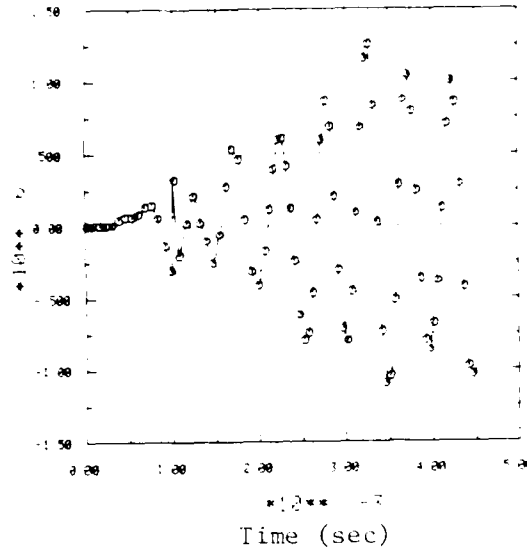Lateral Support Junction (lateral
impact from 40 feet)

Figure 15. Approximate Locations of Elements for Which Vertical Impact Strain Data Was Plotted.

Forward Support

Aft Support

53

Figure 19. Strains in M55 Rocket Undergoing Vertical
Impact (from 40 feet)

Element 24
Strain (in/in)

Time (sec)

Element 25
Strain (in/in)

Time (sec)

Figure 19. (cont'd) Strains in M55 Rocket Undergoing
Vertical Impact (from 40 feet)

45
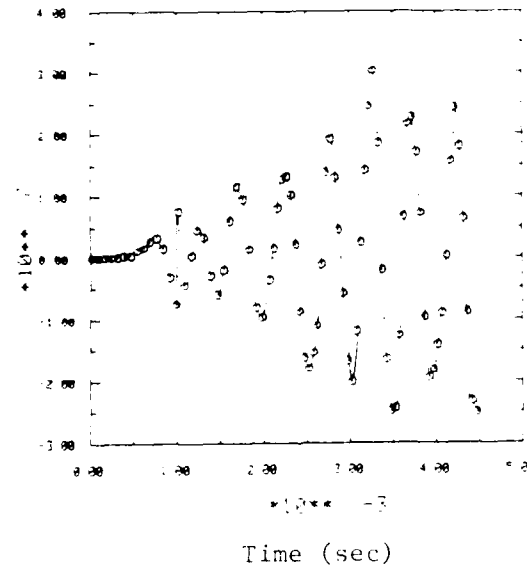
Figure 19. (cont'd) Strains in M55 Rocket Undergoing
Vertical Impact (from 40 feet)
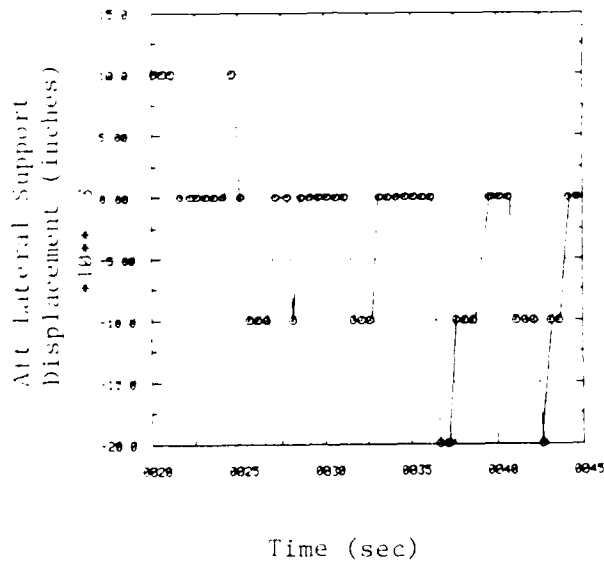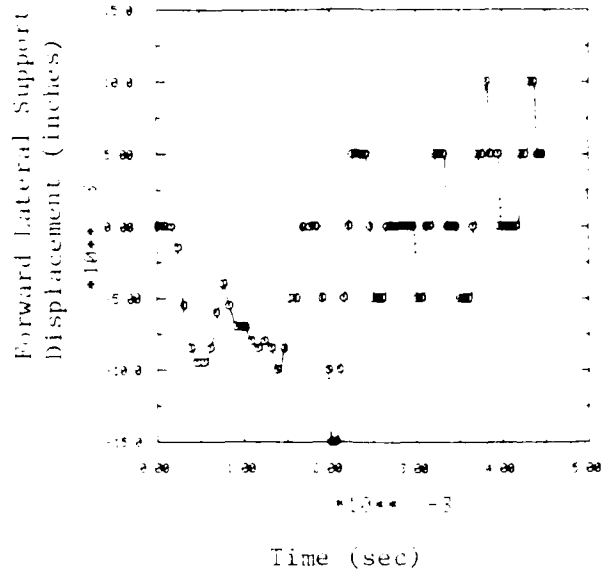
Figure 20. Net Crushing Displacement at Rocket/Tube
Assembly-Lateral Support Junction
(vertical impact from 40 feet)

47

this deflection is not sufficient to cause contact between the support and the impact surface.

Crushing at the rocket tube-support junction also was not sufficient to cause failure in the agent cannister. In fact, yielding of the cross section is not expected for this loading scenario. Figure 20 shows the net crushing displacements at the forward and aft support junctions on the bottom M55 rocket. (Flat regions in these plots were caused by round-off error during plotting of the results. Actual displacement variations occur in this region, but were quite small). Maximum displacement occurs at the aft support and equals 0.02 inches, approximately. From the quasi-static crushing analysis, it was calculated that diametral crushing displacements exceeding 0.18 inches were necessary to induce cannister failure, i.e., cannister strains greater than 4%. The superposition of bending and crushing strains result in a total strain much less than 4%. Therefore, it is considered that cannister leakage is unlikely to be caused by this impact.

3.4 Concluding Remarks

Overall, it should be noted that the analysis methodology is somewhat conservative, particularly because of the assumption that impact surfaces are perfectly rigid. Actual surfaces, and the CAMPACT structure also, will absorb impact energy, thereby reducing cannister strains. Conversely, it must not be forgotten that the rocket structure was idealized in these analyses: aging effects, corrosion, casting, or welding flaws are not assessed or accounted for. Because these latter effects will tend to induce leakage, at lower than expected drop heights, results presented here must be used carefully, assessed in the light of past experience, and compared with actual test data wherever possible.

4.0 REFERENCES

1   Cox, P.A., Pomerening, D.J., "Impact Analysis of the JAMPACT Shipping
    Container," SwRI Report 06-8461, May, 1985.

2   Bathe, K-J, Finite Element Procedures in Engineering Analysis,
    Prentice-Hall, Englewood, Cliffs, 1982.

3   "ADINA: A Finite Element Program for Automatic Dynamic Incremental
    Nonlinear Analysis, (User's Manual)," Report AE 81-1, Adina
    Engineering, Inc., September, 1981.

4   Moore, T.D., ed., Structural Alloys Handbook, Mechanical Properties
    Data Center, 1975.

5   Drawing No. E90-1-21, "Rocket Practice, 115mm, Simulant, EJ, M61
    (assembly)," Department of the Army Chemical Corps, February 21, 1958.

6   Patel, M.R., Finnie, I., "Structural Features and Mechanical Properties
    of Rigid Cellular Plastics," Journal of Materials, JMLSA, Vol. 5, No.
    4, December 1970.

7   Siliva, P.A., Scott, R.J., Michalopolous, C., "Small Craft
    Engineering: Structures," Department of NAME, Report No. 121,
    University of Michigan, 1971.

8   U.S. Department of Agriculture, Wood Handbook (Handbook No. 72), U.S.
    Government Printing Office, Washington, D.C., 1955.

9   Bodig, J., and Jayne, B.A., Mechanics of Wood and Wood Composites, Van
    Nostrand Reinhold, New York, 1982.

Appendix A

Calculations Associated with Longitudinal Impact Analysis

PROJECT NO. 06-8461-001   SPONSOR: H&R
SUBJECT Pallets
BY: SES   DATE: 12MAX 19 85   CHECKED BY: _____ DATE CHECKED _____ 19

22-141 50 SHEETS
22-142 100 SHEETS
22-144 200 SHEETS

References cited frequently in this calculations are

1. Bodig, J. and Jayne, B.A. _Mechanics of Wood Composites_,
   Van Nostrand, New York, 1982.

2. U.S. Department of Agriculture, _Wood Handbook_, Forest Products
   Laboratory Handbook No. 72, 1955.

3. Drawings cited are of the M55 pallet and wing for 5 chemical
   pallets, Army Material Corps Drawings C-20-6-62 through
   C-20-6-69, 1960.

4. Roark, R.J. _Formulas for Stress and Strain_, 5th
   Edition, McGraw-Hill, 1975.

5. Blevins, R.D. _Formulas for Natural Frequency and Mode Shape_,
   Van Nostrand-Reinhold, New York, 1979.

PROJECT NO. 06-8461-001   SPONSOR. H&R
SUBJECT Long't'l Impact
BY SES   DATE 25 FEB 19 85   CHECKED BY ____ DATE CHECKED ____ 19 ...

I Determine Effective Areas for Burster-Agent Cannister Elements

Dimensions and properties of burster casing
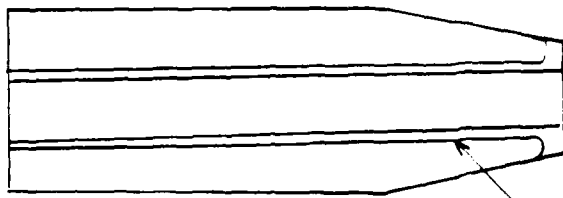
idealized as tube for entire warhead length

Burster Casing (FM34 region)

D_i 1.740 in

$t = 0.034$ in

Take as 6061-T6 aluminum
$\sigma_y = 38.8 \cdot 10^3 \; lb/in^2$
$\sigma_u = 42 \cdot 10^3 \; lb/in^2$
$E = 10 \cdot 10^6 \; lb/in^2$

Ref. D90-2-63

JF Analysis / SwRI

Agent Cannister (Cylindrical Region)

$D_o = 4.442$ in

$t = 0.0578$ in

take as 6061-T6 aluminum

$\sigma_y = 38.8 \cdot 10^3 \; lb/in^2$

$\sigma_u = 42 \cdot 10^3 \; lb/in^2$

Ref. D-90-2-63

PROJECT NO. _____ SPONSOR: _____
SUBJECT: Long'l Impact: Burster + Cannister Composite
BY _____ SES _____ DATE: 15 FEB 19 85 CHECKED BY: _____ DATE CHECKED: _____ 19 ___

Cross section area and area moment of inertia: (burster)

$$A_{burster} = \pi \left[\left(\frac{D_i + 2t}{2}\right)^2 - \left(\frac{D_i}{2}\right)^2 \right] = 0.189 \text{ in}^2$$

$$I_{burster} = \frac{\pi}{4} \left[\left(\frac{D_i + 2t}{2}\right)^4 - \left(\frac{D_i}{2}\right)^4 \right] = 0.0746 \text{ in}^4$$

Cross section area, moment of inertia: (cylindrical agent cannister)

$$A_{agent} = \pi \left[\left(\frac{D_0}{2}\right)^2 - \left(\frac{D_0 - 2t}{2}\right)^2 \right] = 0.796 \text{ in}^2$$

$$I_{agent} = \frac{\pi}{4} \left[\left(\frac{D_0}{2}\right)^4 - \left(\frac{D_0 - 2t}{2}\right)^4 \right] = 1.913 \text{ in}^4$$

composite area, moment of inertia (prismatic region of agent cannister

$$A_{total} = A_{burster} + A_{agent} = 0.9851 \text{ in}^2$$

$$I_{total} = I_{burster} + I_{agent} = 1.9876 \text{ in}^4$$

let $D_0 = 4.442$ in for composite

$$D_i = 2 \left[-\frac{A_{total}}{\pi} + \left(\frac{D_0}{2}\right)^2 \right]^{1/2} = 4.298 \text{ in}$$

PROJECT NO _____ SPONSOR _____
SUBJECT _____
BY _____ DATE: _____ 19 _____ CHECKED BY _____ DATE CHECKED ____ 19

In the tapered region- composite of insert, cannister and burster casing is represented by 2 finite elements

Element Nodes	Area based on Average Diameter Btwn Nodes	Area of Burster	Total Area
9-10	.5970 in²	.189 in²	0.7860 in²
10-11	.797	.189	0.9187 in²

Element Nodes	Average O.D. Btwn Nodes	I.D. Necessary to Achieve Total Area in Composite Element
9-10	3.350 in	3.197 in
10-11	4.077	3.931
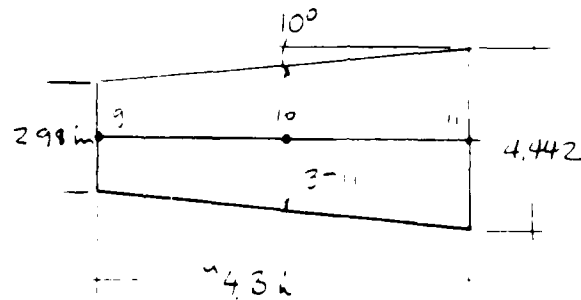
PROJECT NO _____ SPONSOR _____
SUBJECT _____
BY _____ DATE: _____ 19 ____ CHECKED BY _____ DATE CHECKED ____ 19 ___

22:141 50 SHEETS
22:142 100 SHEETS
22:144 200 SHEETS

AMPAD

Summary of Results for Composite Burster and Agent Casing Elements

Element Between Node Numbers	Total or Composite Area (in)²	O.D. of Element	I.D. of Element
9-10	.7860	3.350	3.197
10-11	.9187	4.077	3.931
11-12	.9851	4.442	4.298
12-13	.9851	4.442	4.298
13-14	.9851	4.442	4.298
14-15	.9851	4.442	4.298
15-16	.9851	4.442	4.298
16-17	.9851	4.442	4.298
17-18	.9851	4.442	4.298
18-19	.9851	4.442	4.298

PROJECT NO _____ SPONSOR _____
SUBJECT _____
BY _____ DATE _____ 19 CHECKED BY _____ DATE CHECKED _____ 19

II. Longitudinal-Impact Model, Longitudinal Natural Frequencies

$$f_i = \frac{\lambda_i}{2\pi L}\left[\frac{E}{\mu}\right]^{\frac{1}{2}}, \quad i = 1, 2, 3, \ldots$$

$$L = 72.208 \text{ in}$$

$$E = 10 \times 10^6 \frac{lb}{in^2}$$

$$\mu = \frac{57 \, lbs}{\left[\frac{\pi}{4}(4.442^2 - 4.325^2) - .223\right]in^3} = \frac{0.303 \, lb}{386 \frac{in}{s^2}}$$

$$= 2.560 \, \sigma^3 \, \frac{lb\text{-}s^2}{in^4}$$

for fixed-free B.C.'s

$$\lambda_i = \left(\frac{2i-1}{2}\right)\pi \qquad i = 1, 2, 3, \ldots$$

$$\lambda_1 = 1.571$$

$$\lambda_2 = 4.712$$

$$\lambda_3 = 7.854$$

$$\lambda_5 = 11.00$$

Reference R.D. Blevins, _Formulas for Natural Frequency and Mode Shape_, Van Nostrand, New York, 1979.

hence,

$$f_1 = 216.4 \text{ Hz}$$

$$f_2 = 679.2$$

$$f_3 = 042$$

$$f_4 \quad 1515$$

PROJECT NO _____ SPONSOR: _____

SUBJECT _____

BY ___SES___ DATE 12 MAR 19 65 CHECKED BY: _____ DATE CHECKED ___ 19 __

III Buckling Analysis of longitudinal Rocket Impact Case
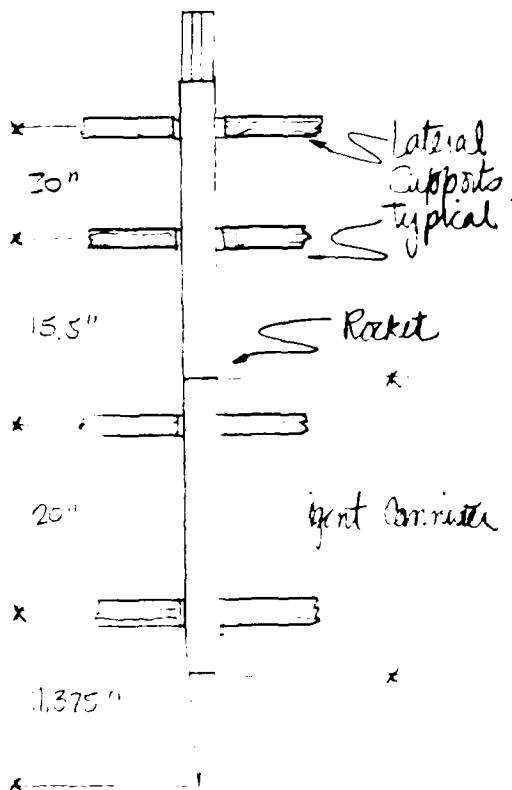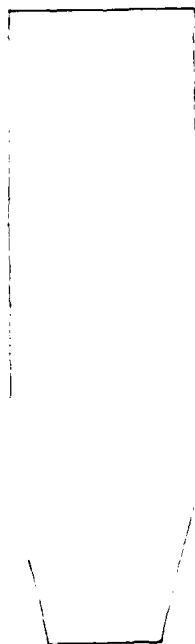
- Lateral Supports, Typical
- 30"
- 15.5"
- Rocket
- 20"
- Vent Barrisette
- 1.375"

We consider first the simple Euler beam problem, assuming
the agent cannister can be considered as a uniform beam
We ignore the effect of the launching tube and the water
on bending stiffness to obtain preliminary, conservative results.

from Blevins,

$$P_{cr} = \frac{\pi^2 E I}{L^2}$$

$$= \frac{\pi^2 \cdot 10 \times 10^6 \frac{lb}{in^2} \cdot 1.919 \, in^4}{(20 in)^2}$$

$$P_{cr} = 473494 \, lb$$

$E_{al} = 10 \cdot 10^6 \, lb/in^2$

$D_0 = 4.442 \, in$

$D_i = 4.326 \, in$

$I_{al} = 1.9 \quad in^4$
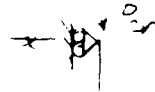
assume this force acts uniformly over cross sectional area

$$A_{cannister} = \frac{\pi}{4}\left(4.442^2 - 4.326^2\right) \quad (\text{ignoring both in})$$

$$A_{cann} = 0.7988 \, in^2$$

$$\sigma_{cr} \equiv \frac{P_{cr}}{A_{cann}} = \frac{473494 \, lb}{0.7988 \, in^2} = \underline{592743 \frac{lb}{in^2}}$$

Note: $\sigma_{cr} > \sigma_{yield}$

Now consider local circumferential buckling modes of the
repair cannister since the influence of the internal
fluid on the buckling characteristics.

from Roark, for a long thin walled circular tube, ends
not constrained, under uniform longitudinal pressure:

actual canister → model

$E_{al} = 10 \times 10^6$

$D_0 = 4.442$ in , $r = 2.221$ in

$t = 0.0578$

$v = 0.3$
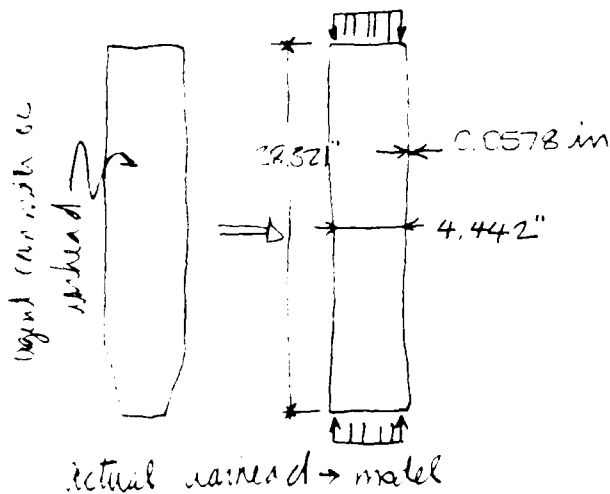
$$^2\sigma_{theo} = \frac{1}{\sqrt{3}} \frac{E_{al}}{\sqrt{1-v^2}} \frac{t}{r} \quad , \quad for \quad \frac{r}{t} > 10 \ \ \& \ \ L >> 1.72 \sqrt{rt}$$

$$= \frac{1}{\sqrt{3}} \cdot \frac{10 \cdot 10^6 \frac{lb}{in^2}}{[1-0.3^2]^{\frac{1}{2}}} \cdot \frac{0.0578 \, in}{2.221 \, in}$$

$$^2\sigma_{theo} = 157506 \frac{lb}{in^2}$$

PROJECT NO   SPONSOR
SUBJECT
BY LES   DATE 3 MAR 19 85   CHECKED BY _____   DATE CHECKED ___ 19

to account for out-of-roundness and material imperfections take

$$^2\sigma_{cr} = 0.40\ ^2\sigma_{theo} \quad [\text{as recommended in Rork}]$$

$$^2\sigma_{cr} = 5002 \frac{lb}{in^2}$$

$$\frac{r}{t} = \frac{2.221}{0.0578} = 38 >> 10 \qquad OK$$

$$L = 28.321 in >> 1.72\sqrt{2.221 in \cdot 0.0578 in} = 0.616 in \quad OK$$

note $^2\sigma_{cr} > \sigma_{yield}$

consider also the tapered section of the canister,

if it is assumed that the ends are held circular then the critical axial +66 in buckling load is,
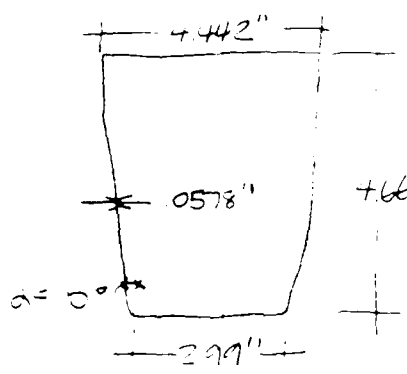
$$\sigma_{cr} = \frac{\pi E_{al} \, t^2 \cos^2 \alpha}{\sqrt{3(1-\nu^2)}} \quad , \quad \frac{R_e}{t} > 10$$

$E_{al} = 10 \times 10^6 \frac{lb}{in^2}$ $\qquad \nu = 0.3 \qquad t = 0.0578$

$\alpha = 10°$ $\qquad A_{zp} = \pi(R^2 - (R_T - t)^2) = .7961$

$R_T = 4.442 \, in$

$2 R_B = 2.99 \, in$

$$\sigma_{cr} = \frac{2\pi \cdot 10 \times 10^6 \frac{lb}{in^2} \, (0.0578 \, in)^2 \, (\cos^2 10°)}{\left[3 \cdot (1 - 0.3^2)\right]^{1/2}}$$

$$P_{cr} = 124030 \, lb$$

take as, $\sigma_{theo} = P_{cr}/A_{zp} = \frac{124030 \, lb}{.7961 \, in^2} = 154771 \frac{lb}{in^2}$

account for out-of-roundness, etc.

$$\sigma_{cr} = 0.37 \, \sigma_{theo} \qquad \left[\text{as recommended by Roark}\right]$$

$$\sigma_{cr} = 57265 \frac{lb}{in^2}$$

PROJECT NO _____ SPONSOR _____

SUBJECT _____

BY _____ DATE: ____ 19 ____ CHECKED BY _____ DATE CHECKED ____ 19

22-141 50 SHEETS
22-142 100 SHEETS
22-144 200 SHEETS

Now consider local beam-like and circumferential buckling of
the Twister casing
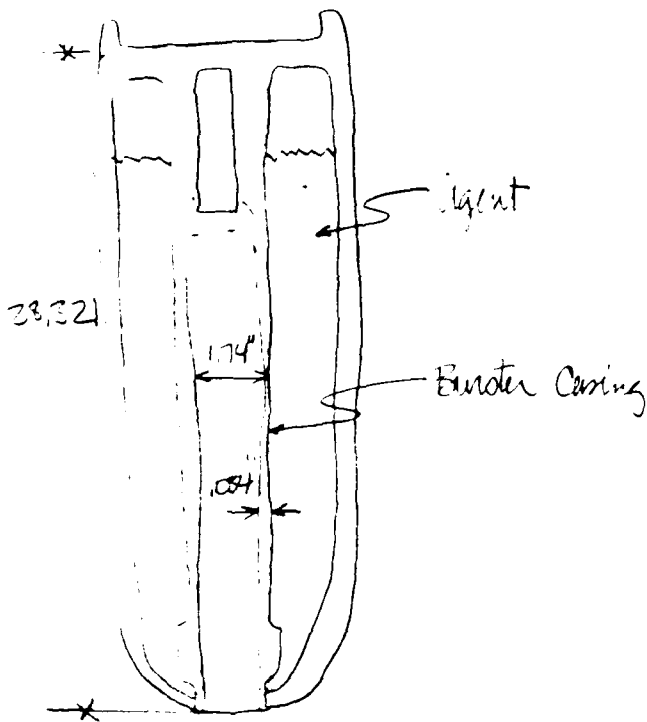
Actual Bulkhead

Model for Twister
Buckling (Euler Beam)

$E_{al} = 10 \times 10^6 \frac{lb}{in^2}$

$D_i = 1.74$ in

$t = 0.034$ in

$L = 38.321$ in

$I_{area} = 0.07457$ in^4

$A_{booster} = .1895$ in^2

from Roark,

$$P_{cr} = \frac{\pi^2 EI}{L^2} = \frac{\pi^2 \cdot 10 \cdot 10^6 \frac{lb}{in^2} \cdot 0.07457 \, in^4}{(38.321 \, in)^2}$$

$$P_{cr} = 9175 \, lb$$

Now

$$\sigma_{theo} = \frac{P_{cr}}{A_{booster}} = \frac{9175 \, lb}{.1895 \, in^2} = 48420 \frac{lb}{in^2}$$

PROJECT NO _____ SPONSOR _____
SUBJECT _____
BY ___SES___ DATE 2 MAR 19 65 CHECKED BY _____ DATE CHECKED 19

22 141 50 SHEETS
22 142 100 SHEETS
22 144 200 SHEETS

Summary of Buckling Results for Longitudinal Impact

Case	Mode Description	Theoretical Buckling Value	Included Buckling Value	Remarks
1	Column mode buckling of agent (annular) between lateral supports (acts as free-free beam)	192,143 psi	same	Actual B.C.'s unknown theoretical value >>> yield aluminum
2	Circumferential buckling of agent approximated as uniform beam	157,616 psi	63,412 psi	Buckling value may be lower if uniform beam assumption is unconservative
3	Circumferential buckling of tapered section of agent (annular, acting as annular ring)	169,171 psi	57,265 psi	Actual B.C.'s unknown
	Circumferential buckling of agent inside ring (acts as free ring)	...	...	actual B.C.'s unknown, the clamped end effects if more fully more taken into ... direct B.C. value is probably a conservative ...

* Because this value is less than that computed for annular columns, buckling of agent annular (case 1-3) this is taken as the governing critical stress for buckling of unstiffened ...

PROJECT NO _____ SPONSOR _____
SUBJECT _____
BY E̅   DATE 25114/09   CHECKED BY _____ DATE CHECKED   19

IV. Characteristics of "Interaction" Model (CAMPACT impact effects)

Estimate the added weight for pallet interaction and estimate

  — In the CAMPACT there are eight pallets arranged as shown

ends of pallets
(6 rockets/
pallet)
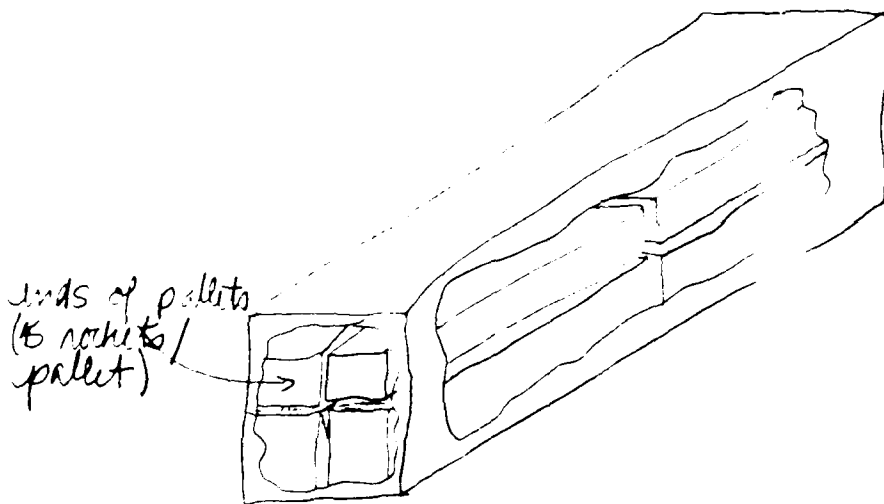
  for an __end__ campact impact we assume
that $\dfrac{1}{4 \times 15} \cdot A_{\substack{campact\\end}}$

acts in initiating motion of one rocket and
that each rocket sees its own weight plus
$\frac{1}{5}$ of the pallet to which it belongs (less rocket
weights) plus $\frac{1}{5}$ of the pallet above it
during impact. That is,

PROJECT NO _____ SPONSOR _____
SUBJECT _____
BY _____ DATE ____ 19 __ CHECKED BY _____ DATE CHECKED ____ 19 __

22-141 50 SHEETS
22-142 100 SHEETS
22-144 200 SHEETS

proposed the following model

Rocket FE model

$$\frac{1}{15}\left[W_{pallet} + \{W_{pallet} - 15\,W_{rocket}\}\right]$$

spring representing foam properties under crushing and an impact area $\frac{1}{60} A_{2nd\ impact}$
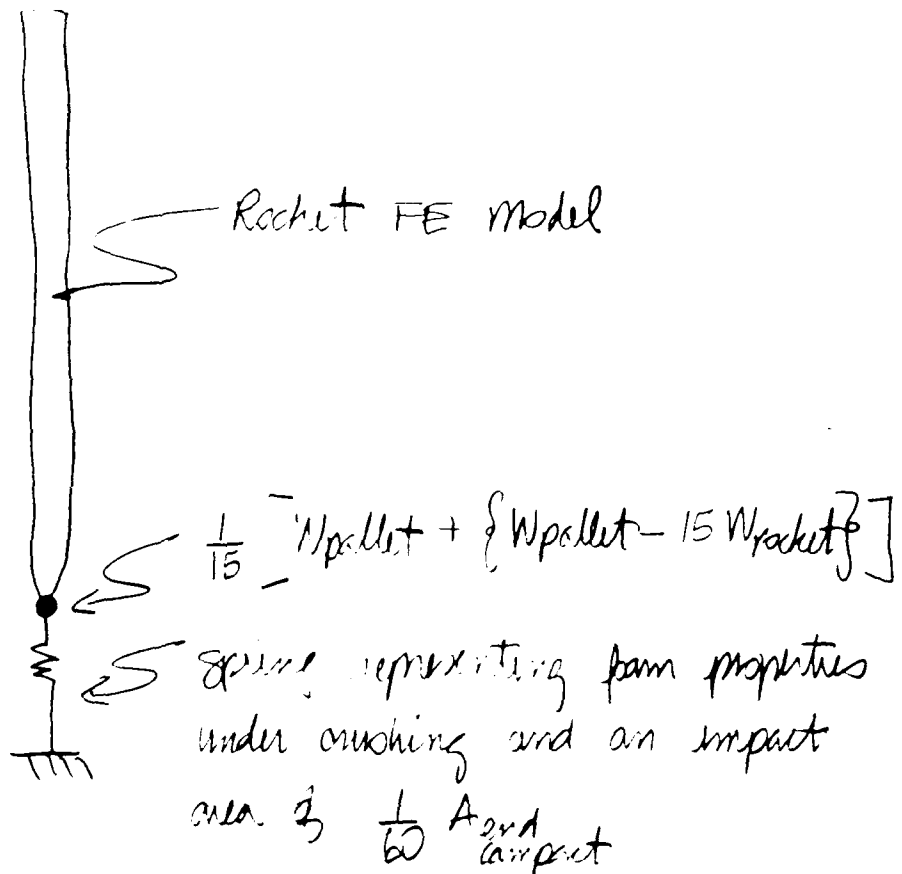
The concentrated mass is at the nose of the rocket because it is assumed no pallet loads pass through rocket, but through pallet elements a launching tubes only.

PROJECT NO _____   ?ONSOR _____
SUBJECT _____
BY _____   DATE ____ 19 _____ CHECKED BY _____   DATE CHECKED   19

The concentrated mass is,

$$W_{con} = \frac{1}{15} \left[350 \text{ os} - \left[1350 \text{ lb} - (15 \times 57 \text{ lbs}) \right] \right] \cdot \frac{1}{386.4} \frac{\text{sec}^2}{\text{in}}$$

$$N_{con} = \frac{23 \text{ lb-sec}^2}{386.4 \text{ in}}$$

$$W_{con} = 0.3183 \frac{\text{lb-sec}^2}{\text{in}}$$

PROJECT NO _____ SPONSOR _____
SUBJECT _____
BY _____ SES _____ DATE 23MAR 19 S5   CHECKED BY _____   DATE CHECKED ____ 19

Compute characteristics of foam spring to estimate
interaction effects between rockets and foam.

Based on work done by Sam Romesburg we adopt an
element that is 36 inches long and has the following
cross-sectional area.

                                          ends of pallets
                                          40 rocket ends =
                                          4 pallets / 15 rockets/pallets
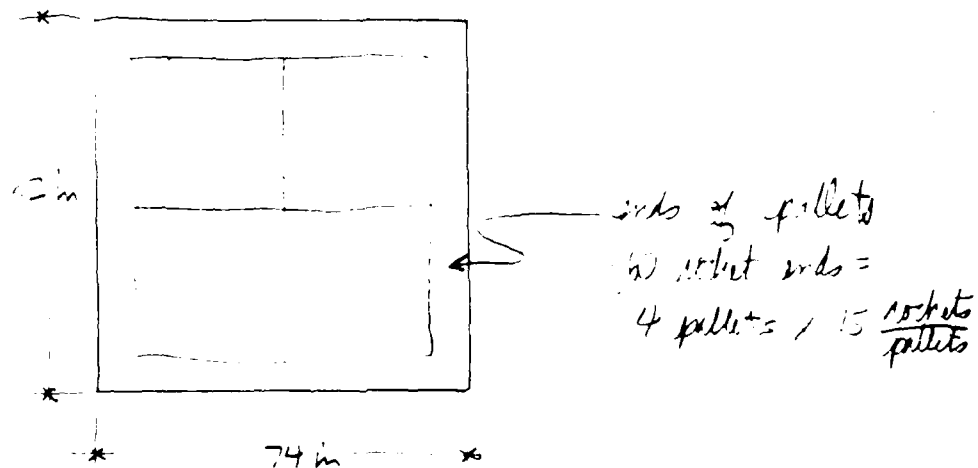
                    74 in

foam area of end of IMPACT

take as cross section area of foam "spring element" = $\frac{1}{60} \times 62" \times 74 \, in$

                                        = .01 in²

take as length = 36 in.

stress-strain characteristics of foam spring
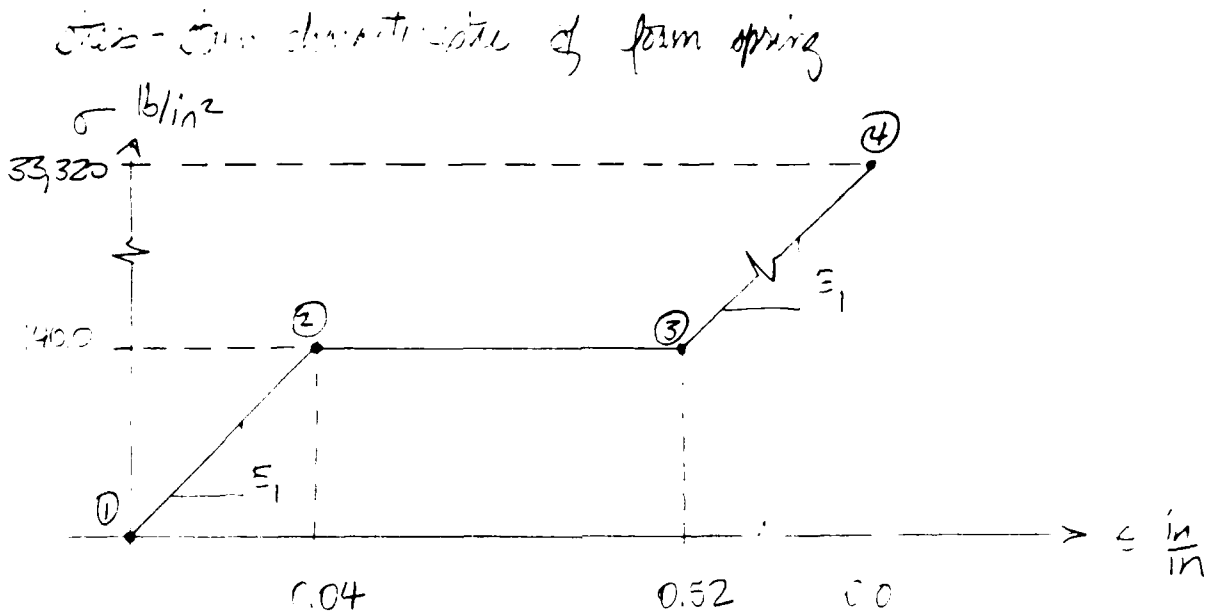
stress-strain points

	ϵ	σ
①	0.0	0.0
②	0.040	140.0
③	0.520	140.0
④	10.000	33320 lb/in²

Appendix B

Calculations Associated with Lateral Impact Analysis

PROJECT NO. 06-8461-001   SPONSOR: H&R
SUBJECT: Pallets
BY SES   DATE: 12 MAR 19 85   CHECKED BY: _____ DATE CHECKED: _____ 19
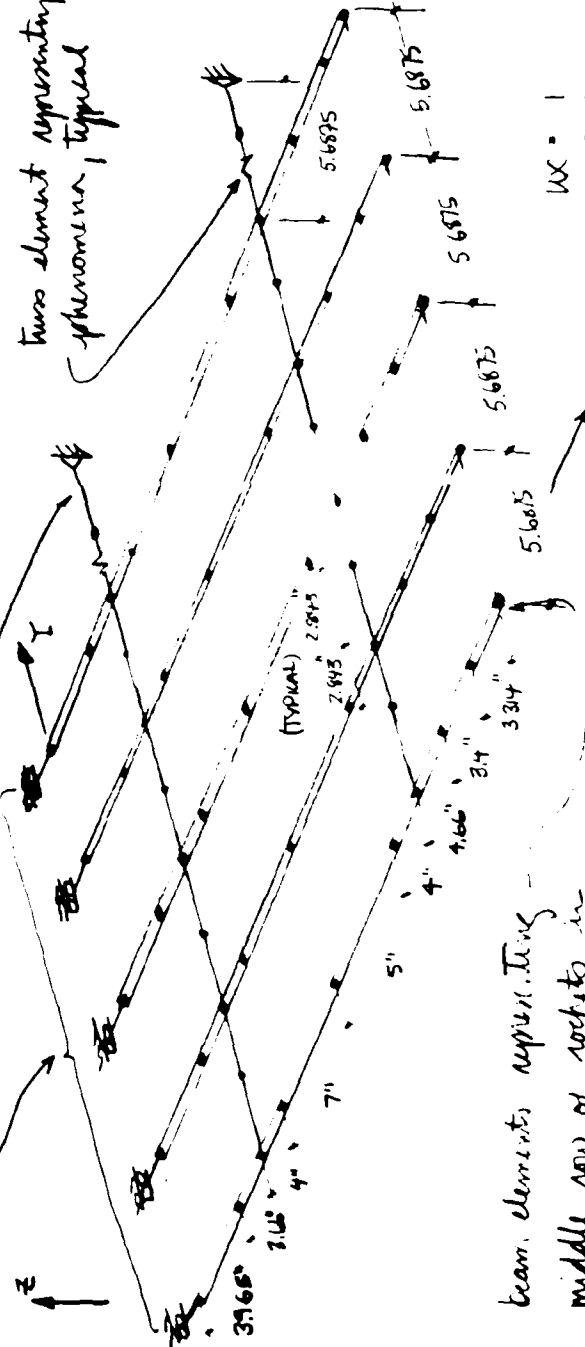
22-141 50 SHEETS
22-142 100 SHEETS
22-144 200 SHEETS

References cited frequently in this calculations are

1. Bodig, J. and Jayne, B.A. <u>Mechanics of Wood Composites</u>, Van Nostrand, New York, 1982.

2. U.S. Department of Agriculture, <u>Wood Handbook</u>, Forest Products Laboratory Handbook No. 72, 1955.

3. Drawings cited are of the M55 rocket & ring for 15 chemical rockets, Army Chemical Corps Drawing D-30-6-62 through D-30-6-69, 1960.

4. Roark, R.J <u>Formulas for Stress and Strain</u>, 5th Edition, McGraw-Hill, 1975.

5. Blevins, R.D. <u>Formulas for Natural Frequency and Mode Shape</u>, Van Nostrand-Reinhold, New York, 1979.

PROJECT NO. 06-8461-001   SPONSOR H&R

SUBJECT Lateral Impact

BY SES   DATE 16 FEB 19 85   CHECKED BY _____ DATE CHECKED ____ 19 ____

I. Finite Element Model

1 = Deleted DOF, 0 = Admissible DOF

PROJECT NO. _____ SPONSOR H & R

SUBJECT _____

BY SES _____ DATE 15 MAY 19 85 CHECKED BY _____ DATE CHECKED ___ 19

NODE NUMBERING

concentrated mass, typical

3 GROUPS OF ELEMENTS   NONLINEAR SPRING   (TRUSSES)
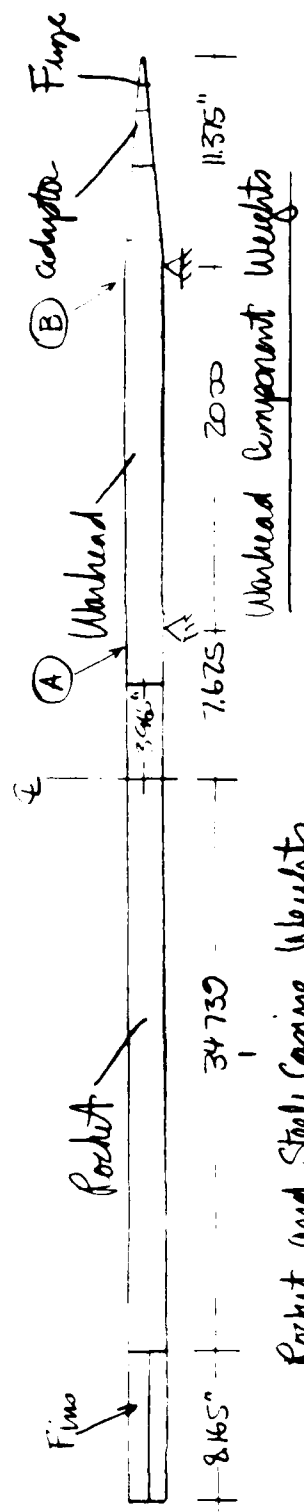
AXIAL SADDLES   (TRUSSES)

ROCKET BEAMS   (BEAMS)

PROJECT NO.: CF-8461-001 SPONSOR: H&R

SUBJECT: Lateral or Vertical Impact Model

BY: SES DATE: 6 FEB 19 85 CHECKED BY: ___ DATE CHECKED: ___ 19 ___

Warhead Component Weights

$$\text{Agent Weight} = 0 \text{ lbs}$$
$$\text{Burster Casing} = 0.4 \text{ lbs}$$
$$\text{Cammrdt Casing} = 12.21 \text{ lbs}$$
$$\text{Fimoton Agent} = \underline{2.9 \text{ lbs}}$$
$$15.51 \text{ lbs}$$

Adapter Component Weights

$$\text{Casing Weight} = 1.221 \text{ lbs}$$
$$\text{Burster Casing} = 0.041 \text{ lb}$$
$$\text{Burster Weight} = \underline{0.31 \text{ lb}}$$
$$1.51 \text{ lb}$$

Fuze Weight
Estimated at 0.1 lb

Rocket and Steel Casing Weights

$$\text{Total Rocket Weight} = 57 \text{ lbs}$$
$$\text{Less Warhead Weight} = 15.61 \text{ lbs}$$
$$\text{Less Adapter Weight} = 1.65 \text{ lbs}$$
$$\text{Less Fuze Weight} = \underline{0.10 \text{ lbs}}$$
$$39.84 \text{ lbs}$$

Ref JF Analysis/Suki
(modified using component lengths
as found in M155 drawings)

PROJECT NO: 8461-001 SPONSOR: H&R

SUBJECT: Impact

BY: _____ DATE: 15 FEB 1985 CHECKED BY: _____ DATE CHECKED: _____ 19

adapter fuze

warhead

△ support

20"

.56" | 4" | 7" | 5" | 4.6 | 3.4" | 3.31"

Node Distribution: see pps

rocket

.3965"

Node Distribution

see pps.

Typical of all Rockets in Center Column

SOUTHWEST RESEARCH INSTITUTE
DEPARTMENT OF ENGINEERING MECHANICS
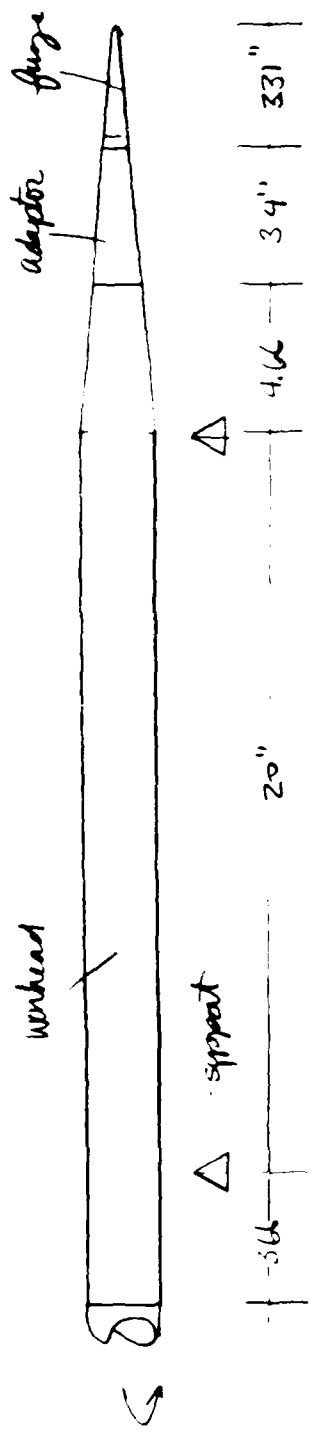COMPUTATION SHEET

SHEET NO
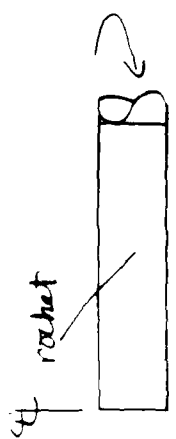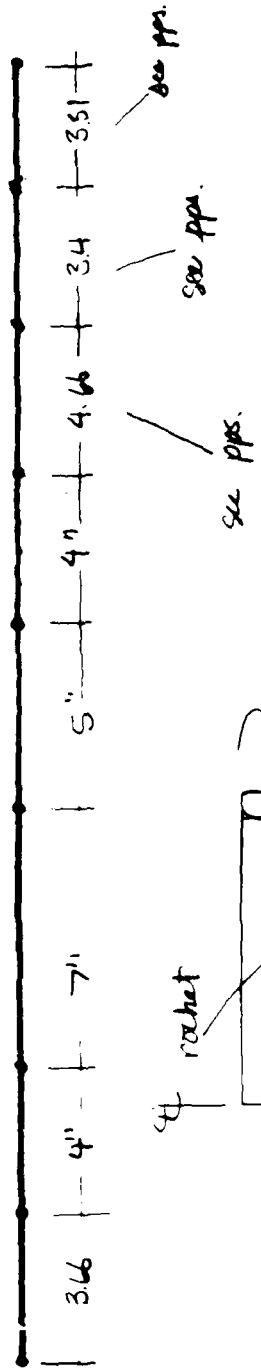65 OF B23

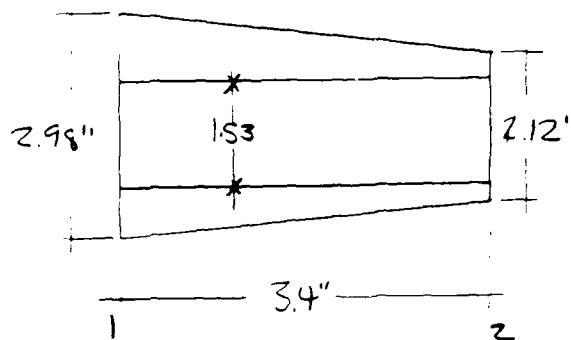PROJECT NO 06-8461-001   SPONSOR H & R
SUBJECT:
BY SES   DATE 5 MAR 19 85   CHECKED BY: DATE CHECKED   19

II Compute Properties of Rocket and Launching Tube tapered

sections:

FUZE ASS'Y (Equivalent Model)

$$1.740 \qquad .610$$

actual bore size, this region

Bore size for equivalent model determined by taking

weighted average of bore sizes on length of bore:

$$D_{i,eq} = \frac{L_1 D_1 + L_2 D_2 + L_3 D_3}{L_1 + L_2 + L_3},$$

$D_1 = 1.37 \ (avg) \qquad L_1 = 2.093$

$D_2 = .248 \qquad L_2 = 0.721$

$D_3 = .541 \qquad L_3 = 0.500$

$$\therefore D_{i,eq} = 1.0 \text{ in}$$

Representing taper section as uniform section beam with average

cross-section properties, compute average D_o

$$D_{o,eq} = \,^1 D_o + \,^2 D_o / 2$$

$$D_{o,eq} = 1.175 \text{ in}$$

PROJECT NO: 06-8461-001   SPONSOR: H&R
SUBJECT:
BY SES   DATE: 15MAR 19 85   CHECKED BY: _____ DATE CHECKED: _____ 19

ADAPTOR ASS'Y (Equivalent Model)

Compute average D_o, (assuming a uniform cylindrical section)

$$D_{o,eq} = \frac{{}^1D_o + {}^2D_o}{2}$$

$$\therefore D_{o,eq} = 2.55 \text{ in}$$

$$D_i = D_i = 1.53 \text{ in}$$

SOUTHWEST RESEARCH INSTITUTE
DEPARTMENT OF ENGINEERING MECHANICS
COMPUTATION SHEET

SHEET NO
87 of 823

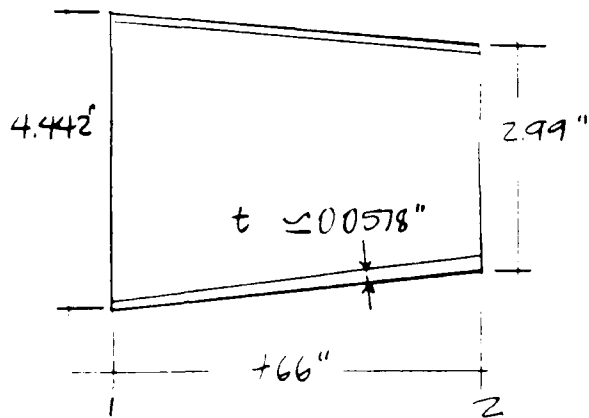PROJECT NO. CG-8461-001   SPONSOR: H & R
SUBJECT
BY SES   DATE: 15 MAR 19 85   CHECKED BY: _____   DATE CHECKED: _____ 19 ___

TAPERED WARHEAD (Equivalent Model)

Representing taper section as uniform section beam with average cross-section properties compute average D_0

$$D_{0,eq} = \frac{{}^1D_0 + {}^2D_0}{2} = 3.716 \text{ in}$$

$$D_i = D_{0,eq} - 2t = 3.6004 \text{ in}$$

SOUTHWEST RESEARCH INSTITUTE
DEPARTMENT OF ENGINEERING MECHANICS
COMPUTATION SHEET

SHEET NO
88 OF 223

PROJECT NO.: 06-8461-001   SPONSOR: H&R
SUBJECT:
BY: SES   DATE: 5 MAR 19 85   CHECKED BY: DATE CHECKED   19

22-141   50 SHEETS
22-142   100 SHEETS
22-144   200 SHEETS

AMPAD

Properties and dimensions used for warhead, rocket and fiberglass shells: (untapered sections)

	Aluminum Warhead	Steel Rocket Motor Casing	Fiberglass Launching Tube
$t =$	0.0578 in	0.096	0.195
$D_o =$	4.442 in	4.442	4.890
$D_i =$	4.3264 in	4.250	4.500
$A =$	0.7961 in^2	1.311	2.876
$I =$	1.913 in^4	3.096	7.9387

PROJECT NO. 06-8461-201   SPONSOR: H/R

SUBJECT _____

BY SES   DATE: 15MAR 19 85   CHECKED BY: _____ DATE CHECKED: _____ 19 ____

III. Compute densities for beam elements representing composite tube and rocket (center-column of rockets):

- weight of launching tube = $\left[\frac{\pi}{4} \left(D_o^2 - D_i^2 \right) \right] L \cdot \rho_{FG}$

$\rho_{FG} = 0.0525 \ lb_f / in^3$ $D_o = 4.890 \ in$

$L = 83\frac{1}{8} \ in$ $D_i = 4.500 \ in$

$W_{Tube} = 12.55 \ lbs$

Density of beams representing fuze (1 beam element)

Fuze is 3.314 in long = L

$W_{FG} = 12.55 \ lbs \cdot \dfrac{3.314 \ in}{83.125 \ in} = 0.500 \ lb$

$W_{FUZE} = 0.10 \ lb$

$D_{o, eq} = 1.175 \ in$

$D_{i, eq} = 10 \ in$

$\rho_{al} = \dfrac{W_{FUZE}}{\frac{\pi}{4} \left\{ D_{o, eq}^2 - D_{i, eq}^2 \right\} \cdot L g} = 0.0002615 \ \dfrac{lb \cdot s^2}{in^4}$

PROJECT NO.: 06-8461-001   SPONSOR: I&R

SUBJECT: _____

BY SES   DATE: 15 MAR 19 85   CHECKED BY: _____   DATE CHECKED: _____ 19 ____

Density of beams representing adaptor (1 beam element)

$L = 34$ in

$D_{o_{eq}} = 2.55$

$D_{i_{eq}} = 1.53$

$W_{adapt} = 1.55 \text{ lb}$

$$\rho_{eq} = \frac{+ W_{adapt}}{\frac{\pi}{4} \{ D_{o_{eq}}^2 - D_{i_{eq}}^2 \} L g} = .00036 1 \frac{lb\text{-}s^2}{in^4}$$

Density of beams representing warhead taper section (1 element)

$L = 4.66$ in

$L_{warhead} = 28.321$ in

$W_{warhead} (total) = 15.51 \text{ lbs}$

$$W_{warhead + agent} = W_{warhead}(total) \cdot \frac{L}{L_{warhead}} = 2.55 \text{ lb}$$

$D_{o_{eq}} = 3.716$ in $D_{i_{eq}} = 3.6004$ in

$$\rho_{eq} = \frac{W_{warhead + agent}}{\frac{\pi}{4} \{ D_{o_{eq}}^2 - D_{i_{eq}}^2 \} L g} = 0.00213 \frac{lb\text{-}s^2}{in^4}$$

SOUTHWEST RESEARCH INSTITUTE
DEPARTMENT OF ENGINEERING MECHANICS
COMPUTATION SHEET

SHEET NO
B11 of 323

PROJECT NO. 06-8461-001   SPONSOR: H&R

SUBJECT:

BY SES   DATE: 15 MAR 19 85   CHECKED BY: _____ DATE CHECKED ____ 19 ___

22-141 50 SHEETS
22-142 100 SHEETS
22-144 200 SHEETS

Density of beams representing warhead, prismatic section (5 elements)

$$L_{5\ elements} = 4 + 5 + 7 + 4 + 3.66\ in = 23.66\ in$$

$$W_{warhead} = W_{warhead\,(total)} \cdot \frac{L}{L_{warhead}} = 12.96\ lb$$

$$D_{o,eq} = 4.442\ in \qquad\qquad D_{i,eq} = 4.3264\ in$$

$$\rho_{eq} = \frac{W_{warhead}}{\frac{\pi}{4}\{D_{eq}^2 - D_{ieq}^2\} \cdot L \cdot g} = .00783\ \frac{lb\ sec^2}{in^4}$$

Density of beams representing steel casing and rocket (1 element)

$$L = 3.965\ in \qquad\qquad L_{rocket} = 34.721\ in$$

$$W_{rocket\,(total)} = 39.84\ lb$$

$$W_{rocket} = W_{rocket\,(total)} \cdot \frac{L}{L_{rocket}} = 4.550\ lb$$

$$D_{o\,eq} = 4.442\ in \qquad\qquad D_{i\,eq} = 4.250\ in$$

$$\rho_{eq} = \frac{W_{rocket}}{\frac{\pi}{4}\{D_{eq}^2 - D_{ieq}^2\} \cdot L \cdot g} = .002267\ \frac{lb\ s^2}{in^4}$$

PROJECT NO __06-8461-00__   SPONSOR __H&R__
SUBJECT _____
BY __SES__   DATE __15MAR__ 19 __85__   CHECKED BY: _____   DATE CHECKED _____ 19 ____

Revised beam properties for lateral and vertical pallet model; missile properties:

Node #'s Beam #'s	Density $\frac{lb-s^2}{in^4}$	E lb/in^2	ν	D_0, D_i in	σ_y lb/in^2	E_T lb/in^2
	.002000	10·10⁶	0.3	1111,1000	38.8·10³	0.885·10⁵
	.000000	10·10⁶	0.0	255,153	38.8·10³	1.885·10⁵
	.00213	10·10⁶	0.0	3.716,3.604	38.8·10³	0.593·10⁵
	.00783	10·10⁶	0.3	4.442,4.324	38.8·10³	0.885·10⁵
	.00783	10·10⁶	0.0	4.442,4.324	38.8·10³	0.593·10⁵
	.00783	10·10⁶	0.3	4.442,4.324	38.8·10³	0.593·10⁵
	.00783	10·10⁶	0.0	4.442,4.324	38.8·10³	0.885·10⁵
	.00783	10·10⁶	0.0	4.442,4.326	38.8·10³	0.885·10⁵
	.002267	30·10⁶	0.33	4.442,4.25	30·10³	1.383·10⁵

PROJECT NO. 06-8461-001   SPONSOR: H & R

SUBJECT:

BY: SES   DATE: 15 MAR 19 85   CHECKED BY: _____   DATE CHECKED: ____ 19 ___

Pilot Model tube Properties Summary

Notes of Beam Element	Beam Element Number	Density of Compo Beam (lb-s²/in⁴)	E (lb/in²)	ν	Do, Di (h)	σ_y (lb/in²)	E_T (lb/in²)
		.000185	1.1×10^6	0.1	4.80, 4.15	$21 \cdot 10^3$	0.0
		.000135	1.1×10^6	0.1	4.80, 4.15	$21 \cdot 10^3$	0.0
		.000135	1.1×10^6	0.1	4.80, 4.15	$21 \cdot 10^3$	0.0
		.000135	1.1×10^6	0.1	4.80, 4.15	$21 \cdot 10^3$	0.0
		.000135	1.1×10^6	0.1	4.80, 4.15	$21 \cdot 10^3$	0.0
		.000135	1.1×10^6	0.1	4.80, 4.15	$21 \cdot 10^3$	0.0
		.000135	1.1×10^6	0.1	4.80, 4.15	$21 \cdot 10^3$	0.0
		.000135	1.1×10^6	0.1	4.80, 4.15	$21 \cdot 10^3$	0.0

PROJECT NO. 06-5461-001   SPONSOR H &K

SUBJECT: Lateral Impact Model

BY SES   DATE: 7 FEB 19 85   CHECKED BY: _____ DATE CHECKED: ____ 19 ___

IV Determination of properties of wooden saddle supports,
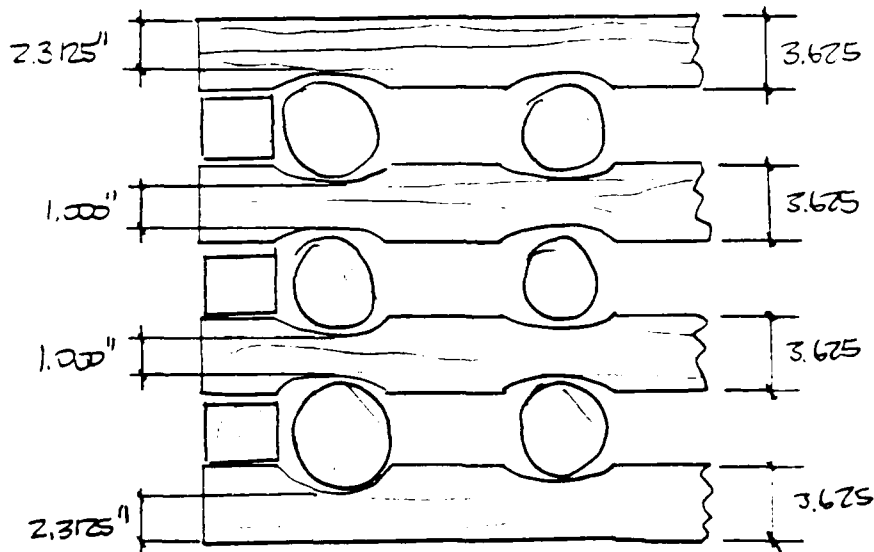
- in the lateral impact model saddle supports are assumed to sustain axial stresses only. Thus saddles are modeled as non-linear isotropic elastic plastic beams with grain (L) direction properties.

- an effective beam depth is calculated to account for variation in saddle depth along its length

- since inelastic stress-strain curves of wood are unavailable assume that $^L\epsilon_{ult} = 10 \times {}^L\epsilon_{yield}$

PROJECT NO.: QS-8451-001   SPONSOR: H4C

SUBJECT: SES

BY SES   DATE: 30 APR 19 85   CHECKED BY: _____   DATE CHECKED: _____ 19 ____

compute effective beam depth for middle saddles

area of this region ≅ 4.8 in²

3.625"   1.00"

31⅛"
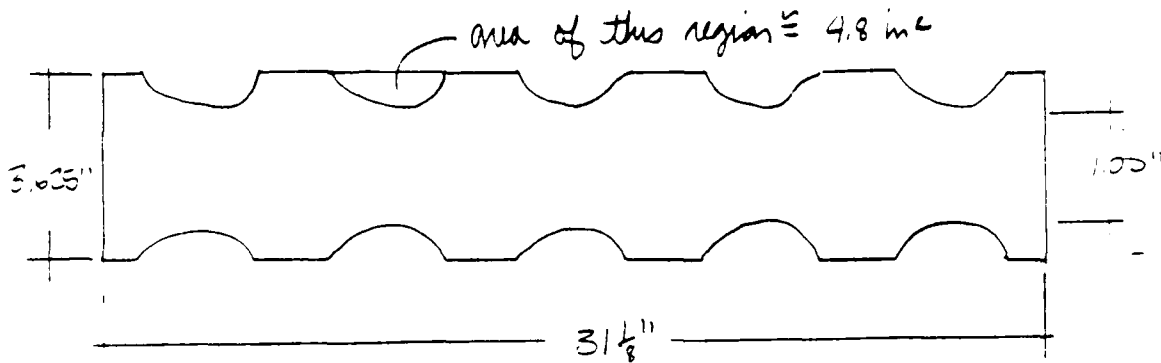
$$W_{eff} = \frac{A_{Tot}}{L} = \frac{3.625" \cdot 31.125" - (10 \cdot 4.80 \text{ in}^2)}{31.125"} =$$

$$W_{eff} = 2.08 \text{ in}$$

compute effective beam depth for upper and lower saddles

31.125

3.625"

area = 4.8 in²
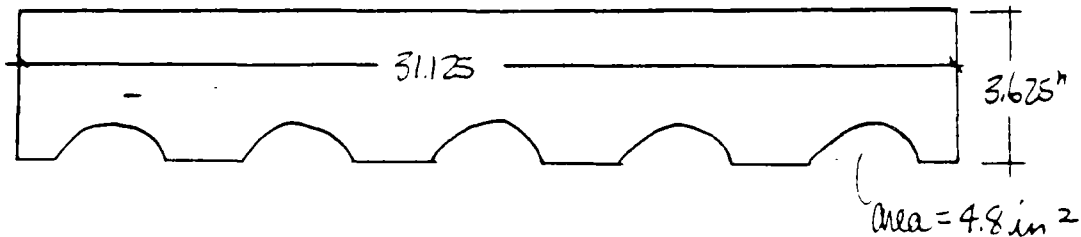
$$W_{eff} = \frac{A_{Tot}}{L} = \frac{3.625 \cdot 31.125 - (5 \cdot 4.8 \text{ in}^2)}{31.125 \text{ in}} = 2.85 \text{ in}$$

SOUTHWEST RESEARCH INSTITUTE
DEPARTMENT OF ENGINEERING MECHANICS
COMPUTATION SHEET

SHEET NO.
E_z of 323

PROJECT NO.: 06-8461-00   SPONSOR: _ _ _ R

SUBJECT: Impact Model

BY: SES   DATE: 17 FEB 9 85   CHECKED BY: _____   DATE CHECKED: _____ 19 _____

Summary of properties for saddle beam finite elements

$$E = 1.353 \cdot 10^6 \ \frac{lb}{in^2}$$

$$\nu = 0.239$$

$$D_o = 2.08 \ in$$

$$D_i = 3.625 \ in \quad (\text{width of saddle})$$

$$\sigma_y = 5700 \ \frac{lb}{in^2}$$

$$E_T = 0 \qquad lb/in^2$$

⎫ "middle 2"
⎬ saddle supports.
⎭

$$E = 1.353 \cdot 10^6 \ \frac{lb}{in^2}$$

$$\nu = 0.239$$

$$D_o = 2.85 \ in$$

$$D_i = 3.625 \ in \quad (\text{width of saddle})$$

$$\sigma_y = 5700 \ \frac{lb}{in^2}$$

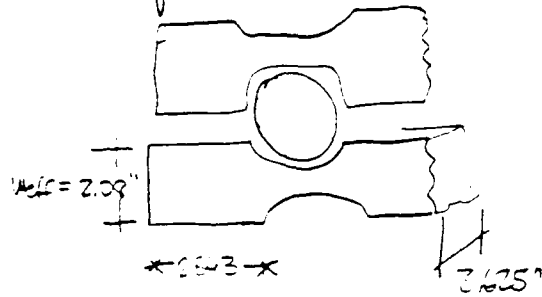$$E_T = 0 \qquad \frac{lb}{in^2}$$

⎫ upper and lower
⎬ saddle supports
⎭

PROJECT NO. 06-8461-001   SPONSOR H&R

SUBJECT _____

BY ____SES____ DATE: 15 MAR 19 85   CHECKED BY: _____ DATE CHECKED: _____ 19 ____

Ⅴ̲ ̲Concentrated̲ ̲masses̲ ̲at̲ ̲nodes̲ ̲3̲ ̲and̲ ̲7̲ ̲represent

2.843 inches of saddle beyond the first socket in

center row

$$W = \rho_{wood} \cdot L \cdot W \cdot D \cdot 2$$

(diagram with dimensions: $\text{AG} = 2.08"$, $\leftarrow 2.843 \rightarrow$, $3.625"$)

$$W = \rho_{wood} \cdot 2.843 \, in \cdot 2.08 \, in \cdot 3.625 \, in \cdot 2$$

$$W_3 = W_7 = 0.35.62 \frac{lb}{ft^3} \cdot \frac{1}{(12)^3} \cdot \frac{1}{386 \frac{in}{sec^2}} \cdot 2.843 \cdot 2.08 \cdot 3.625 \cdot 2$$

$$= 1.39478 \, 10^{-3} \frac{lb-sec^2}{in}$$
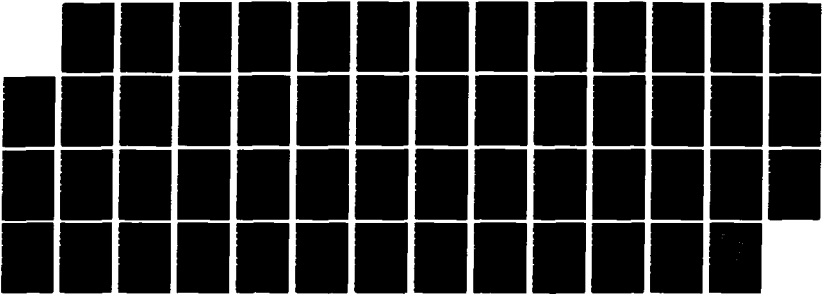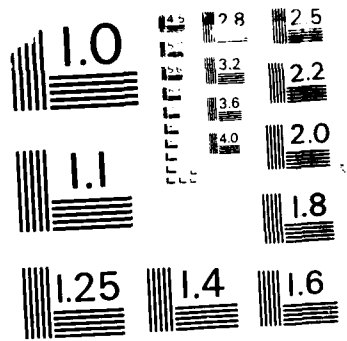
MICROCOPY RESOLUTION TEST CHART

NATIONAL BUREAU OF STANDARDS - 1963

PROJECT NO.: 06-8461-001   SPONSOR: H&R

SUBJECT: _____

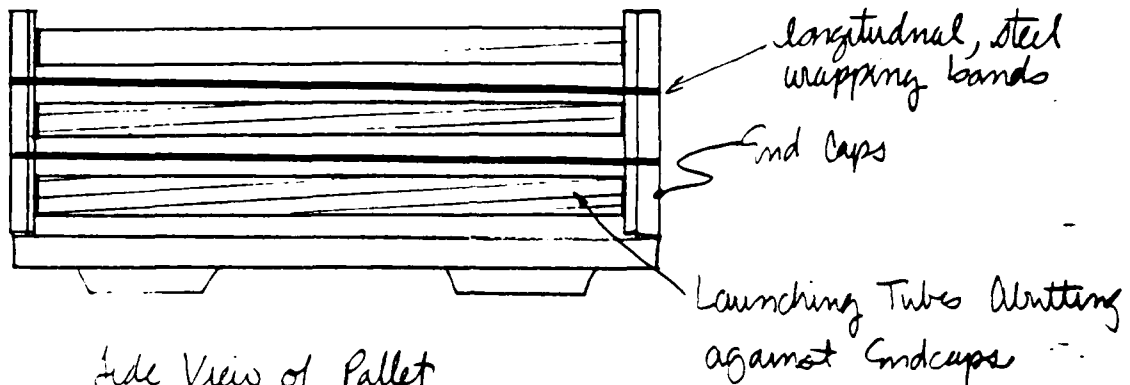BY: SES   DATE: 15 MAR 19 85   CHECKED BY: _____   DATE CHECKED: _____ 19 ___

VI. Effect of end caps on vertical and lateral impact loads

Side View of Pallet
(Stringers Not Shown)

· launching tubes do not fit into holes in end caps, (tubes are 4.890 in dia., holes are 4.000 in dia), but butt against them. A frictional force exists between tube and end cap, but calculations show this force is nominal

· steel bands are assumed to have following properties (equivalent to Signode Corp Hi-Tensile Strength Strapping)

   $'' \times 0.035''$

   Max load = 4360 lb

   Actual load = 0.50 · 4360 = 2180 lb

SOUTHWEST RESEARCH INSTITUTE
DEPARTMENT OF ENGINEERING MECHANICS
COMPUTATION SHEET

SHEET NO.
319 of 323

PROJECT NO.: 06-8461-001   SPONSOR: H&R
SUBJECT: _____
BY: SES   DATE: 1 FEB 19 85   CHECKED BY: _____   DATE CHECKED: ____ 19 ____

Free body diagram of end cap:

Side View   Isometric

$$\Sigma F_x = -4F_s + 15F_t$$

$$F_{t_1} = F_{t_2} = \ldots F_{t_{15}}$$

$$\therefore \quad F_t = \frac{4F_s}{15} = \frac{4 \times 2180\ lb}{15}$$

$$F_t = 581\ lb$$

for Coulomb friction, using $f = 0.50$ (wood on wood, dry)

$$F_{friction} = N \cdot f$$

$$F_{friction} = 0.5 \cdot 581\ lb = 291\ lbs$$

relative to other loads on this system during impact this is so small, that the end cap reactions can be ignored

SOUTHWEST RESEARCH INSTITUTE
DEPARTMENT OF ENGINEERING MECHANICS
COMPUTATION SHEET

SHEET NO.
B20 of B23
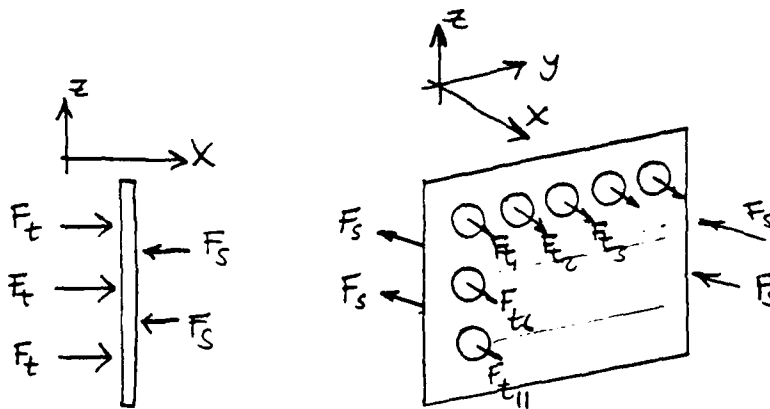
PROJECT NO.: 06-8461-001   SPONSOR: H+R
SUBJECT:
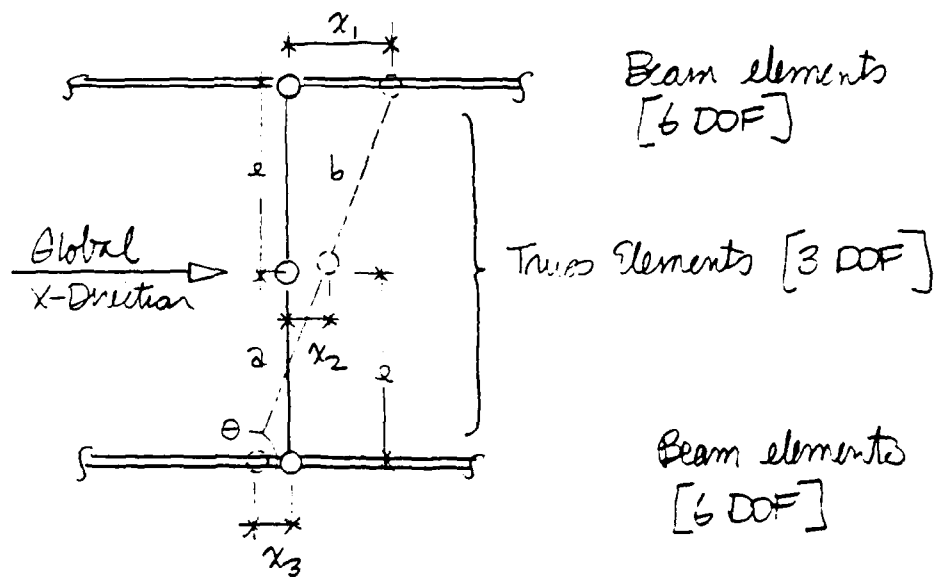BY: SES   DATE: 15 MAR 19 85   CHECKED BY: _____   DATE CHECKED: _____ 19 ____

VII Determination of constraint equations for lateral impact model

the general condition for which equations must be written
is shown in the sketch

Beam elements
[6 DOF]

Truss Elements [3 DOF]

Beam elements
[6 DOF]

it is required that the two truss elements (a, b)
remain collinear under deflections of the beam elements
(x_1, x_3). Hence,

$$x\theta = \frac{x_2 - x_3}{\ell} = \frac{x_1 - x_3}{2\ell}$$

$$\underline{x_2 = \frac{x_1 + x_3}{2}}$$ is the generalized constraint equation

PROJECT NO.: 06-8461-001   SPONSOR: H&K
SUBJECT: _____
BY: SES   DATE: 15 MAR 19 85   CHECKED BY: _____ DATE CHECKED: _____ 19 ____

VIII. Estimate rocket natural frequencies for lateral pallet
model (include launching tube stiffness)

rocket and launching tube, typical

For approximation of the beam bending mode, assume
vertical spring elements are very stiff and compute
natural frequencies for the following cases
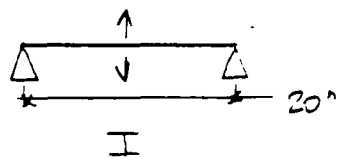
I

$$l = \frac{7.69 + 20 + 11.375}{3} \text{ in}$$

II

III

IV

SOUTHWEST RESEARCH INSTITUTE
DEPARTMENT OF ENGINEERING MECHANICS
COMPUTATION SHEET

SHEET NO
B22 OF B23

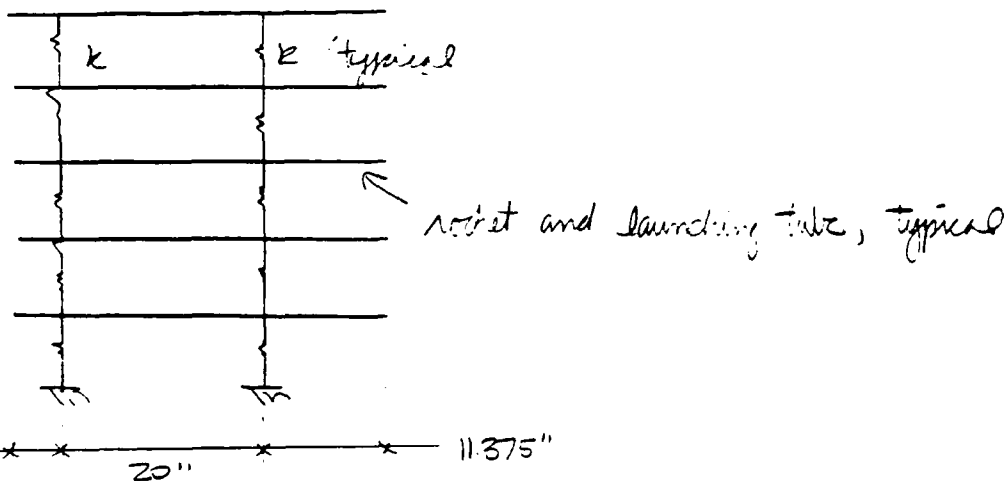PROJECT NO.: OG-8461-001   SPONSOR: H&R

SUBJECT:

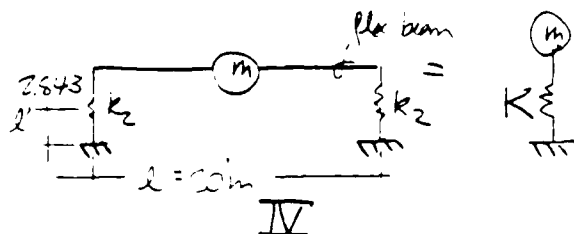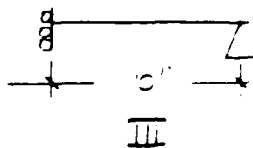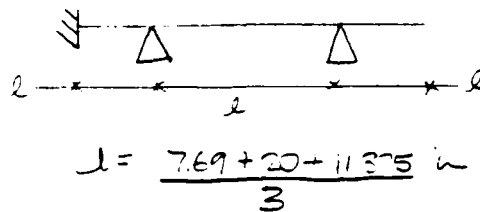BY: SES   DATE: 15 MAR 19 85   CHECKED BY: ___   DATE CHECKED: ___ 19 ___

Case III & I (identical)

from. Blevins. _Formulas for Natural Frequency & Mode Shape_

$$f_i = \frac{\lambda_i^2}{2\pi L^2} \left(\frac{EI}{m}\right)^{\frac{1}{2}}$$

$$\lambda_i = (2i-1)\frac{\pi}{2} = \frac{\pi}{2}$$

$$EI = EI_{al} + EI_{FG} = 10 \cdot 10^6 \cdot 1.919 + 1.1 \cdot 10^6 \cdot 7.938 \quad \frac{lb}{in^2} in^4$$

$$m = \frac{27.6 \, lb}{39 \, in} = \frac{0.7079}{386} \frac{lb \, s^2}{in^2}$$

$$f_i = \frac{(\pi/2)^2}{2\pi \cdot (10 \, in)^2} \cdot \left[\frac{1.919 \cdot 10^7}{0.7079} \frac{lb \, in \, in^4}{in^2 \, lb} \cdot 386 \frac{in}{sec^2}\right]^{\frac{1}{2}}$$

$$f_i = 401 \, Hz$$

Case II

$$f_i = \frac{\lambda_i^2}{2\pi L^2} \left(\frac{EI}{m}\right)^{1/2}$$

$$\lambda_i = 3.393 \times 2 \; spans$$

$$l = 13.02 \, in$$

$$f_i = \frac{3.393 \cdot 2}{2\pi \cdot (13 \, in)^2} \cdot \left(\frac{1.919 \cdot 10^7 \cdot 386}{0.7079}\right)^{\frac{1}{2}}$$

$$f_i = 757 \, Hz$$

SOUTHWEST RESEARCH INSTITUTE
DEPARTMENT OF ENGINEERING MECHANICS
COMPUTATION SHEET

SHEET NO
B23 of B23

PROJECT NO.: 06-8461-001   SPONSOR: H&R

SUBJECT: _____

BY: SCS   DATE: 15MAR9 85   CHECKED BY: _____   DATE CHECKED: _____ 19 ___

Case IV, from Blevins, and Roark. Formulas for Stress & Strain

$$k_1 = \frac{P}{\delta_{center}} = \frac{48EI}{\ell^3}$$

$$= \frac{48 \cdot 1.919 \cdot 10^7 \frac{lb}{in^2} \cdot in^4}{(30 in)^3}$$

$$k_1 = 1.1514 \cdot 10^5 \frac{lb}{in}$$

$$k_2 = \frac{AE}{2\ell'} = \frac{15.08 \, in^2 \cdot 1.353 \cdot 10^6 \frac{lb}{in^2}}{2 \cdot 2.843 \, in} = 3.588 \cdot 10^6 \frac{lb}{in}$$

sum springs

$$k = \frac{1}{\frac{1}{k_1} + \frac{1}{k_2 + k_2}} = \frac{1}{\frac{1}{1.1514 \cdot 10^5} + \frac{1}{2 \cdot 3.588 \cdot 10^6}}$$

$$= \frac{1}{(8.685079 \cdot 10^{-6} + 1.393406 \cdot 10^{-7})}$$

$$= 1.133 \cdot 10^5$$

$$\frac{\omega}{2\pi} = \sqrt{\frac{k}{m}} = \sqrt{\frac{1.133 \cdot 10^5 \, lb/in}{\left(\frac{27.6 \frac{lb \, s^2}{in}}{386}\right) \cdot \frac{20''}{39''}}} = 279 \, Hz.$$

Appendix C

Calculations Associated with Vertical Impact Analysis

SOUTHWEST RESEARCH INSTITUTE
DEPARTMENT OF ENGINEERING MECHANICS
COMPUTATION SHEET

SHEET NO. C-3 OF C-4

PROJECT NO.: 06-8461-001   SPONSOR: H & R
SUBJECT: Pallets
BY: SES   DATE: 12 MAR 19 85   CHECKED BY: _____   DATE CHECKED: ____ 19 __

References cited frequently in this calculations are

1. Bodig, J. and Jayne, B.A. <u>Mechanics of Wood Composites</u>,
Van Nostrand, New York, 1982.

2. U.S. Department of Agriculture, <u>Wood Handbook</u>, Forest Products
Laboratory Handbook No. 72, 1955.

3. Drawings cited are of the M55 rocket packing for 15 chemical
rockets, Army Chemical Corps Drawings D-90-6-62 through
D-90-6-69, 1960.

4. Roark, R.J. <u>Formulas for Stress and Strain</u>, 5th
Edition, McGraw-Hill, 1975.

5. Blevins, R.D. <u>Formulas for Natural Frequency and Mode Shape</u>,
Van Nostrand-Reinhold, New York, 1979.

PROJECT NO.: 06-8461-001   SPONSOR: H&R

SUBJECT: Vertical Impact

BY: SES   DATE: 16 FEB 19 85   CHECKED BY: _____ DATE CHECKED: _____ 19 ___

1 ≡ Deleted DOF, 0 ≡ Admissible DOF

UX = 1   ROTX 1
UY = 0   ROTY = 1
UZ = 1   ROTZ = 1

[PLANE AT Z = -20.0]

steel

Y

[PLANE @ Z = 0]

3.965"
3.66"
4"
7"
6.0625
5"
4"
4.6"
3.4"
3.14"

6.6.25

aluminum

ORIGIN

X

for finite element
model in these regions
see pps.

* truss element representing plywood end cap (typical)
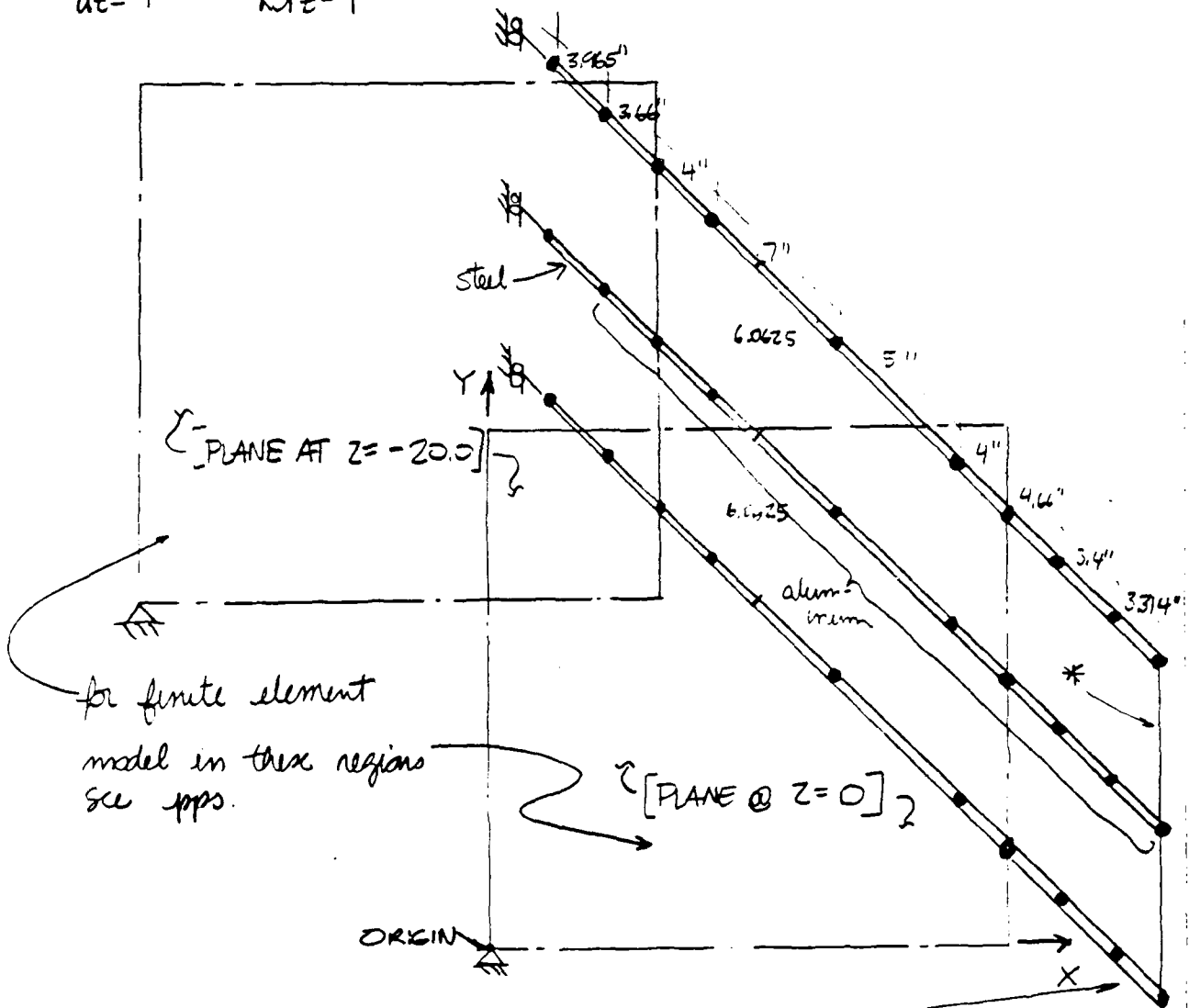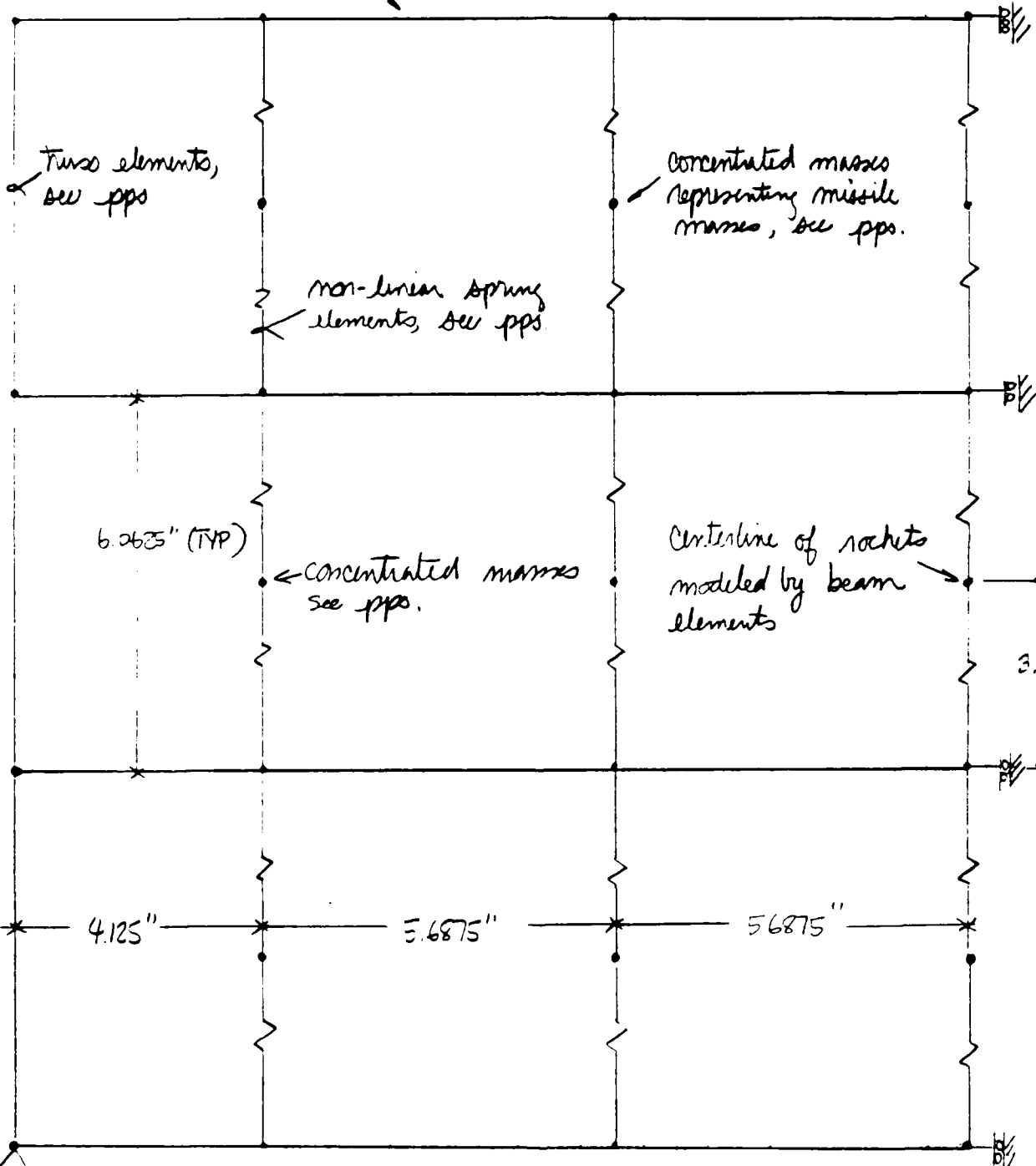
• Densities of rocket elements, pps.

Center column of rockets
represented as beam
elements (composite of
launching tube and M85)
see pps.

PLANE AT Z=

beam element representing
wooden saddle supports
see pps.

Two elements,
see pps

concentrated masses
representing missile
masses, see pps.

non-linear spring
elements, see pps

6.2635" (TYP)

concentrated masses
see pps.

Centerline of rockets
modeled by beam
elements

3.031"
(typical)

4.125"   5.6875"   56875"

UX = 1   ROTX = 1   1 ≡ Deleted DOF   ROTY = 1   UX = 1
UY = 1   ROTY 1   ROTZ = 1   UY = 0
UZ = 1   ROTZ = 0   0 ≡ Admissible DOF   UZ = 1
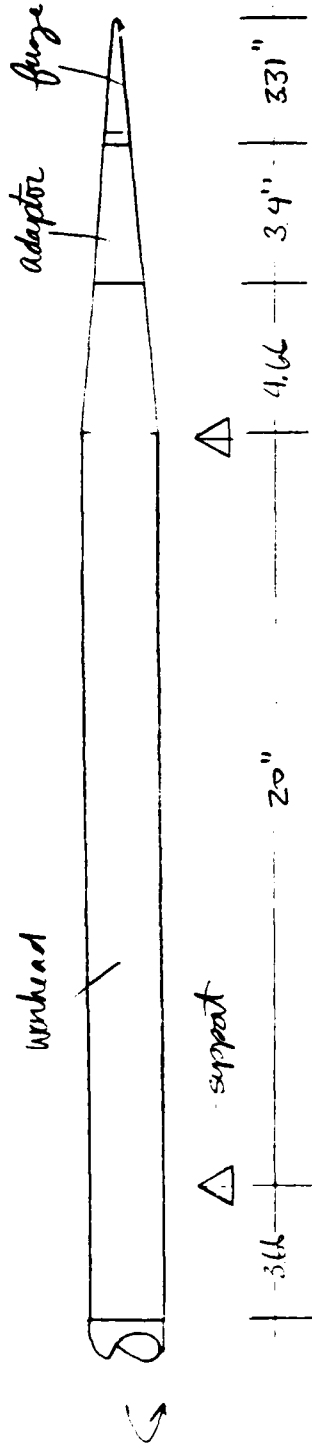   ROTX = 1

SOUTHWEST RESEARCH INSTITUTE
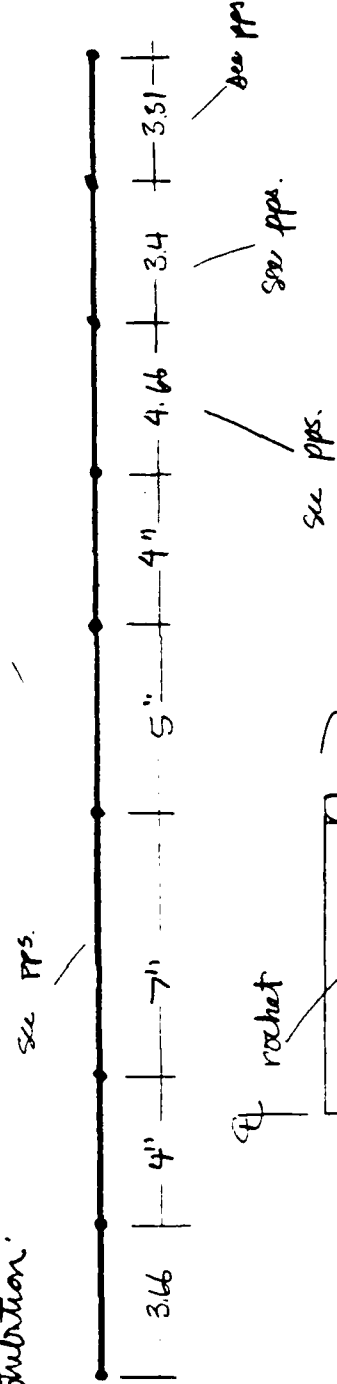## DEPARTMENT OF ENGINEERING MECHANICS
COMPUTATION SHEET

PROJECT NO.: 06-8461-001   SPONSOR: H&R

SUBJECT: Vertical Impact

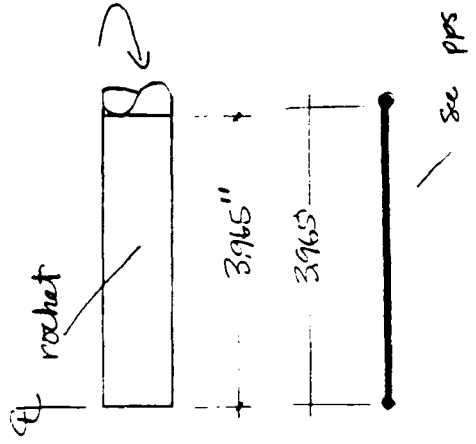BY: SES   DATE: 15 FEB 1985   CHECKED BY: _____   DATE CHECKED: _____ 19 _____

Typical of all Rockets in Center Column

Node Distribution.

Node Distribution

PROJECT NO.: 06-8461-001   SPONSOR: H&R
SUBJECT: Lateral or Vertical Impact Model
BY: SES   DATE: 6 FEB 19 85   CHECKED BY: _____ DATE CHECKED: _____ 19 ___

Rocket

Fins

(A) Warhead

(B) adapter

Fuze

8.165"   34.739   7.625"   3.965"   20.00   11.375"

Warhead Component Weights

Agent Weight = 10 lbs
Burster Casing = 0.41 lbs
Cannister Casing = 2.21 lbs
Burster Agent = 2.9 lbs
—————
15.51 lbs

Adapter Component Weights

Casing Weight = 1.22 lb
Burster Casing = 0.04 lb
Burster Weight = 0.3 lb
—————
1.55 lb

Fuze Weight

Estimated at 0.1 lb
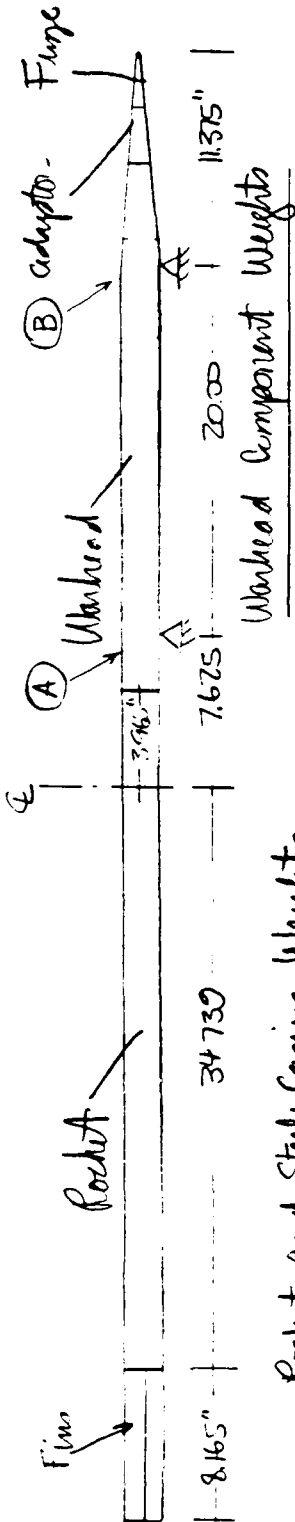
Rocket and Steel Casing Weights

Total Rocket Weight = 57 lbs
Less Warhead Weight = 15.51 lbs
Less Adapter Weight = 1.55 lbs
Less Fuze Weight = 0.10 lbs
—————
39.84 lbs

Ref. JF Amaliya/Suki
(modified using component lengths
as found in M55 drawings)

PROJECT NO.: 06-8461-00   SPONSOR: H&R

SUBJECT:

BY: SES   DATE: 16 FEB 19 85   CHECKED BY: _____   DATE CHECKED: _____ 19 ____

I Compute Concentrated Masses for Rockets & Tubes

Lumping masses of off-center columns of rockets:

- all mass aft of Ⓐ is lumped at Ⓐ
- all mass ahead of Ⓑ is lumped at Ⓑ
- all mass between Ⓐ, Ⓑ is divided equally among Ⓐ, Ⓑ
- these are translational inertias (weights), rotational inertias (weights) are ignored; (in the off-center columns of rockets)

Mass aft of Ⓐ

$$\text{Rocket + Casing} = \frac{W_{Rocket + Casing}}{L_{Rocket + Casing}} \cdot 3.965 \text{ in} = 4.547 \text{ lb}$$

$$\text{Warhead + Agent} = \frac{W_{warhead + agent}}{L_{warhead + agent}} \cdot (7.625 - 3.965 \text{ in}) = 2.004 \text{ lb}$$

$$6.551 \text{ lb}$$

Mass Forward of Ⓑ

Fuze	= 0.1 lb
Adaptor	= 1.55 lb

$$\text{Warhead + Agent} = \frac{W_{warhead + agent}}{L_{warhead + agent}} (11.375" - 3.4" - 3.314") = 2.55 \text{ lb}$$

$$4.203 \text{ lb}$$

SOUTHWEST RESEARCH INSTITUTE
DEPARTMENT OF ENGINEERING MECHANICS
COMPUTATION SHEET

SHEET NO
CL OF C34

PROJECT NO.: 06-8461-001   SPONSOR: H&R
SUBJECT:
BY. SES   DATE: 16 FEB 19 85   CHECKED BY: DATE CHECKED: 19

Mass Between (A) and (B):

$$Warhead + Agent = \frac{W_{warhead + agent}}{L_{warhead + agent}} \cdot 20.00'' = 10.953 \text{ lb}$$

similarly for the launching tube,

Mass aft of (A)

Tube: Total Weight $\frac{L_{aft\ (A)}}{L_{Total}}$

$$= 12.55 \text{ lb} \cdot \frac{7.625}{78.00 \text{ in}} \qquad 1.228 \text{ lb}$$

Mass Forward of (B)

Total Weight $\frac{L_{Fwd\ (B)}}{L_{Total}}$

$$12.55 \text{ lb} \cdot \frac{11.375 \text{ in}}{78.00 \text{ in}} \qquad = \qquad 1.830 \text{ lb}$$

Mass Between (A) and (B)

Total Weight $\cdot \frac{L_{(A)(B)}}{L_{Total}}$

$$12.55 \text{ lb} \cdot \frac{20.00 \text{ in}}{78.00 \text{ in}} \qquad = \qquad 3.218 \text{ lb}$$

PROJECT NO.: 06-8461-001   SPONSOR: H&R

SUBJECT: _____

BY: SES   DATE: 6 FEB 19 85   CHECKED BY: _____   DATE CHECKED: _____ 19 ___

lump masses as follows:

at $\textcircled{A}$ $\dfrac{6.551^{\#} + 1.228^{\#} + \frac{1}{2}(10.953^{\#} + 3.218^{\#})}{386.4 \ \frac{in}{sec^2}} = 3.847 \cdot 10^{-2}$

at $\textcircled{B}$ $\dfrac{4.203^{\#} + 1.830^{\#} + \frac{1}{2}(10.953 + 3.218^{\#})}{386.4 \ \frac{in}{sec^2}} = 3.395 \cdot 10^{-2}$

SOUTHWEST RESEARCH INSTITUTE
DEPARTMENT OF ENGINEERING MECHANICS
COMPUTATION SHEET

SHEET NO. C8 of C34

PROJECT NO.: 06-8461-001   SPONSOR: H & R
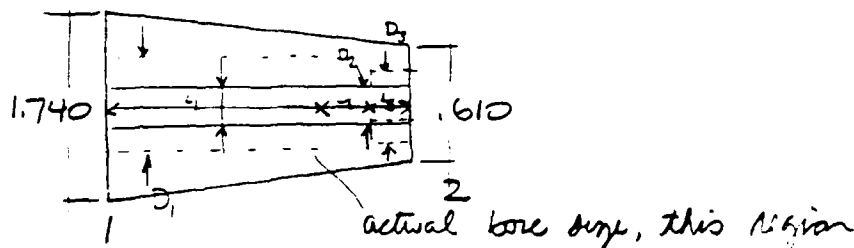SUBJECT:
BY   SES   DATE: 5 MAR 19 85   CHECKED BY: DATE CHECKED   19

II Compute Properties of Rocket and Launching Tube tapered sections:

FUZE ASS'Y (Equivalent Model)

actual bore size, this region

Bore size for equivalent model determined by taking weighted average of bore sizes on length of bore:

$$D_{i,eq} = \frac{L_1 D_1 + L_2 D_2 + L_3 D_3}{L_1 + L_2 + L_3},$$

$D_1 = 1.37$ (avg) $L_1 = 2.093$

$D_2 = .248$ $L_2 = 0.721$

$D_3 = .541$ $L_3 = 0.500$

$\therefore D_{i,eq} = 1.0$ in

Representing taper section as uniform section beam with average cross-section properties, compute average D_o

$$D_{o,eq} = {}^1D_o + {}^2D_o / 2$$

$$D_{o,eq} = 1.175 \text{ in}$$

PROJECT NO. 06-8461-001   SPONSOR: H&R

SUBJECT:

BY. SSS   DATE: 15MAR 19 85   CHECKED BY: _____   DATE CHECKED: ____ 19 ____

ADAPTOR ASS'Y (Equivalent Model)

Compute average D_o, (assuming a uniform cylindrical section)

$$D_{o,eq} = \frac{{}^1D_o + {}^2D_o}{2}$$

$$\therefore D_{o,eq} = 2.55^* \text{ in}$$

$$D_i = D_i = 1.53 \text{ in}$$

SOUTHWEST RESEARCH INSTITUTE
DEPARTMENT OF ENGINEERING MECHANICS
COMPUTATION SHEET

SHEET NO C10 OF C34

PROJECT NO. 06-8461-001   SPONSOR: H & R
SUBJECT: _____
BY: SES   DATE: 15 MAR 19 85   CHECKED BY: _____   DATE CHECKED: _____ 19

TAPERED WARHEAD (Equivalent Model)

$$D_{0,eq} = {}^1D_0 + {}^2D_0 / 2 = 3.716 \text{ in}$$

$$D_i = D_{0,eq} - 2t = 3.6004 \text{ in}$$

Representing taper section as uniform section beam with average cross-section properties compute average D_0

SOUTHWEST RESEARCH INSTITUTE
DEPARTMENT OF ENGINEERING MECHANICS
COMPUTATION SHEET

SHEET NO C10 OF C34
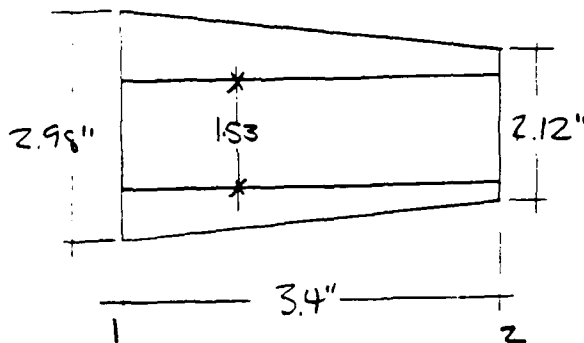
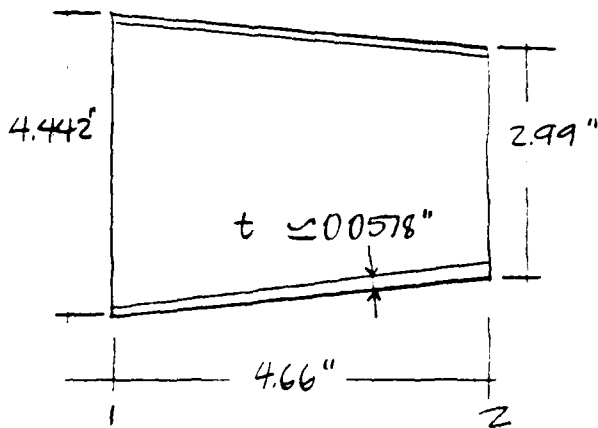PROJECT NO. 06-8461-001   SPONSOR: H & R
SUBJECT: _____
BY: SES   DATE: 15 MAR 19 85   CHECKED BY: _____   DATE CHECKED: _____ 19

TAPERED WARHEAD (Equivalent Model)

Figure: 4.442" (left), 2.99" (right), $t \simeq 0.0578"$, 4.66" (length), points 1 and 2.

Representing taper section as uniform section beam with average cross-section properties compute average D_0

$$D_{0,eq} = {}^1D_0 + {}^2D_0 / 2 = 3.716 \text{ in}$$

$$D_i = D_{0,eq} - 2t = 3.6004 \text{ in}$$

PROJECT NO.: 06-8461-001   SPONSOR: H&R
SUBJECT: _____
BY: SES   DATE 5 MAR 19 85   CHECKED BY: _____   DATE CHECKED: _____ 19 ___

Properties and dimensions used for warhead, rocket and fibrglass shells: (untapered sections)

	Aluminum Warhead	Steel Rocket Motor Casing	Fibrglass Launching Tube
$t =$	0.0578 in	0.096	0.195
$D_o =$	4.442 in	4.442	4.890
$D_i =$	4.3264 in	4.250	4.500
$A =$	0.7961 in^2	1.311	2.876
$I =$	1.913 in^4	3.096	7.9387

PROJECT NO.: 06-8461-001   SPONSOR: HJR

SUBJECT: _____

BY: SES   DATE: 15MAR 19 85   CHECKED BY: _____   DATE CHECKED: ___ 19 ___

III. Compute densities for beam elements representing composite tube and rocket (center-column of rockets):

- weight of launching tube = $\left[\frac{\pi}{4}\left(D_o^2 - D_i^2\right)\right] L \cdot \rho_{FG}$

$\rho_{FG} = 0.0525 \ lb_f/in^3$ $D_o = 4.890 \ in$

$L = 83\frac{1}{8} \ in$ $D_i = 4.500 \ in$

$W_{TUBE} = 12.55 \ lbs$

Density of beams representing fuze   (1 beam element)

Fuze is 3.314 in long = L

$W_{FG} = 12.55 \ lbs \cdot \dfrac{3.314 \ in}{83.125 \ in} = 0.500 \ lb$

$W_{FUZE} = 0.10 \ lb$

$D_{o,eq} = 1.175 \ in$

$D_{i,eq} = 10 \ in$

$\rho_{al} = \dfrac{W_{FUZE}}{\frac{\pi}{4}\left\{D_{o,eq}^2 - D_{i,eq}^2\right\} \cdot L g} = 0.0002615 \ \dfrac{lb\text{-}s^2}{in^4}$

SOUTHWEST RESEARCH INSTITUTE
DEPARTMENT OF ENGINEERING MECHANICS
COMPUTATION SHEET

SHEET NO. C13 OF C34

PROJECT NO.: 06-8461-001   SPONSOR: H&R

SUBJECT: _____

BY: SES   DATE: 15 MAR 19 85   CHECKED BY: _____   DATE CHECKED: _____ 19 ___

Density of beams representing adaptor (1 beam element)

$$L = 34 \text{ in}$$

$$D_{oeq} = 2.55$$

$$D_{ieq} = 1.53$$

$$W_{adapt} = 1.55 \text{ lb}$$

$$\rho_{eq} = \frac{+ W_{adapt}}{\frac{\pi}{4}\{D_{oeq}^2 - D_{ieq}^2\} L g} = .000361 \frac{lb\text{-}s^2}{in^4}$$

Density of beams representing warhead taper section (1 element)

$$L = 4.66 \text{ in}$$

$$L_{warhead} = 28.321 \text{ in}$$

$$W_{warhead} \text{ (total)} = 15.51 \text{ lbs}$$

$$W_{warhead + agent} = W_{warhead} \text{ (total)} \cdot \frac{L}{L_{warhead}} = 2.55 \text{ lb}$$

$$D_{oeq} = 3.716 \text{ in}$$

$$D_{ieq} = 3.6004 \text{ in}$$

$$\rho_{eq} = \frac{W_{warhead + agent}}{\frac{\pi}{4}\{D_{oeq}^2 - D_{ieq}^2\} L g} = .00213 \frac{lb\text{-}s^2}{in^4}$$

PROJECT NO.: 06-8461-001   SPONSOR: H&R

SUBJECT:

BY: SES   DATE: 15MAR19 85   CHECKED BY: _____   DATE CHECKED: _____ 19 ____

Density of beams representing warhead, prismatic section (5 elements)

$$L_{5\,elements} = 4 + 5 + 7 + 4 + 3.66 \text{ in} = 23.66 \text{ in}$$

$$W_{warhead} = W_{warhead(total)} \cdot \frac{L}{L_{warhead}} = 12.96 \text{ lb}$$

$$D_{o,eq} = 4.442 \text{ in} \qquad\qquad D_{i,eq} = 4.3264 \text{ in}$$

$$\rho_{eq} = \frac{W_{warhead}}{\frac{\pi}{4}\{D_{oeq}^2 - D_{ieq}^2\} \cdot L \cdot g} = .00783 \frac{\text{lb sec}^2}{\text{in}^4}$$

Density of beams representing steel casing and rocket (1 element)

$$L = 3.965 \text{ in} \qquad\qquad L_{rocket} = 34.721 \text{ in}$$

$$W_{rocket(total)} = 39.84 \text{ lb}$$

$$W_{rocket} = W_{rocket(total)} \cdot \frac{L}{L_{rocket}} = 4.550 \text{ lb}$$

$$D_{oeq} = 4.442 \text{ in} \qquad\qquad D_{ieq} = 4.250 \text{ in}$$

$$\rho_{eq} = \frac{W_{rocket}}{\frac{\pi}{4}\{D_{oeq}^2 - D_{ieq}^2\} \cdot L \cdot g} = .002267 \frac{\text{lb s}^2}{\text{in}^4}$$

PROJECT NO: 06-8461-001   SPONSOR: H&R

SUBJECT: _____

BY: SES   DATE: 8 MAR 19 85   CHECKED BY: _____   DATE CHECKED: _____ 19 ___

IV. Compute equivalent rectangular beam for middle truss & strut and burndown tubes (@ ½ stiffness and mass)

for rocket beam element properties of

E_{roc} E_{Troc} G_{vra} $I_{roc} = \frac{\pi}{64}(D^4_{oroc} - D^4_{iroc})$

ρ_{roc} D_{oroc} $A_{roc} = \frac{\pi}{4}(D^2_{oroc} - D^2_{iroc})$

ν_{roc} D_{iroc}
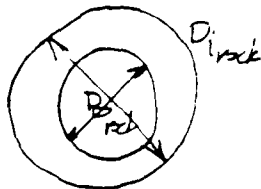
we desire to fulfill mid-plane symmetry conditions,
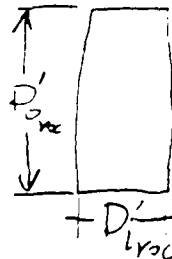
$E'_{roc} = E_{voc}$ $E'_{Troc} = E_{Troc}$

$\rho'_{roc} = \rho_{roc} \frac{\frac{\pi}{4}(D^2_{oroc} - D^2_{iroc})}{D'_{iroc} D_{oroc}}$ $A'_{roc} = \frac{1}{2} A_{roc} = D'_{iroc} D_{oroc}$

$\nu'_{roc} = \nu_{roc}$ $I'_{roc} = \frac{1}{2} I_{roc} = \frac{\pi}{64}(D^4_{ora} - D^4_{iroc})$

adopt a rectangular section of the following dimensions

Rocket Cross Section

Calculations for D_i'.

For the critical pellet model we require that stiffness is preserved.

$$I_{ra}' = \frac{1}{2} I_{roc} = \frac{D_{3ra}^3 D_{ira}'}{12}$$

$$D_{ira}' = \frac{6 I_{roc}}{D_{orac}^3} = \frac{\frac{6\pi}{64}\left[D_{3roc}^4 - D_{iroc}^4\right]}{D_{ora}^3}$$

we desire to have half the full rocket weight:

$$\rho_{ra} A_{ra} L_{roc} = \rho_{ra}' A_{ra}' L_{roc}$$

$$\rho_{ra}' = \frac{\rho_{ra} A_{ra}}{A_{roc}'} = \frac{\rho_{roc} \frac{\pi}{4}\left[D_{oroc}^2 - D_{ira}^2\right]}{D_{ira}' D_{oroc}}$$

PROJECT NO. 06-6461-001   SPONSOR: H & R
SUBJECT: _____
BY: SCS   DATE: 16 FEB 19 85   CHECKED BY: _____ DATE CHECKED: _____ 19

Equivalent Rectangular Beam Properties for Middle Column of Rockets

Material Set No	$E'_{rc} = E_{rc}$	ρ'_{rc}	$\nu'_{rc} = \nu_{rol}$	$D'_{rc} = D_{rc}$	D'_{c} mm	$F'_{trc} = F_{trc}$
1	10.0E6	.000026	0.3	1.175	.1645	0.685E5
2	10.0E6	.0003589	0.3	2.550	.6537	0.6533E5
3	10.0E6	.0001445	0.3	3.716	.1300	0.685E5
4	10.0E6	.001220	0.3	4.442	.1310	0.685E5
5	10.0E6	.0011220	0.3	4.442	.1310	0.685E5
6	10.0E6	.001200	0.0	4.442	.1310	0.685E5
7	10.0E6	.001220	0.0	4.442	.1310	0.685E5
8	10.0E6	.001220	0.0	4.442	.1310	0.685E5
9	3.0E6	.001018	.035	4.442	.2119	1.383E5

Fiberglass Launching Tubes

L-1	1.1E6	.000015	.011	4.250	.4074	0.0

SOUTHWEST RESEARCH INSTITUTE
DEPARTMENT OF ENGINEERING MECHANICS
COMPUTATION SHEET

C18 SHEET NO OF C34

PROJECT NO.: 06-8461-001   SPONSOR: H&R
SUBJECT: _____
BY: SKS   DATE: 15 MAR 19 85   CHECKED BY: _____   DATE CHECKED: _____ 19 ____

I Determination of properties of saddles for vertical impact model
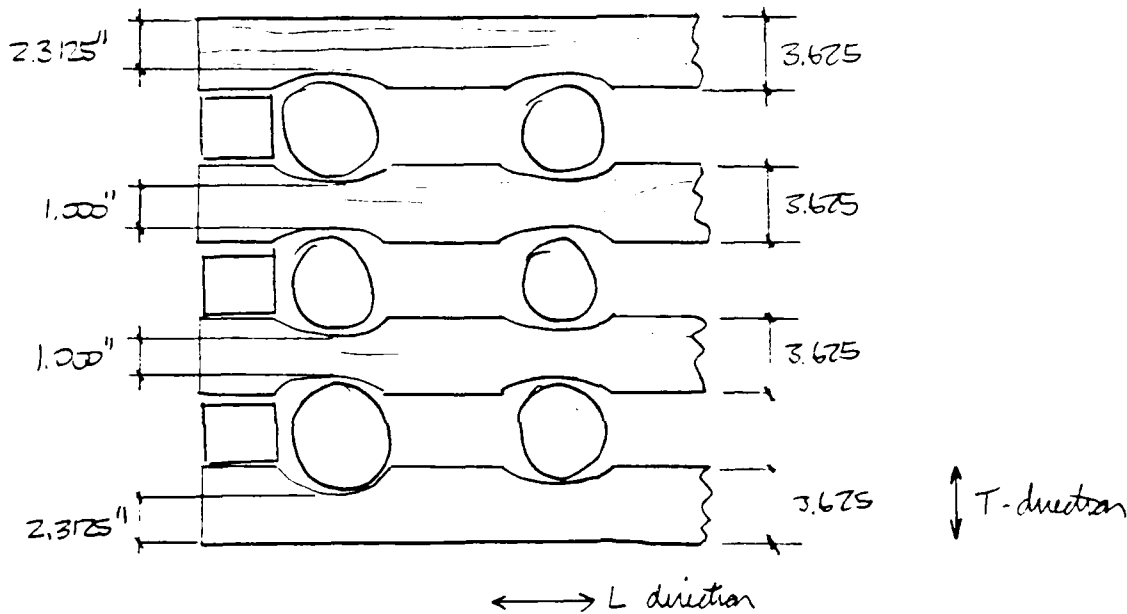
- wood is assumed to be eastern white pine
- for vertical impact model, saddle supports are presumed to undergo bending and shear, but principal stresses result from bending and are in L-direction. Thus, saddles are modeled as nonlinear isotropic elastic-plastic beams with grain (L) direction properties
- an effective beam depth is computed on the following pages to account for variations in saddle depth along its length
- since inelastic behavior of wood unknown, assume that $\epsilon_{ult} = 10 \cdot \epsilon_{yield}$
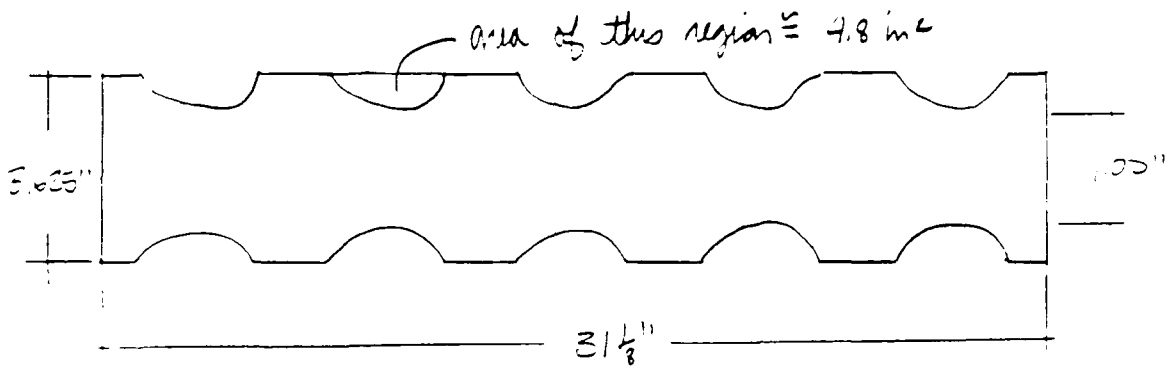
SOUTHWEST RESEARCH INSTITUTE
DEPARTMENT OF ENGINEERING MECHANICS
COMPUTATION SHEET

SHEET NO. C19 OF C24

PROJECT NO. 06-8461-001   SPONSOR: H{R
SUBJECT.
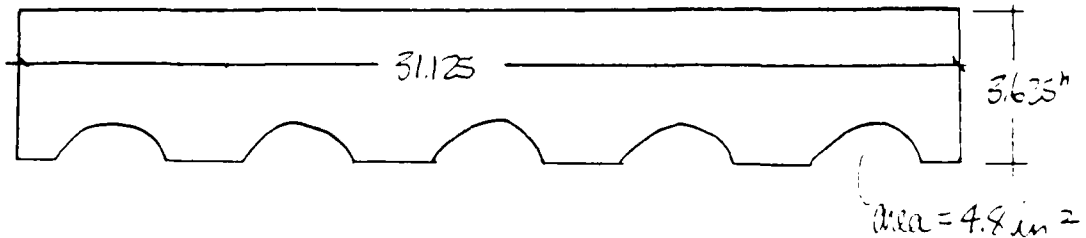BY SES   DATE: 5 MAR 19 85   CHECKED BY: _____   DATE CHECKED: ___ 19 ___

compute effective beam depth for middle saddles

area of this region ≅ 4.8 in²

3.625"

.33"

31⅛"

$$N_{eff} = \frac{A_{Tot}}{L} = \frac{3.625" \cdot 31.125" - (10 \cdot 4.30 \, in^2)}{31.125''} =$$

$$N_{eff} = 2.08 \, in$$

compute effective beam depth for upper and lower saddles

31.125

3.625"

area = 4.8 in²

$$W_{eff} = \frac{A_{Tot}}{L} = \frac{3.625 \cdot 31.125 - (5 \cdot 4.8 \, in^2)}{31.125 \, in} = 2.85 \, in$$

PROJECT NO. 06-8461-001   SPONSOR: H/R
SUBJECT:
BY: SES   DATE: 17 FEB 19 85   CHECKED BY: DATE CHECKED: 19

From Mechanics of Wood Composites, & Wood Handbook:

$$E_L = 1.353 \cdot 10^6 \frac{lb}{in^2}$$

$$\nu_{LT} = 0.0595 \qquad \nu_{LR} = 0.1894$$

$$\nu_{eq} = \nu_{LT} + \nu_{LR}/2 = 0.239$$

$^L\sigma_y \equiv$ fiber stress in grain direction at proportional limit = 5700 $\frac{lb}{in^2}$
(bending, static)

$^L\sigma_u \equiv$ tensile ultimate stress = 12,200 * $\frac{lb}{in^2}$ (uniaxial tension)

$^L\sigma_u$ & $^L\sigma_y$ are for seasoned wood at 12% moisture content (M.C.)

$$^L\varepsilon_y = \frac{^L\sigma_y}{E_L} = 0.0042 \frac{in}{in}$$

assuming that $10^2\varepsilon_y = {}^L\varepsilon_{ult}$, compute E_T (strain-hardening modulus)

$$E_T = \frac{12,200 - 5700 \frac{lb}{in^2}}{(^L\varepsilon_{ult} - {}^L\varepsilon_y)} = 0.172 \cdot 10^6 \frac{lb}{in^2}$$

* this is the value for coastal Douglas-fir given on page 291
of Mechanics of Wood Composites; coastal Douglas fir has orthotropic
and strength properties very near that of eastern white pine.

PROJECT NO.: 06-8461-001   SPONSOR: H & R
SUBJECT: Vertical Impact Model
BY: SES   DATE: 17 FEB 19 85   CHECKED BY: _____   DATE CHECKED: _____ 19 ____

Summary of properties for saddle beam finite elements

$$E = 1.353 \cdot 10^6 \ \frac{lb}{in^2}$$

$$\nu = 0.239$$

$$D_o = 2.08 \ in$$

$$D_i = 3.625 \ in \quad (\text{width of saddle})$$

$$\sigma_y = 5700 \ \frac{lb}{in^2}$$

$$E_T = 0.172 \cdot 10^6 \ lb/in^2$$

"middle 2"
saddle supports

$$E = 1.353 \cdot 10^6 \ \frac{lb}{in^2}$$

$$\nu = 0.239$$

$$D_o = 2.85 \ in$$

$$D_i = 3.625 \ in \quad (\text{width of saddle})$$

$$\sigma_y = 5700 \ \frac{lb}{in^2}$$

$$E_T = 0.172 \cdot 10^6 \ \frac{lb}{in^2}$$

upper and lower
saddle supports

SOUTHWEST RESEARCH INSTITUTE
DEPARTMENT OF ENGINEERING MECHANICS
COMPUTATION SHEET

SHEET NO. C22 of C34

PROJECT NO. 06-8461-001   SPONSOR: H{R
SUBJECT: Vertical Impact Model
BY: SES   DATE: 7-56 19 85   CHECKED BY: _____   DATE CHECKED: _____ 19 ____

VI Determination of cross grain properties of pallet stringer elements

- Stringers are assumed to be eastern white pine
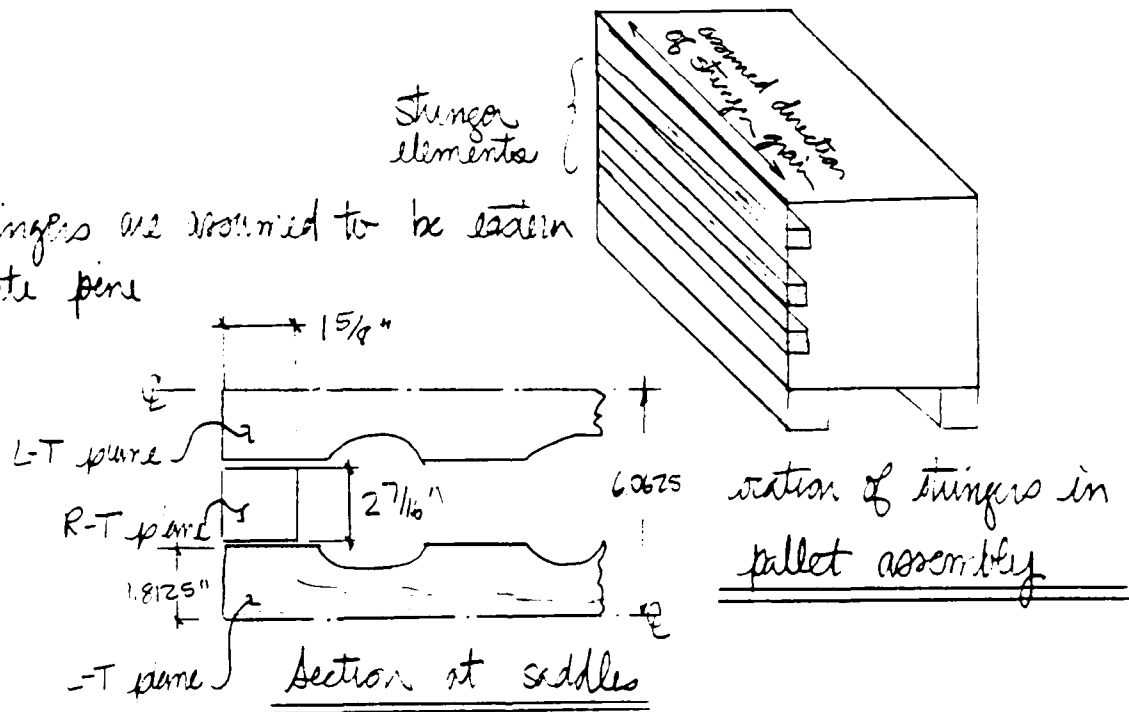
- in the vertical impact model, stringers & saddles cross grain stiffnesses (between saddle supports) are modeled using truss elements with cross-grain properties.

- because ultimate strengths of wood in crushing direction are unknown and to conservatively load the warhead casings assume that wood in cross-grain crushing acts as elastic-perfectly plastic material

SOUTHWEST RESEARCH INSTITUTE
DEPARTMENT OF ENGINEERING MECHANICS
COMPUTATION SHEET

SHEET NO. C23 OF C34

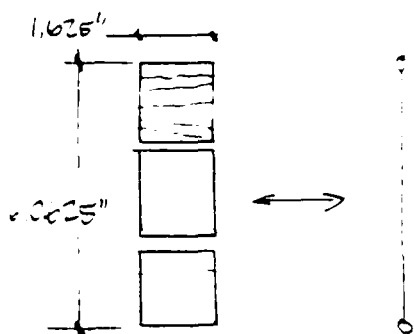PROJECT NO. 06-8461-001   SPONSOR: H&R

SUBJECT

BY: SES   DATE: 15 FEB 19 85   CHECKED BY: _____   DATE CHECKED: _____ 19 ____

From the pallet drawings (see sketch previous page, too) C-90-6-22, to C-90-669 and <u>Mechanics of Wood Composites</u>

$E = 0.064 \cdot 10^6 \frac{lb}{in^2}$ (tangential direction modulus)

σ_y = crushing yield strength, $\perp$ grain, 12% M.C.
$= 510 \ lb/in^2$

$E_T = 0.0$ (i.e. elc-perfectly plastic)

effective portions of saddle / stringer   Equivalent Truss Element

$\nu = \frac{\nu_{LT} + \nu_{RT}}{2} = \frac{.289 + .413}{2} = 0.351$

depth of beam/truss element $\equiv$ width of saddle $= 3.625$ in

Summary of Properties of Equivalent Truss Element

$E = 0.064 \cdot 10^6 \frac{lb}{in^2}$ $\sigma_y = 510 \ lb/in^2$

$\nu = 0.351$ $E_T = 0.0$

$D_0 = 1.625$ in

$D_i = 3.625$ in

PROJECT NO. 06-8461-001   SPONSOR H{R

SUBJECT

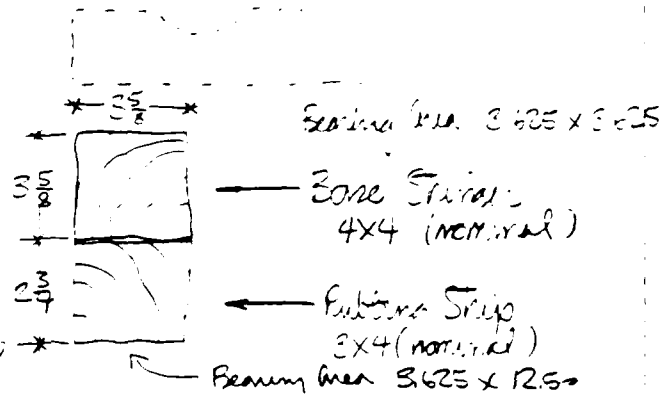BY SES   DATE 18 MAY 19 85 CHECKED BY   DATE CHECKED   19

VII Determine properties of 4×4 base and rubbing strip.

for insertion into vertical pallet model:

we assume that grain runs along
the long dimension of one stringer
and rubbing strip; hence take
longitudinal or T direction properties
for representative truss finite element of
actuators

Section Area 3.625 × 3.625

Base Stringer
4×4 (nominal)

Rubbing Strip
3×4 (nominal)

Bearing Area 3.625 × 12.50

$$E = E_T = 0.064 \, 10^6 \, \frac{lb}{in^2}$$

$$\nu = \nu_{RT} = 0.413$$

$$D_0 = 8.368 \, in$$
$$D_i = 3.625 \, in$$ \} mean contact area, see calcs on next page

$$L = 6.575 \, in$$

$$\sigma_y = 510 \, \frac{lb}{in^2}$$

$$E_T = 0.0 \quad \left[we \; assume \; elastic\text{-}perfectly \; plastic \; material \right]$$

PROJECT NO. 06-6461-001   SPONSOR H&R

SUBJECT:

BY SES   DATE 22 MAY 1985   CHECKED BY: _____   DATE CHECKED: ____ 19 ___

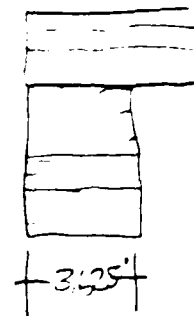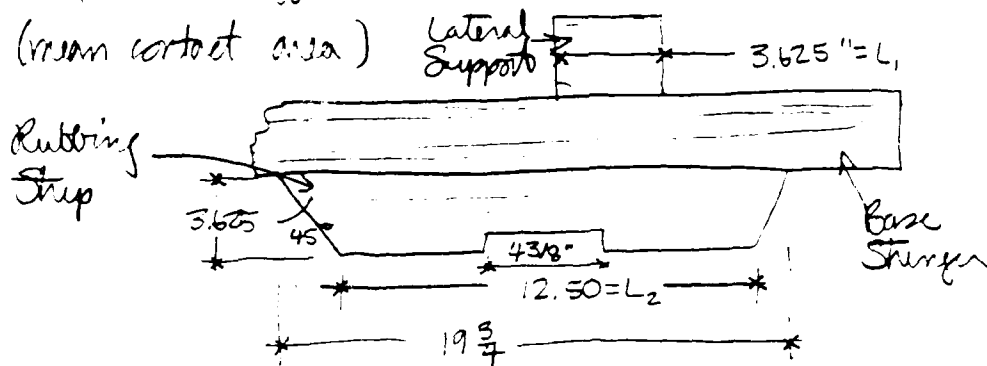compute an effective area for the truss element

(mean contact area)

Figure A
Side View

Figure B
End View

$$area = L \times W$$

$$W = 3.625 \text{ in} \quad (\text{Figure B})$$

$$L = \frac{L_1 + L_2}{2} = \frac{3.625'' + 12.50''}{2} = 8.063 \text{ in}$$

therefore take as $\oslash \, D_i$

8.063 in
3.625 in

PROJECT NO 06-846-001   SPONSOR H/R
SUBJECT _____
BY SES   DATE: 1 FEB 19 85   CHECKED BY _____ DATE CHECKED ____ 19 ___

VIII Effect of end caps on vertical and lateral impact loads

longitudnal, steel
wrapping bands

End Caps

Launching Tubes abutting
against End caps

Side View of Pallet
(Stringers Not Shown)

- Launching tubes do not fit into holes in end caps,
  (tubes are 4.890 in dia., holes are 4.000 in dia), but
  butt against them. A frictional force exists between
  tube and end cap, but calculations show this force
  is nominal

- steel bands are assumed to have following properties
  (equivalent to Signode Corp Hi-Tensile Strength Strapping)

  $\times 0.035$

  Max. load = 4360 lb

  Actual load = 0.50 × 4360 = 2180 lb

PROJECT NO. 06-8461-001   SPONSOR H&R

SUBJECT _____

BY SES   DATE: 1FEB 19 85   CHECKED BY: _____   DATE CHECKED _____ 19 ___

Free body diagram of end cap

Side View   Isometric

$$\Sigma F_x = -4F_S + 15 F_t$$

$$F_{t_1} = F_{t_2} = \ldots F_{t_{15}}$$

$$\therefore \quad F_t = \frac{4F_S}{15} = \frac{4 \times 2180 \text{ lb}}{15}$$

$$F_t = 581 \text{ lb}$$

for Coulomb friction, using $f = 0.50$ (wood on wood, dry)

$$F_{friction} = N \cdot f$$

$$F_{friction} = 0.5 \cdot 581 \text{ lb} = 291 \text{ lbs}$$

relative to other loads on this system during impact this
is so small, that the end cap reactions can be ignored

PROJECT NO __06-8461-001__   SPONSOR __#{R__

SUBJECT _____

BY __SES__   DATE. __18 MAR__ 19 ____   CHECKED BY: _____   DATE CHECKED: _____ 19 ____

IX and Calculations for Weight Check on Vertical Pallet Model

Compute the estimated weight of components in pallet
FE model and compare with ADINA value

Components	Estimated Weight Calculations
1. Rockets at Centerline	3 rockets @ =17 #s @ ½ cross section = 32.56 #
2. Tubes at Centerline	3 tubes @ 12.55 #/tube × ½ cross area × ½ length = 9.4125 #
3. Rockets and Tubes as lumped masses	[21.7 #/rocket + 13.55 × ½ #/tube] × 2 columns × 2 rows = 57.85 #
4. axial Wooden Supports	{[2 interior supports @ .469 #/support] − [2 exterior supports @ 2.013 #/support]} × 2 sets = 13.93 lb
5. Trusses Representing Stringer	× ρ × L × W × H × No. = 3.253 10⁻⁵ lb-s²/in⁴ × 6.063" × .625" × 3.625" × 386.4 in/sec² × 6 = 2.09 lb

---

* ρLWH = 3.253 10⁻⁵ $\frac{lb-s^2}{in^4}$ · 366 $\frac{in}{sec^2}$ · 15.5" × 2.08" × 3.625" = .469 lb

** ρLWH = 3.253 · 10⁻⁵ $\frac{lb-s^2}{in^4}$ · 5864 $\frac{in}{sec^2}$ · 15.5 × 2.25 · 3.625 = 2.013 lb

SOUTHWEST RESEARCH INSTITUTE
DEPARTMENT OF ENGINEERING MECHANICS
COMPUTATION SHEET

SHEET NO C29 OF C34

PROJECT NO. 06-8461-001   SPONSOR H $R
SUBJECT
BY SES   DATE 18 MAR 19 85   CHECKED BY: _____ DATE CHECKED _____ 19 ___

Total weight of pallet model should therefore be about
226.44 lbs

SOUTHWEST RESEARCH INSTITUTE
DEPARTMENT OF ENGINEERING MECHANICS
COMPUTATION SHEET

SHEET NO C30 OF C34

PROJECT NO. 06-8461-001   SPONSOR H & R
SUBJECT.
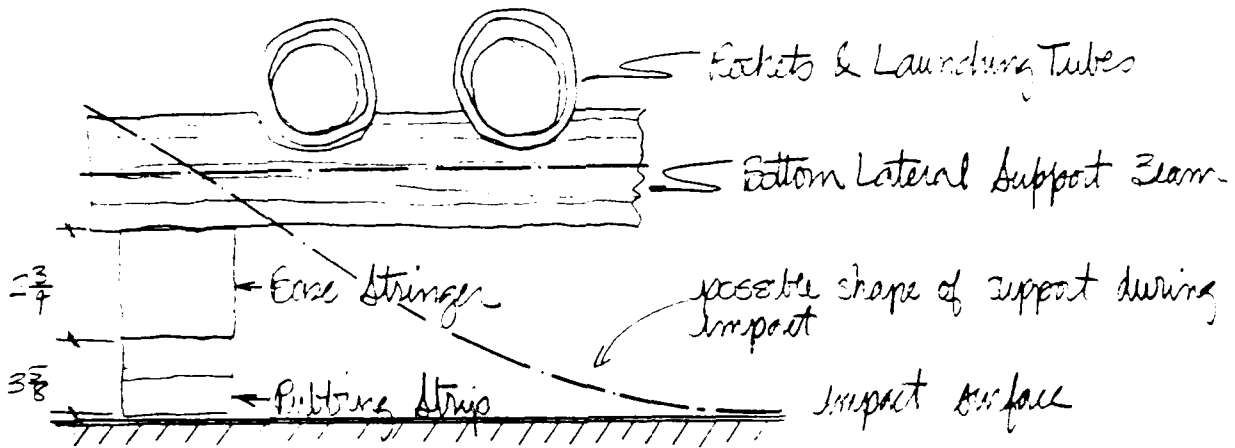BY SES   DATE 30 MAY 19 85   CHECKED BY: _____ DATE CHECKED: ____ 19 ___

X Compute characteristics of "contact"-type elements representing contact of lateral support beams with impacted surface

Actual Conditions at Base of Pallet

To address possible contact between the lateral support beam and the impact surface a "contact" type element is introduced
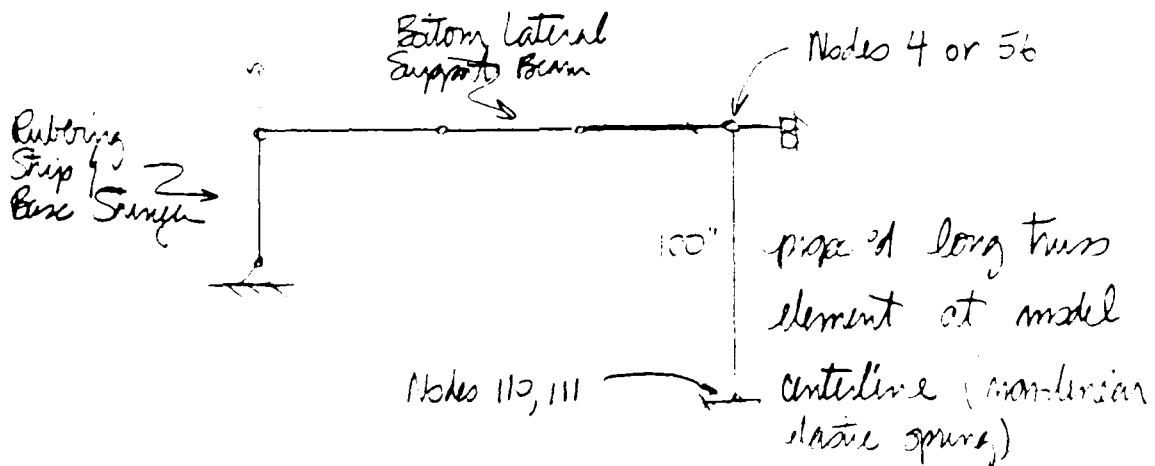
SOUTHWEST RESEARCH INSTITUTE
DEPARTMENT OF ENGINEERING MECHANICS
COMPUTATION SHEET

SHEET NO.
_____ OF _____

PROJECT NO. _____ SPONSOR _____
SUBJECT _____
BY _____ DATE _____ 19 ___ CHECKED BY _____ DATE CHECKED _____ 19 _____

Stress-strain pairs for contact element

ϵ	σ	E	lb.
0.0	0.0	$2.632 \cdot 10^3$	①
0.03375	157.8	$2.632 \cdot 10^3$	②
0.090	450		
0.100	1100		
0.105	5000		
0.1050+	25000		
0.500	$18 \cdot 10^6$		

SOUTHWEST RESEARCH INSTITUTE
DEPARTMENT OF ENGINEERING MECHANICS
COMPUTATION SHEET

SHEET NO. ___ OF ___

PROJECT NO. _____ SPONSOR _____
SUBJECT _____
BY _____ SES _____ DATE ___ 19 __ CHECKED BY: _____ DATE CHECKED _____ 19 _____

the nonlinear elastic spring model is made lower than
the right of the resulting strip so that the deflected
element length > 0 and strains are small

Desired $\sigma - \epsilon$ characteristic

i.e.,

$$E = \frac{1}{100} E_{min}$$
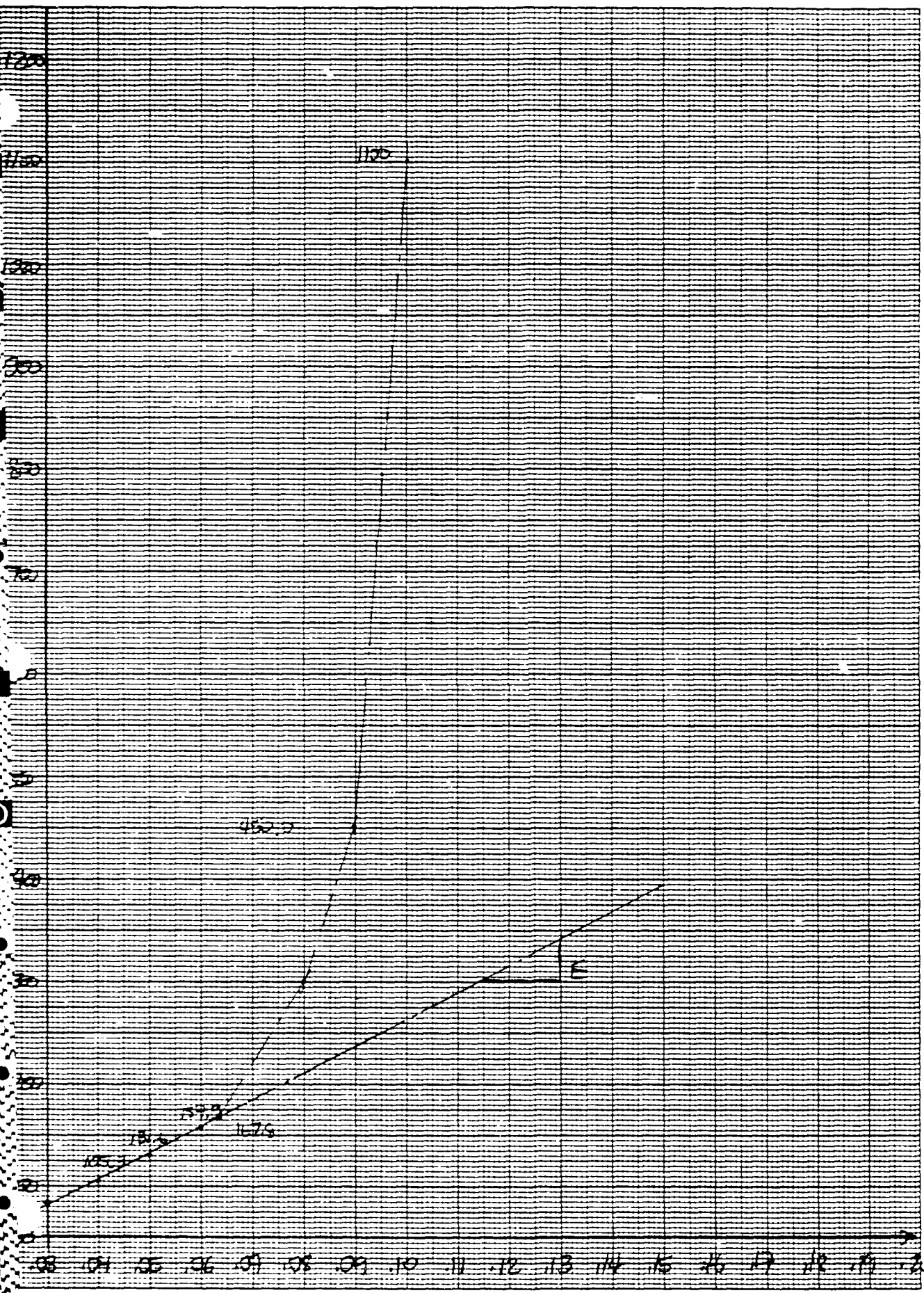
$$E_* = 10 \, E_{max}$$
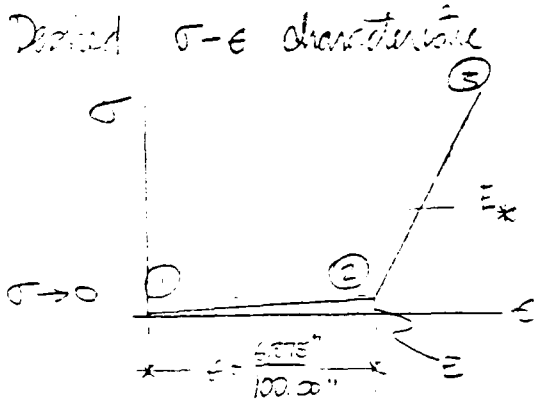
where E_{min}, E_{max} are the maximum and minimum
elastic moduli in the vertical pallet model:

$$E_{min} = 0.652 \times 10^5 \frac{lb}{in^2} \text{(nonlinear spring)}$$
$$E_{max} = 30 \times 10^6 \frac{lb}{in^2} \quad (\text{steel})$$

$$E = 0.652 \times 10^3 \frac{lb}{in^2} \qquad E_* = 30 \times 10^7 \frac{lb}{in^2}$$

PROJECT NO. 06-8461-001   SPONSOR: H&R

SUBJECT:

BY SFS   DATE 15 MAR 19 85   CHECKED BY: DATE CHECKED   19

VERTICAL PALLET IMPACT — CRUSHING
STRAIN CHARACTERISTIC (Tabulated from FE Analysis)

Load on Base (psi)	Equivalent Force (lbs)	Displacement (in)	Maximum Agent Cannister Strain (in/in)
100	1032	-0.0070729	———
200	2065	-0.1414590	———
215	2220	-0.1732060	.0003759
230	2375	-0.1866720	.0007900
245	2529	-0.0200865	.0012480
260	2684	-0.0215479	.0016700
280	2891	-0.0235544	.0023410
300	3097	-0.0256826	.0031480
302	3118	-0.0258998	.0032200
330	3407	-0.0291410	.0045300
360	3716	-0.0328180	.0058900
390	4026	-0.0366443	.0072260
420	4336	-0.0406022	.0085976
450	4646	-0.0446598	.0101640
480	4956	-0.0487896	.0114288
510	5265	-0.0529537	.0131389
540	5575	-0.0571719	.014298
570	5885	-0.0614017	.0159640
600	6194	-0.0656658	.0170400
650	6711	-0.0727966	.0196700
700	7227	-0.0799129	.0210100
840	8672	-0.0998594	.0268000
840	8672	-0.1138230	.0279000
840	8672	-0.1377820	.0288610
840	8672	-0.1888510	.0326000

Appendix D

Crushing/Buckling Loads of Pallet During Longitudinal Impact

PALLET AXIAL BUCKLING/CRUSH LOAD

LAUNCHING TUBES

$$D_0 = 4.89 \text{ in} \qquad E = 1.1 \times 10^6 \text{ PSI}$$
$$D_i = 4.50 \text{ in} \qquad \sigma_y = 38,800 \text{ PSI}$$

$$L_{O/A} = 30.98 \text{ in} \;\; , \text{ OVERALL LENGTH}$$

$$L = 20 \text{ in.} \overset{MAX}{,} \text{ LENGTH BETWEEN TRANSVERSE WOODEN SPACERS}$$

$$r = \text{radius of gyration} = \sqrt{I/A}$$

$$I = \frac{\pi}{64}(D_0^4 - D_i^4) = \frac{\pi}{64}\left[(4.89)^4 - (4.50)^4\right] = 7.94 \text{ in}^4$$

$$A = \frac{\pi}{4}(D_0^2 - D_i^2) = \frac{\pi}{4}\left[(4.89)^2 - (4.50)^2\right] = 2.876 \text{ in}^2$$

$$r = \sqrt{I/A} = 1.66 \text{ in.}$$

THE EULER FORMULA GIVES THE BUCKLING STRESS FOR SLENDER COLUMNS AS:

$$\sigma = \frac{P}{A} = \frac{C\pi^2 E}{(L/r)^2}$$

WHERE $C = 1.0$ for PINNED ENDS
$= 4.0$ for CLAMPED ENDS

CONSERVATIVELY ASSUME THAT $C = 1.0$ FOR THIS CASE. BETWEEN THE SPACERS THE STRESS TO CAUSE BUCKLING IS:

$$\sigma = \frac{(1.0)\,\pi^2\,(1.1\times10^6)}{(20\text{in}/1.66)^2} = 74,900 \text{ PSI} \gg \sigma_y$$

THUS, IT APPEARS THAT THE LAUNCHING TUBES WILL CRUSH BEFORE THEY WILL BUCKLE. THE CRUSHING LOAD PER TUBE IS:

$$F_{cr} = \sigma_y A = (38,900 \text{ psi})(2.876 \text{ in}^2)$$
$$= \underline{\underline{111,600 \text{ lb}}}$$

IN ADDITION TO THE LAUNCHING TUBES, THERE ARE EIGHT (8) LONGITUDINAL WOODEN STRINGERS. BETWEEN THE TRANSVERSE WOODEN SPACERS THEIR CROSS-SECTION PROPERTIES ARE:

$$A = .58 \text{ in} \times 3 \tfrac{5}{8} \text{ in} = 5.89 \text{ in}^2$$

$$I_{MIN} = \tfrac{1}{12}(3.625)(1.625)^3 = 1.296 \text{ in}^4$$

$$r_{MIN} = \sqrt{I/A} = 2.132 \text{ in}$$

$$L = 20 \text{ in}, \quad \text{MAX. UNSUPPORTED LENGTH}$$

$$\sigma_{cy} = 3,670 \text{ psi} \qquad E = 1.35 \times 10^6 \text{ psi}$$
$$\sigma_{cult} = 4,800 \text{ psi}$$

THE BUCKLING STRESS IS, FROM EULER'S FORMULA:

$$\sigma = \frac{C \pi^2 E}{(L/r)^2} = \frac{1.0(\pi)^2(1.35 \times 10^6)}{(20/2.132)^2}$$
$$= 151,370 \text{ psi} \ggg \sigma_y$$

THUS, AS FOR THE LAUNCHING TUBES, THE STRINGERS WILL CRUSH RATHER THAN BUCKLE. THE MINIMUM

CRUSHING LOAD IS:

$$F_{sp} = \sigma_{c_Y} A = (3,670 \text{ psi})(5.89 \text{ in}^2)$$
$$= \underline{\underline{21,620 \text{ lb}}}$$

THE TOTAL LONGITUDINAL CRUSH LOAD FOR THE PALLET IS THE SUM OF THE CRUSH LOADS FOR ALL LAUNCHING TUBES AND LONGITUDINAL WOODEN STRINGERS. IT IS:

$$F_{CR} = 15 \cdot F_{LT} + 8 \times F_{sp} = 15(111,600) + 8(21,620)$$
$$= 1.847 \times 10^6 \text{ lb}$$

IF THIS LOAD IS GREATER THAN THAT REQUIRED TO CRUSH THE FOAM, THEN THE ASSUMPTION THAT THE ROCKET CAN BE ISOLATED FROM THE LAUNCHING TUBE AND PALLET FOR LONGITUDINAL IMPACT INSIDE THE CAMPACT, IS GOOD. THE FOAM CRUSHING LOAD IS COMPUTED FOR THE DOOR AREA AND DIVIDED BY FOUR (4) TO OBTAIN A CONSERVATIVE ESTIMATE FOR THE "MAXIMUM RESISTANCE" FELT" BY THE BOTTOM (DOOR END) PALLET DURING A LONGITUDINAL DROP. THIS FORCE IS

$$F = (\sigma_c)_{FOAM} \frac{1}{4} A_{DOOR}$$

WHERE

σ_c = FOAM CRUSHING STRENGTH = 140 psi

A = CAMPACT INNER DOOR AREA

= 86 × 74 = 6364 in²

THESE VALUES GIVE:

$$F = (140\ psi)(\tfrac{1}{4})(6364\ in^2)$$

$$= 222,700\ lb\ <<\ 1.85 \times 10^6\ lb$$

THEREFORE IT APPEARS THAT THE PALLETS WILL NOT COLLAPSE AXIALLY WITHIN THE CAMPACT AND THAT THE ROCKET IS EFFECTIVELY ISOLATED FROM THE REMAINDER OF THE STRUCTURE DURING A LONGITUDINAL IMPACT

Appendix E

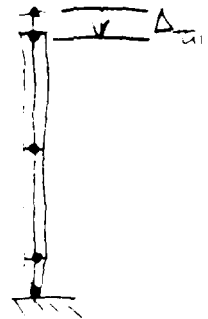Calculation of Equivalent Crush Forces: Longitudinal and Lateral Impacts
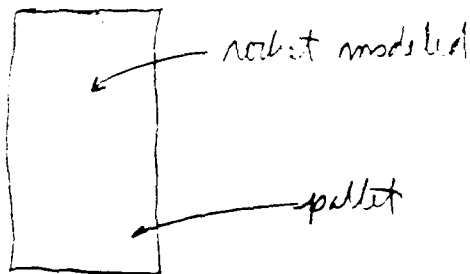
SOUTHWEST RESEARCH INSTITUTE
DEPARTMENT OF ENGINEERING MECHANICS
COMPUTATION SHEET

SHEET NO
E1 OF

PROJECT NO _Oc-9461-001_   SPONSOR _H&R_
SUBJECT _____
BY _____SES_____ DATE _5 MAY 85_ CHECKED BY _____ DATE CHECKED ____ 19 __

<u>Equivalent Static Crush Force for Longitudinal Impact</u>

Compute the equivalent static crush force for longitudinal impact by equilibrating the kinetic energy (KE) at pallet impact with the work done deforming the structure.

rocket modelled

pallet

Longitudinal Impact
(single rocket modeled)

Schematic of FE model

the governing equation is

$$F \Delta = \tfrac{1}{2} m v^2$$

$\tfrac{1}{2} m v^2$ is computed from impact velocity and pallet mass.

impute rs for pallet

$$m_{pallet} = \frac{1350\,lb}{386.4\,in/s^2}$$

$$v_{final} = 608.7\,\frac{in}{sec}$$

$$\tfrac{1}{2}mv^2 = 6.4725 \cdot 10^5\ lb\text{-}in$$

Maximum displacement of rocket at tail

$$max_{tail} = 1.1837\,in \quad @\ t = 0.3603\ sec \ (from\ FE\ analysis)$$

$$F_{avil} = \frac{rs}{L} = \frac{6.4725 \cdot 10^5\ lb\text{-}in}{1.1837\ in}$$

$$\underline{F_{avil} = 5.468 \cdot 10^5\ lb \qquad LONGITUDINAL\ IMPACT}$$

SOUTHWEST RESEARCH INSTITUTE
DEPARTMENT OF ENGINEERING MECHANICS
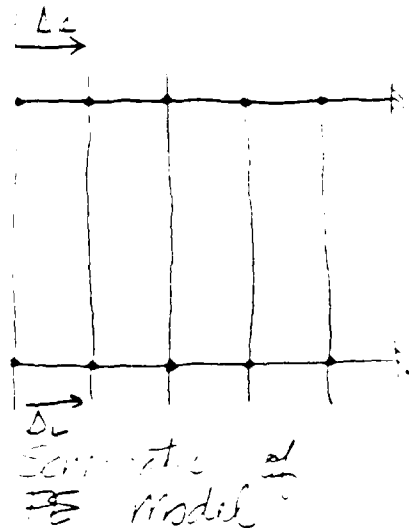COMPUTATION SHEET

SHEET NO E3 OF

PROJECT NO. 05-8461-001   SPONSOR H&R
SUBJECT
BY SES   DATE 28 MAY 85   CHECKED BY _____ DATE CHECKED ___ 19 ___

Equivalent Static Force in Lateral Impact

Compute the equivalent static force for a lateral impact of the pallet from 40 feet by applying the maximum computed (from FE analysis) dynamic displacement as a static displacement to the structure. The resultant static force is the equivalent force.
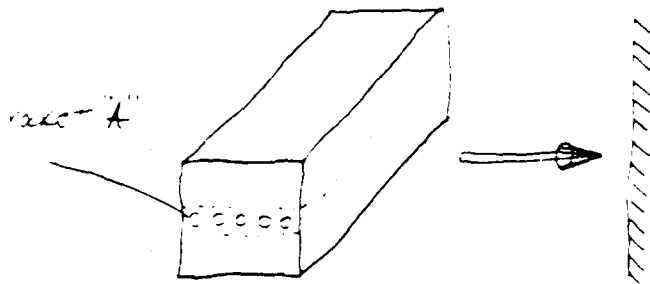
lateral impact
(Middle section is modeled)

Geometry of FE model

The governing equation is

$$F \cdot \Delta = \tfrac{1}{2} m v^2$$

$\tfrac{1}{2} m v^2$ is computed from the impact velocity

SOUTHWEST RESEARCH INSTITUTE
DEPARTMENT OF ENGINEERING MECHANICS
COMPUTATION SHEET

SHEET NO $\underline{\text{E4}}$ OF $\underline{\text{E4}}$

PROJECT NO $\underline{\text{06--846-001}}$ SPONSOR: $\underline{\text{H&R}}$
SUBJECT $\underline{\hspace{6cm}}$
BY $\underline{\text{SES}}$ DATE $\underline{\text{28 MAY 85}}$ CHECKED BY: $\underline{\hspace{3cm}}$ DATE CHECKED $\underline{\hspace{1.5cm}}$ 19 $\underline{\hspace{1cm}}$

compute KE to pallet

$$m_{pallet} = \frac{1350 \text{ lbs}}{386.4 \text{ in/s}^2} \left.\begin{array}{c} \\ \\ \end{array}\right\} \text{from KE analysis}$$

$$v_{avg} = 608 \text{ in/s}$$

$$KE = \frac{1}{2} m v^2$$

$$= \frac{1350}{386.4} \frac{lb-s^2}{in} \cdot \frac{1}{2} \cdot \left(608.7 \frac{in}{s}\right)^2$$

$$KE = 6.4735 \cdot 10^5 \text{ lb-in}$$

maximum displacements of strut A

$$\overset{max}{u} = .16026 \text{ in } @ .004105 \text{ sec}$$

$$\overset{max}{u_R} = 0.90125 \text{ in } @ .00605 \text{ sec}$$

take average $\Delta_{avg} = 1.03 \text{ in}$

$u \neq u_R$ because some "rocking" of pallet
occurs at impact)

$$F_{equiv} = \frac{KE}{\Delta} = \frac{6.4735 \cdot 10^5 \text{ lb-in}}{1.03 \text{ in}}$$

$$\underline{F_{equiv} = 6.2795 \cdot 10^5 \text{ lb.}} \quad \text{LATERAL IMPACT}$$
$$\text{FROM 40 FEET}$$

END

DATE

FILMED

DTIC

4/88